

INFORMATION TO USERS

This material was produced from a microfilm copy of the original document. While the most advanced technological means to photograph and reproduce this document have been used, the quality is heavily dependent upon the quality of the original submitted.

The following explanation of techniques is provided to help you understand markings or patterns which may appear on this reproduction.

- 1. The sign or "target" for pages apparently lacking from the document photographed is "Missing Page(s)". If it was possible to obtain the missing page(s) or section, they are spliced into the film along with adjacent pages. This may have necessitated cutting thru an image and duplicating adjacent pages to insure you complete continuity.**
- 2. When an image on the film is obliterated with a large round black mark, it is an indication that the photographer suspected that the copy may have moved during exposure and thus cause a blurred image. You will find a good image of the page in the adjacent frame.**
- 3. When a map, drawing or chart, etc., was part of the material being photographed the photographer followed a definite method in "sectioning" the material. It is customary to begin photoing at the upper left hand corner of a large sheet and to continue photoing from left to right in equal sections with a small overlap. If necessary, sectioning is continued again — beginning below the first row and continuing on until complete.**
- 4. The majority of users indicate that the textual content is of greatest value, however, a somewhat higher quality reproduction could be made from "photographs" if essential to the understanding of the dissertation. Silver prints of "photographs" may be ordered at additional charge by writing the Order Department, giving the catalog number, title, author and specific pages you wish reproduced.**
- 5. PLEASE NOTE: Some pages may have indistinct print. Filmed as received.**

Xerox University Microfilms

300 North Zeeb Road
Ann Arbor, Michigan 48106

75-11,916

MacKINNON, David John, 1944-
AN ANALYSIS OF THE FLUCTUATIONS IN LASER LIGHT
CAUSED BY THE MOTION OF ATMOSPHERIC SCATTERERS.

The University of Arizona, Ph.D., 1974
Physics, optics

Xerox University Microfilms, Ann Arbor, Michigan 48106

AN ANALYSIS OF THE FLUCTUATIONS IN LASER LIGHT
CAUSED BY THE MOTION OF ATMOSPHERIC SCATTERERS

by

David John MacKinnon

A Dissertation Submitted to the Faculty of the
DEPARTMENT OF ATMOSPHERIC SCIENCES
In Partial Fulfillment of the Requirements
For the Degree of
DOCTOR OF PHILOSOPHY
In the Graduate College
THE UNIVERSITY OF ARIZONA

1 9 7 4

THE UNIVERSITY OF ARIZONA

GRADUATE COLLEGE

I hereby recommend that this dissertation prepared under my
direction by David John MacKinnon
entitled An Analysis of the Fluctuations in Laser Light
Caused by the Motion of Atmospheric Scatterers
be accepted as fulfilling the dissertation requirement of the
degree of Doctor of Philosophy

Reginald M. Herman
Dissertation Director

Nov 14, 1974
Date

After inspection of the final copy of the dissertation, the
following members of the Final Examination Committee concur in
its approval and recommend its acceptance:*

<u>William D. Sellers</u>	<u>10/17/74</u>
<u>Henry A. Wei</u>	<u>11-1-74</u>
<u>R. D. Smith</u>	<u>11-14-74</u>
<u>John A. Reager</u>	<u>11-15-74</u>
<u> </u>	<u> </u>

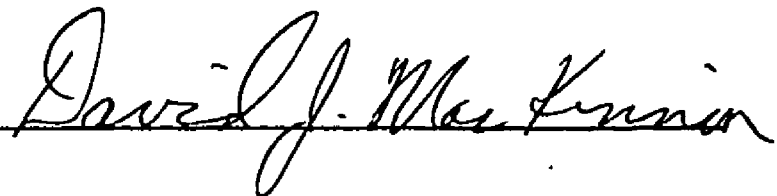
*This approval and acceptance is contingent on the candidate's
adequate performance and defense of this dissertation at the
final oral examination. The inclusion of this sheet bound into
the library copy of the dissertation is evidence of satisfactory
performance at the final examination.

STATEMENT BY AUTHOR

This dissertation has been submitted in partial fulfillment of requirements for an advanced degree at The University of Arizona and is deposited in the University Library to be made available to borrowers under rules of the Library.

Brief quotations from this dissertation are allowable without special permission, provided that accurate acknowledgment of source is made. Requests for permission for extended quotation from or reproduction of this manuscript in whole or in part may be granted by the head of the major department or the Dean of the Graduate College when in his judgment the proposed use of the material is in the interests of scholarship. In all other instances, however, permission must be obtained from the author.

SIGNED:

A handwritten signature in cursive script, reading "David J. MacKinnon", written over a horizontal line.

ACKNOWLEDGMENTS

Beloved, do not be surprised at the fiery ordeal among you, which comes upon you for your testing, as though some strange thing were happening to you (1 Peter 4:12).

In the spirit of trying to uphold a standard of quality for this degree my committee has spent a great deal of time and personal effort. For this thanks must go to Dr. William Sellers, Dr. Carl Tomizuka, and especially to Dr. Henry Hill. I must give special thanks to Dr. John Reagan and extra special thanks to Dr. Benjamin Herman, my advisor, for efforts spent beyond the call of duty.

To my friends who came through this long period with me, all I can say is that I sincerely appreciate your help.

To Marian, Sophie (the dog), and the Wilderness, you maintained my inner spirit.

TABLE OF CONTENTS

	Page
LIST OF TABLES	vii
LIST OF ILLUSTRATIONS	viii
ABSTRACT	ix
1. INTRODUCTION AND SYNOPSIS	1
1.1 Introduction	1
1.2 Synopsis	4
1.2.1 Light Scattered in a Continuous Bistatic Source-receiver System . .	4
1.2.2 Intensity Correlation Function . .	10
1.2.3 Temporal Intensity Correlation Function: $R_I(\vec{r}_s, \vec{r}_s, t)_p$	16
1.2.4 Analysis of the Number Density Terms in (1.9a) and (1.9b)	25
1.2.5 Spatial Intensity Correlation Function: $R_I(\vec{r}_s, \vec{r}'_s, 0)_p$	29
1.2.6 Current Correlation Function	31
1.2.7 Results	34
1.2.8 Attenuation Fluctuations	37
1.2.9 Power Spectrum	38
1.2.10 Conclusions	38
2. THE CAUSES OF THE FLUCTUATIONS OF SCATTERED LASER LIGHT	40
2.1 Optical Properties of Atmospheric Scatterers	41
2.1.1 Molecules	41
2.1.2 Particulates	46
2.1.3 Turbulent Refractive Inhomogeneities	57
2.2 Coherence	60
2.2.1 Temporal Coherence	60
2.2.2 Spatial Coherence	63
2.3 Interaction of the Laser Light with the Atmospheric Scatterers	66
2.4 Effects of Scatterers between Laser the Source and Scattering Volume	67
2.4.1 The Effects of the Turbulence Component of the Scattered Light on the Transmitted Laser Light . .	67

TABLE OF CONTENTS--Continued

	Page
2.4.2 The Effects of the Rayleigh and Particulate Components of the Scattered Light on the Transmitted Laser Light	78
2.5 Effects of the Atmospheric Scatterers at the Scattering Volume	79
2.5.1 Turbulence Component of the Scattered Light	79
2.5.2 The Rayleigh and Particulate Components of the Scattered Light	80
2.6 The Scattering Volume	81
2.6.1 The Scattering Volume for Pulsed and Continuous Illumination	81
2.7 General Formulation of the Intensity Correlation Function of the Scattered Light	84
2.7.1 The Intensity Correlation Function from the Continuously Illuminated Atmospheric Scatterers	89
2.8 Effects of the Atmospheric Scatterers Between the Scattering Volume and the Receiver	105
2.8.1 Turbulent Refractive Inhomogeneities	105
2.8.2 Molecular (Rayleigh) and Particulate Effects	108
2.9 Transmittance Fluctuations	108
2.10 Receiver Effects	109
2.10.1 Photocurrent Correlation Function for One Spatial Coherence Area	112
2.10.2 Photocurrent Correlation Function for Many Spatial Coherence Areas	114
2.10.3 Filtering the Photanode Current	115
2.10.4 The Statistical Properties of the Filtered, Photoanode Current	116
2.11 Chapter Summary	121
3. RESULTS	123
3.1 The Photoanode Current Fluctuations for the University of Arizona Monostatic Lidar	123
3.2 Estimating the True Mean Photocurrent.	131
3.3 Photocurrent Fluctuations for the Monostatic System when the Scatterer Noise is Greater than the Shot Noise	139

TABLE OF CONTENTS--Continued

	Page
4. CONCLUSIONS	142
APPENDIX A: THE FIELD AMPLITUDE OF THE SINGLE SCATTERED LASER LIGHT	145
A.1 The Scattered Light to the Receiver . .	147
APPENDIX B: MAGNITUDE OF THE SINGLE SCATTERED LIGHT FROM MOLECULES (RAYLEIGH COM- PONENT) AND PARTICULATES IN THE TRANSMITTED LASER BEAM	150
B.1 Scattering and Attenuation	150
B.2 Forward Scattered Light	153
B.3 Attenuation on a Slant Path	154
B.4 Calculation of the Forward Scattered Light	155
APPENDIX C: CALCULATION OF THE INTENSITY CORRE- LATION FUNCTION OF THE MOLECULES AND PARTICULATES	163
C.1 Particulates	164
C.2 Analysis of Term (2b)	167
C.3 Brownian Motion	168
C.4 Turbulent Motion	170
C.5 Analysis of Term (1) and Term (2a) . .	173
C.6 Complete Expression for $R_I^C(t)_p$	178
C.7 Molecules	178
C.8 Calculation of the Field Correlation Function of the Particulates and Molecules	180
C.8.1 Particulates	180
C.8.2 Molecules	181
C.9 The Statistical Moments of the Inten- sity Distribution	181
APPENDIX D: CONVERSION OF LIGHT TO CURRENT . . .	184
D.1 Filtering the Photoanode Current . . .	185
APPENDIX E: TRANSMITTANCE FLUCTUATIONS	188
LIST OF REFERENCES	198

LIST OF TABLES

Table	Page
2.1 The Transverse Coherence Length, TCL, of the Transmitted Laser Light as a Function of Range, $ \vec{r} $, in Weak Turbulence	73
2.2 The Variance of the Transmitted Laser Light Log-intensity (σ_L^2) as the Light Passes Through a Weakly Turbulent Medium with Increasing Range, $ \vec{r} $	76
2.3 The Maximum Transverse Separation, MTS, of the Received Scattered Light as a Function of Increasing Range Through a Homogeneous, Weak ($C_n^2=1 \times 10^{-16}$) Turbulent Atmosphere	107
3.1 The Total Flux Collected by the Receiver ($\langle F \rangle$) as a Function of Range (R) for the University of Arizona Monostatic Laser Propagating Vertically	132
3.2 The Photoanode Current ($\langle i \rangle$), Variance (σ_i^2), and Signal-to-Noise Ratio (S_N) as a Function of Range for the University of Arizona Monostatic Lidar	133
3.3 The Values of S_N as a Function of the Error Spread About the Mean, $\pm X\%$, and the Confidence Level, $Y\%$	136
B.1 The Ratio of the Volume Scattering Coefficients in the Forward and Backward Directions	154
B.2 The Normal Flux Density Ratio, $Q(R)$, as a Function of Range For a Vertically Propagating Laser Beam With Particulates	161
E.1 Fluctuation States for Particulates in Brownian Motion	196

LIST OF ILLUSTRATIONS

Figure		Page
1.1	Geometry of the Bistatic Source-Receiver System	6
2.1	The Number Density of Molecules, $N(r)$ (Solid Curve), and its Component Parts (Dotted Curves) Along the Path of the Light Beam	43
2.2	The Young's Double Slit Experiment	63
2.3	The Relative Position of the Instantaneous Scattering Volume at Time 0 (Solid Boundaries) and Time t (Dashed Boundaries).	88
2.4	The Spherical Phase Surfaces of Two Scatterers at O and P have a Path Difference of $\Delta = \lambda/16$ at the Separation Length d on the Receiver Surface .	101
A.1	The Geometry of the Transmitted Laser Beam and the Forward Scattered Light	145
A.2	The Geometry of the Scattered Light Arriving at a Point on the Receiver (R)	147
B.1	A Volume Containing Many Scatterers Upon Which is Normally Incident a Differential of Monochromatic Flux Density $I_\lambda d\omega$	151
B.2	Description of the Laser Beam and Scattering Volume	157

ABSTRACT

By means of correlation functions the statistics of light fluctuations caused by the motions of atmospheric scatterers are developed. The light fluctuations are influenced by the physical properties of the scattering medium (number density fluctuations of the scatterers, Brownian and turbulent motion of the scatterers, and the perturbations in the transmitted light caused by turbulent refractive inhomogeneities), the optics of the source-receiver system (receiver aperture size), and the noise characteristics of the receiver (photocurrent shot-noise). All the previously mentioned effects are included in a photocurrent correlation function (the photocurrent is the measurable quantity associated with the received light). From this correlation function, the first and second moments of the probability distribution and the mean time between independent values of the photocurrent are obtained. The results are applied to a typical radar system and, then, to the University of Arizona lidar system. First, the results show that the received radar signal (photocurrent) fluctuates according to an exponential distribution (Rayleigh); this is substantiated by experiment. Second, the lidar photocurrent fluctuations are found to be normally distributed with a mean directly proportional to the number of molecules and particulates in the scattering

volume; the variance is dominated by shot-noise. The large receiver apertures typically employed in systems like the University of Arizona lidar cause the dominance of shot-noise in the fluctuations. It is shown that changing some of the lidar's geometric configurations (e.g., reducing receiver aperture size and/or reducing the size of the scattering volume) will allow the fluctuations associated with the scatterer motion to dominate shot-noise.

CHAPTER 1

INTRODUCTION AND SYNOPSIS

1.1 Introduction

Lidar systems are now being regularly used to remotely detect the atmospheric structure of aerosols. Fluctuations in the light intensity scattered from those aerosols create an uncertainty in the true atmospheric structure. This paper is an attempt to analyze the physical processes which cause these fluctuations. Correlation functions are chosen as the vehicle for this analysis because of the ease by which certain physical processes can be evaluated. Included in the analysis are the effects of number density fluctuations of the scatterers, Brownian and turbulent motion of the scatterers, and phase perturbations caused by turbulent refractive inhomogeneities. The results are sufficiently general to be applied to most lidar systems as well as typical radar systems.

Smith (1965) discusses some work related to the fluctuations in scattered laser light received from particulate and molecular scatterers. Smith presents some actual examples of laser light scattered from the atmosphere as the laser beam propagates at increasing range with the receiver looking directly along the laser beam path (monostatic

system; these examples were taken from a series of experiments performed by Collis and Ligda 1964). When the laser light was received and converted into a photocurrent, the most notable property of the photocurrent was smaller fluctuations than expected. Smith expected the photocurrent to exhibit the larger fluctuations of a Rayleigh distributed photocurrent. This result is based upon the assumption that the laser light is scattered from randomly distributed, independent scatterers (Marshall, Hitschfeld, and Wallace 1953); the assumption seems quite reasonable and is discussed further in this dissertation. In order to account for the observed smaller fluctuations, Smith gives several hypotheses. All of these hypotheses incorporate some means of averaging the laser light over several independent values. This averaging causes the statistical variance of the fluctuation to be reduced by the square root of the number of independent values, thus explaining the smaller fluctuations. This dissertation reaches conclusions similar to those just stated. Further, the effects of the photoelectric conversion and the variations in the transmission of the laser light are analyzed; these factors are not discussed by Smith.

In Chapter 2, the photocurrent correlation function is calculated in terms of the intensity correlation function of the scattered light incident on the receiver. Recall that the photocurrent correlation function is a statistical

average of the product of two values of the photocurrent at two separate times; the intensity correlation function is similarly defined. From the photocurrent correlation function the first two statistical moments of the photocurrent probability distribution are obtained, as well as the independence time of the photocurrent. This information is used to calculate the relative magnitudes of the experimental error in the photocurrent for typical lidar systems.

Using the University of Arizona monostatic facility operating under normal conditions as a typical lidar system, the photocurrent fluctuations are indeed calculated to be smaller than the Rayleigh distributed photocurrent as indicated by Smith (1965). Even more surprising is the result that the photocurrent fluctuations associated with the scatterer motion (scatterer noise) are far below the shot noise. It is shown that the size of the scattering volume and the collecting aperture of the lidar system principally determine the number of spatial coherence areas contained within the collecting aperture. As the number of coherence areas is increased, the fluctuations in the collected laser light are reduced. Since the scatter noise is a property of the collected light and the shot noise is a property of the photocurrent itself, then increasing the number of spatial coherence areas reduces the scatter noise but not the shot noise. The number of coherence areas associated with typical lidar systems is so large that the scatter noise is found to be far

below the shot noise. Finally, it is of interest to consider lidar systems in which the number of coherence areas are small (diffraction limited). Under such conditions a whole new set of interesting problems arise. The results discussed in the previous paragraph are present in Chapter 3.

In conclusion some of the original work in this dissertation was placed into the Appendices, because its inclusion in an already cumbersome text would have lead to unnecessary confusion.

The synopsis which follows is a condensation of some of the more salient contributions brought forth in this dissertation. The synopsis references portions of the main text where more detailed information can be found.

1.2 Synopsis

1.2.1 Light Scattered in a Continuous Bistatic Source-receiver System

Consider a continuous, narrow beam of quasimonochromatic (laser) light illuminating a region of space containing molecular and particulate scatterers. Let a receiver view a portion of the illuminated space in order to collect the light scattered from the molecules and particulates (atmospheric scatterers). The received light is from those scatterers in the source-receiver common volume (scattering volume) yet the phase and amplitude of the received light is modified by the medium between both the source and the

scattering volume and the scattering volume and receiver. Mathematically, a transmitted, scalar component of the light field, E_t , which arrives at the scattering volume from the source can be expressed as

$$E_t = E_L e^{-k\alpha} + \sum_i E_{mi} e^{-k\alpha_i} + \sum_j E_{pj} e^{-k\alpha_j} + \text{H.O.T.} \quad (1.1)$$

where E_L is the light source field attenuated by the molecules and particulates along the path, according to $e^{-k\alpha}$, where $k = 2\pi/\lambda$ (λ - wavelength) and α [meter] is the attenuation parameter which includes the absorption and scattering of the laser light out of the beam. The second and third terms represent the single scatter contributions from the molecules and particulates, respectively; these terms are similarly adjusted for attenuation. The higher order terms [H.O.T.] that appear in (1.1) represent multiple scattering contributions. However for the weakly scattering medium envisioned for this paper, these terms can be neglected.

When the summation is performed over the molecular contribution, the resultant field can be divided into two components due to small and large scale correlation lengths in the spatial number density distribution of the molecules. The resultant field component from the molecules whose spatial number density correlation length is small compared to the wavelength (λ) of the (laser) light, is called the Rayleigh component, while the component which typifies large

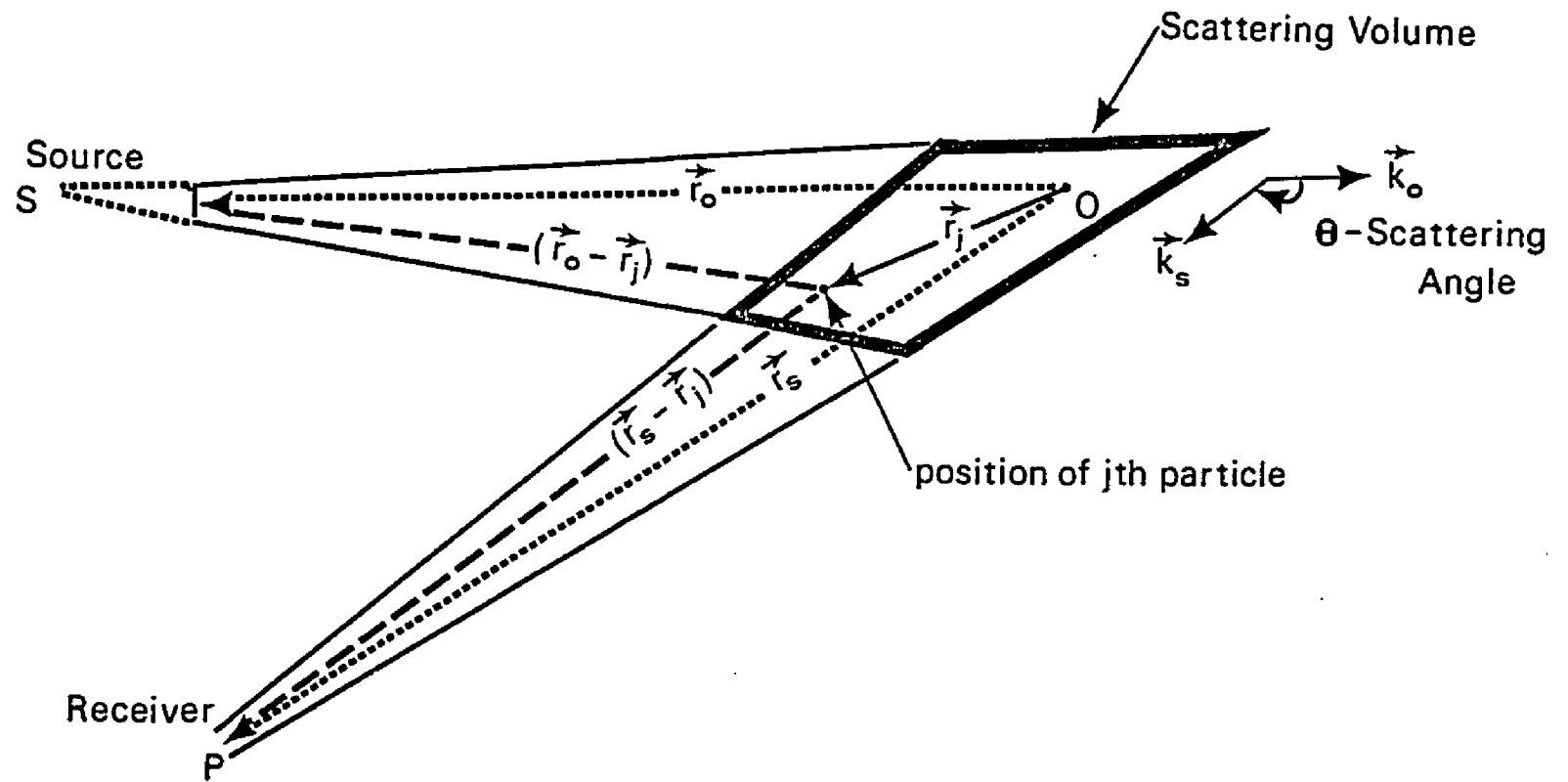


Fig. 1.1 Geometry of the Bistatic Source-Receiver System.

scale correlation lengths (turbulent refractive inhomogeneities) with respect to λ , is called the eddy component. The Rayleigh component of the scattered light appears in all directions, while the eddy component appears primarily in the forward direction (the larger the eddy compared to λ , the closer to the forward direction is the scattered light). The molecular field component in (1.1) can now be written as

$$\sum_i E_{mi} e^{-k\alpha_i} = E_m^e + E_m^R = \sum_i E_{mi}^{\ell} e^{-k\alpha_i} + \sum_i E_{mi}^s e^{-k\alpha_i} \quad (1.1a)$$

where the superscripts e and R refer to the eddy and Rayleigh field components, respectively, while the superscripts ℓ and s refer to the large and small number density correlation lengths, respectively.

The light field which arrives at the receiver is expressed in a manner similar to (1.1) except that the scatterers within the scattering volume now act as the source for the light arriving at the receiver. A complete expression for the light field arriving at the receiver from one scatterer within the scattering volume can be found after some preliminary simplification; this expression can be immediately extended to a collection of scatterers. First, the medium is assumed to be non-absorbing, so that attenuation of the light is caused strictly by scattering. Second, the eddy term, E_m^e , is assumed to arise from weak, homogeneous, and

isotropic refractive turbulence consisting of eddies ranging in size from the inner scale of turbulence (ℓ_0) of 1.2 cm to an outer scale (L_0) of 10 m. Furthermore, since a typical (laser) wavelength is $\lambda \sim 7 \times 10^{-5}$ cm, the eddy component appears essentially in the forward direction and scatters little light out of the beam. Consequently, E_m^e does not attenuate the transmitted light, but modifies its amplitude and phase. To express this modification, E_m^e is combined with the transmitted light field arriving at both the scattering volume and the receiver, where the combination is expressed by a new light field with a perturbed amplitude and phase. In addition since E_m^e appears only along the transmission paths, there are no E_m^e sources in the scattering volume which contribute light to the receiver for the bistatic system (see Fig. 1.1) collecting light away from the forward direction of the initial source. Finally, for the weak scattering medium envisioned, it can be shown that the contributions along the path from the scattering volume to the receiver of E_m^R and $E_p = \sum_j E_{pj} e^{-k\alpha_j}$ are negligible (see Appendix B) compared to the other terms in (1.1 and 1.1a). Therefore, a component of the light field from one scatterer arriving at a point P on the receiver at time t $[\bar{E}_j(\vec{r}_s, t)]$ for the bistatic source-receiver system depicted in Figure 1.1 can be expressed with respect to some arbitrary origin in the common volume according to

$$E_j(r_s, t) = \quad (1.2)$$

$$A_j \angle (\vec{r}_o - \vec{r}_j), (\vec{r}_s - \vec{r}_j), t \quad (a)$$

$$\times e^{i \angle \vec{\omega} t + \vec{k}_{oj} (\vec{r}_o - \vec{r}_j) - \vec{k}_{sj} (\vec{r}_s - \vec{r}_j)} \quad (b)$$

$$\times e^{i \{ \gamma \angle (\vec{r}_o - \vec{r}_j), t \} + \gamma \angle (\vec{r}_s - \vec{r}_j), t \}} \quad (c)$$

$$\times e^{-k \{ \alpha \angle (\vec{r}_o - \vec{r}_j), t \} + \alpha \angle (\vec{r}_s - \vec{r}_j), t \}} \quad (d)$$

$$\times e^{iq_j(t)} \quad (e)$$

where term (1.2a) is a component of the electric field amplitude which arrives at the receiver (P) from the j th scatterer within the common volume adjusted for the perturbation of E_m^e from the source to the scatterer $\angle (\vec{r}_o - \vec{r}_j) \angle$ and from the scatterer to the receiver $\angle (\vec{r}_s - \vec{r}_j) \angle$; in this case (1.2a) is a real number. The time dependence expresses the changing amplitude not only as the scatterer moves $\angle \vec{r}_j \equiv \vec{r}_j(t) \angle$ but also as the refractive eddies move. Term (1.2b) expresses the phase of the scattered light in terms of the geometric path from the source to point P on the receiver (ω is the light frequency, \vec{k}_{oj} and \vec{k}_{sj} are the propagation vectors whose absolute values equal $2\pi/\lambda$ and whose directions are along the incident and scattered light paths for the j th particle, respectively; these vectors change direction in time as the scatterer moves. Term (1.2c) denotes the perturbation

in the phase of the light (expressed by γ) caused by the refractive turbulence. Term (1.2d) represents the attenuation of the light. Finally, Term (1.2e) accounts for the temporal coherence of the light where $q_j(t)$ is a phase factor (between 0 and 2π) for the j th particle at time t . If two scattering events occur at time t_1 and time t_2 ($t_1 \neq t_2$), then

$$\begin{aligned} \langle e^{i[\bar{q}_j(t_1) - q_j(t_2)]} \rangle &= \begin{aligned} &\approx 1 \text{ for } |t_1 - t_2| \leq t_c \\ &\approx 0 \text{ for } |t_1 - t_2| > t_c \end{aligned} \end{aligned} \quad (1.2f)$$

where $\langle \rangle$ denotes the ensemble average and t_c is the temporal coherence time of the light.

1.2.2 Intensity Correlation Function

If the assumption of stationarity in the mean properties of the scattering medium is assumed, then the statistical properties of the light intensity fluctuations at the receiver can be expressed in terms of an intensity correlation function. This function contains information on the mean and variance of the intensity probability distribution, the mean time between independent values of the intensity, and the spectral distribution of the light fluctuations. The most general form of the intensity correlation function $\langle I(\vec{r}_s, 0) I(\vec{r}'_s, t) \rangle$ denoted symbolically by $R_I(\vec{r}_s, \vec{r}'_s, t)$ expresses the correlation of the intensity for both space and time according

to

$$R_I(\vec{r}_s, \vec{r}'_s, t) \equiv \langle I(\vec{r}'_s, 0) I(\vec{r}_s, t) \rangle \quad (1.3)$$

The expression denotes an average over all the possible values which the intensity may assume at two arbitrary points, \vec{r}_s and \vec{r}'_s in space and at two arbitrary times t_1 and t_2 . For the case discussed here \vec{r}_s denotes, as before, some point on the receiver, while \vec{r}'_s is an adjacent point on the receiver. Finally, from the stationarity assumption the correlation in time depends only on the time delay t between the two arbitrary times here defined as $t_1=0$ and $t_2=t$, and hence in (1.3) t_1 is set equal to 0 and t_2 equal to t .

The intensities expressed in (1.3) are directly related to the light fields of the scatterers expressed by (1.2) according to

$$\begin{aligned} I(\vec{r}_s, 0) &= E(\vec{r}_s, 0) E^*(\vec{r}_s, 0) \\ &= \sum_i E_i(\vec{r}_s, 0) \sum_j E_j^*(\vec{r}_s, 0) \end{aligned} \quad (1.4)$$

where the * superscript denotes the complex conjugate of the light field and the expression is summed over all the scatterers contained in the scattering volume. An expression similar to (1.4) exists for $I(\vec{r}'_s, t)$. The light field expressions in (1.4) can be individually summed over the molecular (Rayleigh component) and particulate field contributions so

that

$$E(\vec{r}_s, 0) = E_m(\vec{r}_s, 0) + E_p(\vec{r}_s, 0) \quad (1.5)$$

where the m and p subscripts denote the separate contributions of the molecules¹ and particulates, respectively. Using (1.4) and (1.5) in (1.3) results in an expression containing sixteen terms. Ten of these sixteen terms involve products of terms similar to $\langle E_m(\vec{r}_s, 0) E_p^*(\vec{r}'_s, t) \rangle$; these terms are zero because the motions of the molecules and particulates and, therefore, the associated, scattered light fields are assumed independent (see 2.7). The six terms which are left boil down to the expression given by

$$\begin{aligned} R_I(\vec{r}_s, \vec{r}'_s, t) &= R_I(\vec{r}_s, \vec{r}'_s, t)_m + R_I(\vec{r}_s, \vec{r}'_s, t)_p \\ &+ 2 R_e \left[\overline{R_E}(\vec{r}_s, \vec{r}'_s, t)_m R_E^*(\vec{r}_s, \vec{r}'_s, t)_p \right] + 2 \langle I_m \rangle \langle I_p \rangle \end{aligned} \quad (1.6)$$

where R_e in front of the $\left[\right]$ brackets denotes the real portion of the quantity contained within, $\langle I_m \rangle$ and $\langle I_p \rangle$ are the mean intensities of the molecular and particulate portions of the light, respectively, and $R_E(\vec{r}_s, \vec{r}'_s, t)$ with the appropriate subscripts signifies the field correlation function of the molecules and particulates, generally given by

$$R_E(\vec{r}_s, \vec{r}'_s, t) = \langle E(\vec{r}_s, 0) E^*(\vec{r}'_s, t) \rangle \quad (1.7)$$

1. Note: superscript R is deleted from expression (1.1a).

From (1.6) the effects of the molecules and particulates can be analyzed separately; the particulate component will be analyzed in detail, while the molecular component can be extracted by analogy.

1.2.2a Particulates. The field component of the j th particulate scatterer, generally expressed by (1.2) must be simplified for the analysis to follow. First, for the weak turbulence assumed, (1.2a) will assume its unperturbed, time-independent, free-space value denoted by A_j . Second, (1.2d) is neglected and discussed later, since it is negligible in most cases. Using this modified form of (1.2), and (1.3) and (1.4), the particulate intensity correlation function is given by

$$R_I(\vec{r}_s, \vec{r}'_s, t)_P = \left\langle \sum_{i=1}^{N(0)} \sum_{j=1}^{N(0)} \sum_{k=1}^{N(t)} \sum_{l=1}^{N(t)} A_i A_j A_k A_l \right\rangle \quad (1.8)$$

(a)

$$\exp \{i[\phi_i(0, \vec{r}_s) - \phi_j(0, \vec{r}_s) + \phi_k(t, \vec{r}'_s) - \phi_l(t, \vec{r}'_s)]\} \rangle \quad (b)$$

where

$$\phi_j(t, \vec{r}_s) = -\vec{k}_j \cdot \vec{r}_j + \gamma_{oj}(t) + \gamma_{sj}(t) - \vec{k}_{sj} \cdot \vec{r}_s + q_j(t)$$

where $\vec{k}_j = \vec{k}_{oj} - \vec{k}_{sj}$, and $\gamma_{oj}(t)$ and $\gamma_{sj}(t)$ are the phase terms in the brackets of (1.2c) and $q_j(t)$ is as defined by (1.2e). In (1.8b), i appears in front of the $[\]$ brackets and as a subscript, the former denotes $\sqrt{-1}$, while the latter is a sum index. Further, portions of the phase representation

expressed in (1.2b) do not appear in (1.8) because they are common to all ϕ terms in (1.8b) and would cancel. Finally $N(0)$ and $N(t)$ denote the total number of particles in the scattering volume at time 0 and time t , respectively.

The analysis of (1.8) begins by summing over the indices; this leads to three independent sums given by

$$R_I(r_s, r'_s, t)_p = (1.9a) + (1.9b) + (1.9c)$$

$$(1.9a) \quad \begin{array}{c} \text{for } i=j \text{ and } k=l \\ = < \sum_{i=1}^{N(0)} |A_i|^2 \sum_{j=1}^{N(t)} |A_j|^2 > \end{array}$$

$$(1.9b) \quad \begin{array}{c} \text{for } i=l \text{ and } j=k, \text{ but } i \neq j \\ = < \sum_{i=1}^{N'(t)} |A_i|^2 \sum_{j=1}^{N'(t)} |A_j|^2 \times \exp \{i[\phi_i(0, \vec{r}_s) - \phi_i(t, \vec{r}'_s) - i[\phi_j(0, \vec{r}_s) - \phi_j(t, \vec{r}'_s)]]\} > \end{array}$$

$$(1.9c) \quad \begin{array}{c} \text{for } i=k, j=l; i \neq j \\ = 0 \end{array}$$

In (1.9a) the individual intensities from each particle are denoted by the $|A_i|^2$ terms where $N(0)$ and $N(t)$ account for the motions into and out of the scattering volume between time 0 and t . In (1.9b) $N'(t)$ is the number of particles from the original $N(0)$ which remain within the scattering volume after time t ; only the particles that remain can have a correlated phase. The $< >$ brackets refer to an

ensemble average over all the positions the particles may assume within the scattering volume and all the realizations the turbulent medium may assume along the two-way transmission path. Finally (1.9c) expresses all remaining terms which contain factors which involve the initial phase position of the particles. When the ensemble average is taken over the initial phase positions of the particles, the result yields

$$\langle e^{-i\phi_j(0)} \rangle = 0, \text{ for } \phi_j(0) \text{ random} \quad (1.10)$$

As a consequence of (1.10) all terms in (1.9c) are zero.

The exponential which appears in (1.9b) has a complete expression written as

$$\begin{aligned} & \langle \exp i \{ \vec{k}_i \cdot [\vec{r}_i(t) - \vec{r}_i(0)] - \vec{k}_j \cdot [\vec{r}_j(t) - \vec{r}_j(0)] + (\vec{k}_{sj} - \vec{k}_{si}) \cdot \vec{r}_s \\ & \quad - (\vec{k}_{sj} - \vec{k}_{si}) \cdot \vec{r}'_s + [\vec{q}_i(0) - \vec{q}_i(t) - \vec{q}_j(0) + \vec{q}_j(t)] \} \rangle \end{aligned} \quad (1.11)$$

$$+ [\vec{\gamma}_{oi}(0) + \vec{\gamma}_{si}(0) - \vec{\gamma}_{oi}(t) - \vec{\gamma}'_{si}(t) - \vec{\gamma}_{oj}(0) - \vec{\gamma}_{sj}(0) + \vec{\gamma}_{oj}(t) + \vec{\gamma}'_{sj}(t)] \rangle$$

where the terms \vec{k}_i, \vec{k}_j (time dependence not expressed) denote the appropriate scattering vectors for the i and j th particles, respectively, and the $\langle \rangle$ brackets denote the expectation value or ensemble average which can be taken independent of the summation terms over $N'(t)$ in (1.9b). Using (1.2f) only those particles i and j which are within a temporal coherence length Δt denoted as t_c/C , where C is the speed of

light remain correlated over the ensemble average, at time 0 and t so that

$$\langle \exp i\{q_i(0) - q_j(0) - q_i(t) + q_j(t)\} \rangle \approx 1 \quad (1.12)$$

1.2.3 Temporal Intensity Correlation

Function: $R_I(\vec{r}_s, \vec{r}_s, t)_p$

In order to discuss the temporal characteristics of the scattered light arriving at a point on the receiver from particles i and j , and then from a larger collection of particles and molecules, it is assumed that $\vec{r}_s = \vec{r}'_s$ (implies $\vec{k}_s = \vec{k}'_s$ for all i and j), therefore (1.11) becomes (with 1.12 assumed)

$$\begin{aligned} & \langle \exp i\{\vec{k} \cdot [\vec{r}_i(t) - \vec{r}_i(0)] - \vec{k} \cdot [\vec{r}_j(t) - \vec{r}_j(0)] \\ & + [\gamma_{oi}(0) - \gamma_{oj}(0) + \gamma_{si}(0) - \gamma_{sj}(0) - \gamma_{oi}(t) + \gamma_{oj}(t) - \gamma_{si}(t) + \gamma_{sj}(t)] \} \rangle \end{aligned} \quad (1.13)$$

where the ' is dropped in $\gamma'_{si}(t)$ and $\gamma'_{sj}(t)$ since $\vec{r}_s = \vec{r}'_s$, and the subscripts on the \vec{k} 's are dropped, since $\vec{k}_i \approx \vec{k}_j$. It can be shown that for the weak, homogeneous, isotropic turbulence assumed in this paper that $\gamma_{oi}(0) - \gamma_{oj}(0)$ depends only on

$$\frac{|k_o \times [\vec{r}_i(0) - \vec{r}_j(0)]|}{|\vec{k}_o|} = \tilde{\ell}_o$$

where \times denotes cross-product. There exists an $\tilde{\ell}_o$ such that

$$\begin{aligned} \langle e^{i[\bar{\gamma}_{oi}(0) - \gamma_{oj}(0)]} \rangle &= \begin{cases} \approx 1 & \text{for } \tilde{\ell}_o \leq \tilde{\ell}_{tc} \\ \approx 0 & \text{for } \tilde{\ell}_o > \tilde{\ell}_{tc} \end{cases} \end{aligned} \quad (1.14)$$

where $\tilde{\ell}_{tc}$ is defined as the transmitted, turbulent coherence length. This length is nothing more than the point beyond which the difference between the optical paths of the transmitted light arriving at i and j fluctuates randomly between more than say $-\lambda/4$ and $\lambda/4$, thereby causing

$$\langle e^{i[\bar{\gamma}_{oi}(0) - \gamma_{oj}(0)]} \rangle \approx 0$$

as expressed by (1.14). A relation similar to (1.14) exists for $(\gamma_{si}(0) - \gamma_{sj}(0))$ and the associated coherence length ($\tilde{\ell}_{rc}$) will be called the received turbulence coherence length. In addition the terms $[\bar{\gamma}_{oi}(t) - \gamma_{oj}(t)]$ and $[\bar{\gamma}_{si}(t) - \gamma_{sj}(t)]$ have coherence lengths $\tilde{\ell}_{tc}$ and $\tilde{\ell}_{rc}$ associated with them respectively. Therefore all particles i and j which have the appropriate components of relative separation less than $\tilde{\ell}_{tc}$ and $\tilde{\ell}_{rc}$ at time 0 and t will satisfy the condition that all γ terms appearing in the second line of (1.13) vanish. Therefore, using this condition and (1.12) expression (1.9b) becomes

$$\begin{aligned} \langle \sum_{i=1}^{N'(t)} |A_i|^2 \sum_{\substack{j=1 \\ i \neq j}}^{N'(t)} |A_j|^2 \rangle &= \langle \exp i\{\vec{k} \cdot [\vec{r}_i(t) - \vec{r}_i(0)] - \vec{k} \cdot [\vec{r}_j(0) \\ &\quad - \vec{r}_j(t)]\} \rangle \end{aligned} \quad (1.15)$$

where $\langle \rangle$ is separated since the movement of particles i and

j can be evaluated independently of the total number of particles within the scattering volume. Term (1.15) has the stipulation that it includes only those particles i and j whose components of separation are less than the temporal coherence length (t_c/C) , and the transmitted and received, turbulent coherence length $(\tilde{l}_{tc}$ and $\tilde{l}_{rc})$ both at time 0 and t . These three lengths define what can be called a mutual coherence volume, MCV. So only those particles i and j whose components of separation remain less than the dimensions of an MCV at time 0 and t stay correlated during time 0 and t . As a result the scattering volume (V) can be partitioned into V/MCV subvolumes within each of which there are $N''(0) \angle \bar{N}''(0) = (MCV/V) N'(0) \angle$ particles. For each MCV only $N''(t)$ of the original $N''(0)$ remain within the dimensions of an MCV after time t . Therefore (1.15) can be written as

$$\left[\frac{V}{MCV} \right]^2 < \sum_{i=1}^{N''(t)} \sum_{\substack{j=1 \\ i \neq j}}^{N''(t)} |A_i|^2 |A_j|^2 > \quad (1.16)$$

where each summation term in (1.15) is multiplied by the total number of subvolumes (V/MCV) when $N'(t)$ is changed to $N''(t)$.

If ΔZ_i is denoted as the component of $\vec{r}_i(t) - \vec{r}_i(0)$ in the direction \vec{K} and if K is the absolute value of \vec{K} , then the exponential part of (1.15) becomes

$$< \exp i \angle \vec{K} (\Delta Z_i - \Delta Z_j) \angle > \quad (1.17)$$

Assuming the Brownian (B) and the turbulent motion (T) of the particles are independent and if $\Delta Z_i = \Delta Z_i^B + \Delta Z_i^T$, then (1.17) becomes

$$\langle \exp i \sqrt{K} (\Delta Z_i^B - \Delta Z_j^B) \rangle \langle \exp i \sqrt{K} (\Delta Z_i^T - \Delta Z_j^T) \rangle \quad (1.18)$$

The expressions in (1.18) can be calculated by averaging the exponential over all possible displacements i and j . For this purpose a generalized displacement probability function has been developed after Wang and Uhlenbeck (1945), given by

$$G(\Delta Z_i, \Delta Z_j, t) = \frac{1}{\pi \bar{\sigma}_i \bar{\sigma}_j (1 - \bar{\rho}^2)^{\frac{1}{2}}} \exp \left\{ \frac{-1}{(1 - \bar{\rho}^2)} \right. \\ \left. \times \left(\frac{\Delta Z_i^2}{\bar{\sigma}_i^2} + \frac{\Delta Z_j^2}{\bar{\sigma}_j^2} - 2 \bar{\rho} \frac{\Delta Z_i \Delta Z_j}{\bar{\sigma}_i \bar{\sigma}_j} \right) \right\} \quad \text{[cm}^{-2}] \quad (1.19)$$

where $\bar{\sigma}_i^2 = \langle \Delta Z_i^2 \rangle$ and $\bar{\rho} \bar{\sigma}_i \bar{\sigma}_j = \langle \Delta Z_i \Delta Z_j \rangle$.

1.2.3a Brownian Motion. Integrating the product of the first term in the $\langle \rangle$ brackets of (1.18) and expression (1.19) over the limits of an MCV, it can be shown that

$$\langle \exp i \sqrt{K} (\Delta Z_i^B - \Delta Z_j^B) \rangle = \exp \left[-\frac{K^2}{4} (\bar{\sigma}_i^2 + \bar{\sigma}_j^2 - 2 \bar{\rho} \bar{\sigma}_i \bar{\sigma}_j) \right] \quad (1.20)$$

where $\bar{\rho} = \bar{\rho}_B = 0$ since the motion of a Brownian particle is non-correlated at all times with the motion of any other Brownian particle. Further,

$$\overline{\sigma}_i^2 = \frac{4k_B T}{m_i \beta_i^2} \{ \exp(-\beta_i t) + \beta_i t - 1 \}$$

$$\beta_i = \frac{k_B T}{m_i D_i}$$

where k_B is Boltzmann's constant, T is the Kelvin temperature, m_i is the mass of the particles, D_i is the diffusion coefficient of the particle in air (or water or whatever) [cm^2/sec], and t is the time.

1.2.3b Turbulent Motion. The diffusion of particles in a turbulent field has many similarities to Brownian motion. For homogenous, isotropic, and stationary turbulence the probability of displacement distributions is most likely to be Gaussian (Hinze 1959), as expressed by (1.19). However, unlike Brownian motion turbulent motion causes some correlated movement between two separated particles. The assumptions for turbulent motion are exactly the same as presented in the previous section on Brownian motion with a few exceptions. Since all the particles are assumed to move along with the turbulent fluid (air, water, etc.), the displacements are independent of the scatterer size and mass, so that

$$\overline{\sigma}_i = \overline{\sigma}_j = \overline{\sigma}_T \quad (1.21)$$

Hinze (1959) states that for small diffusion times in homogeneous turbulence, the correlation function (\tilde{C}) of

the displacement components of two fluid elements depend on the mean separation, $\langle \Delta r_{ij}(t) \rangle (= \langle |\vec{r}_i(t) - \vec{r}_j(t)| \rangle)$ according to

$$\tilde{C} = \frac{\langle \Delta z_i \Delta z_j \rangle}{\bar{\sigma}_T^2} = \left[\bar{I} - \frac{11}{9} \frac{\bar{A}}{(\overline{u'})^2} (\epsilon \langle \Delta r_{ij}(t) \rangle)^{2/3} \right] \quad (1.22)$$

$$\tilde{C} = 0 \quad \langle \Delta r_{ij}(t) \rangle \gg \Lambda_0$$

where \bar{A} is some absolute constant, $\overline{(u')^2}$ is the mean square fluctuation velocity of the turbulent air, and ϵ is the eddy dissipation, and Λ_0 is the integral scale of turbulence. Batchelor (1959) shows that for particles whose separation is in the inertial subrange

$$\langle \Delta r_{ij}^2(t) \rangle - \Delta r_{ij}^2(0) = C_0 \left(\frac{\epsilon t^3}{\Delta r_{ij}^2(0)} \right)^\beta \Delta r_{ij}^2(0) \quad (1.23)$$

where C_0 is a constant, $\Delta r_{ij}(0)$ is initial separation, β is a power constant. Batchelor found for small t , $\beta = 2/3$ and for intermediate t , $\beta = 1$. For the purposes of this dissertation a simpler relation valid for all time is proposed according to

$$\frac{d}{dt} \langle \Delta r_{ij}^2(t) \rangle = \Gamma \langle \Delta r_{ij}^2(t) \rangle \quad (1.24)$$

where Γ is a constant. Upon integration (1.24) yields

$$\langle \Delta r_{ij}^2(t) \rangle - \Delta r_{ij}^2(0) = (e^{\Gamma t} - 1) \Delta r_{ij}^2(0) \quad (1.25)$$

The characteristics of (1.25) are simpler than and sufficiently analogous to (1.23) and will be used in place of (1.23). An explicit relation similar to (1.25) for $\langle r_{ij}(t) \rangle$ has not been found in the literature. Such a relation must be found in order that (1.22) can be completely defined so that it may eventually be used for $\bar{\rho} = \bar{\rho}_T$ in (1.20). To this end it is assumed that

$$\frac{d}{dt} \langle \Delta r_{ij}(t) \rangle = \Gamma' \langle r_{ij}(t) \rangle \quad (1.26)$$

where Γ' is a constant. Upon integration, (1.26) yields

$$\langle \Delta r_{ij}(t) \rangle - \Delta r_{ij}(0) = (e^{\Gamma' t} - 1) \Delta r_{ij}(0) \quad (1.27)$$

If $\Delta r_{ij}(t)$ is randomly distributed according to the exponential distribution

$$p[\Delta r_{ij}(t)] d[\Delta r_{ij}(t)] = \frac{1}{\langle \Delta r_{ij}(t) \rangle} e^{-\frac{\Delta r_{ij}(t)}{\langle \Delta r_{ij}(t) \rangle}} d[\Delta r_{ij}(t)] \quad (1.28)$$

then from (1.28) it follows that

$$\langle \Delta r_{ij}^2(t) \rangle = 2 \langle \Delta r_{ij}(t) \rangle^2 \quad (1.29)$$

and substitution of (1.29) into (1.24) immediately yields

(1.26) with $\Gamma' = \Gamma/2$. Unfortunately, (1.28) cannot be substantiated. However a relation similar to (1.26) seems physically sound based on (1.23) and (1.24). Therefore, for lack of a better relation, (1.27) will be used.

Equation (1.27) can now be used in (1.22) where (1.22) is slightly modified for the purposes of this dissertation to extend the correlation relation to longer periods of time, so that

$$\begin{aligned}\tilde{C} &= \angle \bar{1} - \left[\frac{\langle \Delta r_{ij}(t) \rangle}{\Lambda_0} \right]^{2/3} &< \Delta r_{ij}(t) \rangle \leq \Lambda_0 \\ \tilde{C} &= 0 &< \Delta r_{ij}(t) \rangle > \Lambda_0\end{aligned}\quad (1.30)$$

where (1.30) must now be averaged over all possible initial separations $\angle \bar{\Delta r}_{ij}(0) \angle$ within the mutual coherence volume. In this connection it is equally probable that $\Delta r_{ij}(0)$ may assume any value. Consequently, the turbulent correlation function, $\bar{\rho}_T$, which is equivalent to $\bar{\rho}$ in (1.19) is

$$\bar{\rho}_T = \langle \tilde{C} \rangle = \frac{\langle \langle \Delta Z_i \Delta Z_j \rangle \rangle}{\sigma_T^2} = \frac{1}{(\text{MCV})} \int_{\text{MCV}} \tilde{C} \, dV(\Delta r_{ij}(0)) \quad (1.31)$$

The solution to (1.31) is quite difficult for odd shaped, mutual coherence volumes. Yet, when (1.31) is integrated for a spherical MCV of diameter D , the result is

$$\bar{\rho}_T = 1 - \frac{9}{11} \left(\frac{D}{\Lambda(t)} \right)^{2/3} \quad \Lambda(t) \geq D \quad (1.32a)$$

$$\bar{\rho}_T = (1 - \frac{9}{11}) (\frac{\Lambda(t)}{D})^3 \quad \Lambda(t) < D \quad (1.32b)$$

where $\Lambda(t) = \Lambda_0 \exp(-\Gamma' t)$. If at time $t = 0$, Λ_0 is $\geq D$ then all particles within the MCV will have some correlation in their initial displacements; the greater Λ_0 is than D the closer the average correlation of the particles in the volume $\langle \bar{\rho}_T \rangle$ approaches 1, as shown by (1.32a). As time progresses the correlation becomes less as the particles mean relative separations $\langle \Delta r_{ij}(t) \rangle$ increase. If $\Lambda_0 < D$ initially, then there are some particles within the MCV which have no correlation in their initial displacements. Therefore, the average correlation of the particles in the MCV is small (1.32b) and decreases rapidly as time increases. The previously defined conditions will hold for any odd shaped MCV; the spherical MCV was chosen for the simplicity of explanation. Finally, the probability distribution of the displacements caused by turbulence is written as

$$G_T(\Delta Z_i, \Delta Z_j, t) = \frac{1}{\pi \bar{\sigma}_T^2 (1 - \bar{\rho}_T^2)^{\frac{1}{2}}} \exp \left\{ \frac{1}{(1 - \bar{\rho}_T^2)^{\frac{1}{2}}} \right. \\ \left. \frac{(\Delta Z_i^2 + \Delta Z_j^2 - 2\bar{\rho}_T \Delta \bar{Z}_i \Delta \bar{Z}_j)}{\bar{\sigma}_T^2} \right\} \langle \bar{cm}^{-2} \rangle \quad (1.33)$$

Integrating the product of the second term in the $\langle \rangle$ brackets of (1.18) and expression (1.33) over an MCV yields

$$\langle \exp \{ iK(\Delta Z_i^T - \Delta Z_j^T) \} \rangle = \exp \langle -K^2/4 (2\bar{\sigma}_T^2 (1 - \bar{\rho}_T)) \rangle \quad (1.34)$$

The complete expression for the phase term (1.17) influenced by Brownian and turbulent motion can now be written as

$$\langle \exp \{ iK(\Delta z_i - \Delta z_j) \} \rangle = \exp \left\{ -\frac{K^2}{4} [\overline{\sigma}_i^2 + \overline{\tau}_j^2 + 2\overline{\sigma}_T^2 (1-\overline{\rho}_T)] \right\} \quad (1.35)$$

Equation (1.35) completes the analysis of the phase term of (1.15)

1.2.4 Analysis of the Number Density Terms of (1.9a) and (1.9b)

The particle number densities are uniformly distributed according to the Junge power distribution within size interval increments over which a mean intensity $\overline{|A^i|^2} = I^i$ is calculated. Let f_i be the fraction of the total number of particles in the i th increment. For a well-mixed, stationary distribution $f_i = v_i/v_p$ where v_i is the total mean number of particles in i th interval and v_p is the total mean number of particles of all sizes within the scattering volume. Finally, let f'_i be the fractional ratio of the original f_i that remains after time t . Such a difference occurs because smaller particles escape from the scattering volume faster than the larger ones, thereby changing the fractional ratio in each size range of the original distribution. From (1.9a), and (1.9b) [using (1.16)] the following can be written

$$(1.9a) = \langle N(0)N(t) \rangle \sum_{i=1}^J \sum_{j=1}^J f_i f_j I^i I^j \quad (1.36)$$

$$(1.9b) = \left[\frac{V}{MCV} \right]^2 \langle \bar{N}'(t) \rangle^2 \left\{ \sum_{i=1}^J \sum_{j=1}^J f_i' f_j' I^i I^j - \sum_{j=1}^J (f_j')^2 (I^j)^2 \right\}$$

where J is the number of size intervals. By employing statistical relationships developed by Chandrasekhar (1943) and after lengthy calculations, it can be shown that

$$\begin{aligned} \langle N(0)N(t) \rangle &= v_p^2 + \langle \bar{I} - \bar{P}(t) \rangle v_p \\ \langle \bar{N}'(t) \rangle^2 &= v_p'^2 \langle \bar{I} - \bar{P}'(t) \rangle^2 + v_p' \langle \bar{I} - \bar{P}'(t) \rangle \end{aligned} \quad (1.37)$$

$$f_i' = f_i \langle \bar{I} - P_i'(t) \rangle$$

where v_p has been defined, v_p' is the mean number of particles of all sizes within a mutual coherence volume, $\bar{P}(t)$ is the mean probability of escape for all sizes of particles from the scattering volume (V), $\bar{P}'(t)$ is the mean probability of escape for all sizes of particles from the mutual coherence volume (MCV) and, finally, $P_i'(t)$ is the mean probability of escape for the i th sized particle from the MCV. Using (1.35), (1.36), and (1.37), the complete temporal, intensity correlation function can be written as (after some manipulation)

$$R_I(\vec{r}_s, \vec{r}_s, t)_p = \{v_p^2 + \langle \bar{I} - \bar{P}(t) \rangle v_p\} A^*(t) + \quad (1.38)$$

$$v_p^2 \langle \bar{I} - \bar{P}'(t) \rangle^2 \{A^*(t) - B^*(t)\} C^*(t)$$

where

$$A^*(t) = \sum_{i=1}^J \sum_{j=1}^J f_i^1 f_j^1 I_i^1 I_j^1$$

$$B^*(t) = \sum_{j=1}^J \langle \bar{f}_j^1 I_j^1 \rangle^2$$

$$C^*(t) = \exp \left\{ -\frac{K^2}{4} \langle \bar{\sigma}_i^2 + \bar{\tau}_j^2 + 2\sigma_T^2 (1 - \bar{\rho}_T) \rangle \right\}$$

A relation similar to (1.38) can be developed (see Appendix C) for the molecules and is given by

$$R_I(\vec{r}_s, \vec{r}_s, t)_m = \bar{I} \{v_m^2 + \bar{\sigma}_m^2 \langle \bar{I} - \bar{P}'(t) \rangle^2\} C_m^*(t) \quad (1.39)$$

$$C_m^*(t) = \exp \left\{ -\frac{K^2}{2} \langle \bar{\sigma}_m^2 + \bar{\sigma}_T^2 (1 - \bar{\rho}_T) \rangle \right\}$$

where \bar{I} is the intensity per molecule, v_m is the mean number of molecules in the scattering volume V , $\bar{P}'(t)$ is the mean probability of escape of a molecule from an MCV, $\bar{\sigma}_m^2$ is the mean square displacement for molecules in Brownian motion. The other terms have the same meanings as for (1.38). Finally, terms for $R_E(\vec{r}_s, \vec{r}_s, t)_p$ and $R_E(\vec{r}_s, \vec{r}_s, t)_m$ can be found along lines similar to (1.38) and (1.39); the respective relations are (see Appendix C).

$$R_E(\vec{r}_s, \vec{r}_s, t)_p = v_p [\bar{I} - \bar{P}'(t)] \sum_{j=1}^J f_j^i I_j^j \exp\{-\frac{K^2}{4} [\bar{\sigma}_j^2 + \bar{\sigma}_T^2]\} \quad (1.40)$$

$$R_E(\vec{r}_s, \vec{r}_s, t)_m = \bar{I} \{v_m [\bar{I} - P'(t)] \exp\{-\frac{K^2}{4} [\bar{\sigma}_m^2 + \bar{\sigma}_T^2]\} \} \quad (1.41)$$

Expressions (1.38), (1.39), (1.40), and (1.41) can be substituted into (1.6) $[\vec{r}_s = \vec{r}_s']$ from which the first two moments of the intensity distribution can be found so that

$$\lim_{t \rightarrow 0} R_I(\vec{r}_s, \vec{r}_s, t) = \langle I^2 \rangle = 2(\langle I_p \rangle + \langle I_m \rangle)^2 \quad (1.42)$$

$$\lim_{t \rightarrow \infty} R_I(\vec{r}_s, \vec{r}_s, t) = \langle I \rangle^2 = (\langle I_p \rangle + \langle I_m \rangle)^2 \quad (1.43)$$

where (1.43) and (1.44) have utilized

$$\lim_{t \rightarrow 0} \{\bar{\sigma}_i^2, \bar{\sigma}_T^2, \bar{\sigma}_m^2\} = 0, \quad \lim_{t \rightarrow 0} \{\bar{P}(t), \bar{P}'(t), P_i'(t), P'(t)\} = 0$$

$$\text{and } \lim_{t \rightarrow \infty} \{\bar{\sigma}_i^2, \bar{\sigma}_T^2, \bar{\sigma}_m^2\} = \infty, \quad \lim_{t \rightarrow \infty} \{\bar{P}(t), \bar{P}'(t), P_i'(t), P'(t)\} = 1$$

$$\text{in addition } \langle I_p \rangle = \sum_{j=1}^J v_j I_p^j; \quad \langle I_m \rangle = v_m \bar{I}_m$$

The results expressed by (1.42) and (1.43) are exactly the same results which are obtained for the first two statistical moments of Rayleigh (exponential) distributed light for which the mean intensity is the sum of the individual intensities from each scatterer. Although (1.42) and (1.43) do not prove the scattered light intensity is Rayleigh distributed, the results do not contradict this conclusion.

In this connection, the so-called Rayleigh distribution of the intensity is given by

$$P(I) dI = \frac{1}{\langle I \rangle} \exp \left(-\frac{I}{\langle I \rangle} \right) dI \quad (1.44)$$

where $\langle I \rangle$ is given by (1.43) and $p(I)$ is the probability density of the intensity.

1.2.5 Spatial Intensity Correlation

Function: $R_I(\vec{r}_s, \vec{r}'_s, 0)_p$

In order to examine the spatial characteristics of the light arriving at the receiver from particles i and j , and then from a larger collection of particles and molecules, equation (1.8) has been set with $t=0$ so that $R_I(\vec{r}_s, \vec{r}'_s, 0)_p$ contains information only about the spatial variations of I as caused by spatial variations in the phase of the scattered light. With this in mind equation (1.11) becomes

$$\begin{aligned} & \langle \exp i \{ \angle (\vec{k}_{sj} - \vec{k}_{si}) \cdot \vec{r}_s - (\vec{k}'_{sj} - \vec{k}'_{si}) \cdot \vec{r}'_s \\ & \quad + \angle \bar{q}_i(0) - q_i(0) - q_j(0) + q_j(0) \} \\ & \quad + \angle \bar{\gamma}_{si}(0) - \gamma'_{si}(0) - \gamma_{sj}(0) + \gamma'_{sj}(0) \} \rangle \end{aligned} \quad (1.45)$$

where the meaning and analysis of the q term in (1.45) are the same as before, and the γ 's are the phase perturbations induced by the turbulence as the light travels from the i th and j th scatterers to position \vec{r}_s and \vec{r}'_s (for the light paths to \vec{r}'_s a prime superscript appears on the γ 's). Evaluating

the vector terms in the first line of (1.45) yields

$$\langle \exp i\left\{\frac{2\pi}{\lambda} (r_i - r_j) - \frac{2\pi}{\lambda} (r'_i - r'_j) + \text{rest of (1.45)}\right\} \rangle \quad (1.46)$$

where the r 's in (1.46) are the straight line distances from the scatterers to the points on the receiver in question. The condition required of the phase term in the exponential of (1.46) is that, for any pair of particles and any two points on the receiver, when the phase term is less than $\pi/8$, the intensity on the receiver between those two points is essentially uniform. For the case in which the incident light is temporarily coherent over the scattering volume, the q terms in (1.46) can be eliminated. Finally, for the weak turbulence considered the γ terms are negligible compared to changes in the r 's. From these assumptions it can be shown from (1.46) that the separation of the two points on the receiver, denoted by d , defines a circular area ($\pi d^2/4$) within which the received intensity is essentially uniform according to (see 2.7.1b)

$$r_{ij}^{\perp} = \frac{\lambda R^2}{8d^2} \quad (1.47)$$

where λ is the wavelength of the light, R is the distance from the scattering volume to receiver and r_{ij}^{\perp} is the separation component of the particles i and j perpendicular to the

direction of the scattered light. Therefore, if r_{ij}^{\perp} is set equal to the largest dimension of the scattering volume's cross-section in the plane of the receiver surface, then all the particles within the scattering volume will form a spot of almost uniform intensity on the receiver surface of diameter d . This spot is commonly called a coherence area. A receiver may subtend many coherence areas each having a different mean intensity due to the changed phase orientation of the scatterers relative to each coherence area. It is assumed that, due to the unpredictability of determining the phase relationships among the large number of randomly positioned scatterers over each coherence area, the distribution of intensity with time (see 1.44) and space are analogous.

The spatial distribution of intensity is important because of the typically large receivers needed to collect sufficient light for measurement via a photo-electric current. This introduces the next point; the measurement of intensity.

1.2.6 Current Correlation Function

Most generally the light is received by a large collector and focused to a photo-tube which puts out a current characteristic of the collected intensity plus the photo-tube's own noise characteristics (shot-noise is its primary source). It can be shown that the correlation function for the photocurrent $\overline{R}_i(t) \equiv \langle i(0)i(t) \rangle$ where $i(0)$ is the photocurrent at time 0 which has been filtered through a RC

circuit to reduce shot-noise (see Appendix D) is given by

$$R_i(t)_f = \langle i(0)i(t) \rangle_f = (M^2 - M) \langle i' \rangle^2 + MR_i'(t)_f \quad (1.48)$$

where

$$R_i'(t)_f = \frac{\mu e}{4(RC)_f} (\alpha \mu e \langle F' \rangle) e^{-t/(RC)_f} + (\alpha \mu e)^2 R_F'(t)$$

where subscript f denotes the filtered value, M is the number of coherence areas on the collector's surface, $\langle i' \rangle$ is the mean photocurrent from one coherence area, $R_i'(t)_f$ is the filtered current correlation function from one coherence area, μ is the gain factor of the photomultiplier tube, e is the magnitude of the electronic charge, $(RC)_f$ is the time constant of the filter, α is the electron conversion efficiency of the photo cathode (electron/joules), $\langle F' \rangle$ is the mean flux of the scattered light collected by one coherence area, while $R_F'(t)$ is the flux correlation function, written as

$$R_F'(t) = \langle F'(0) F'(t) \rangle \quad (1.49)$$

where $F'(0)$ and $F'(t)$ are the fluxes of the scattered light collected by one coherence area at time 0 and t , respectively. Both $\langle F' \rangle$ and $R_F'(t)$ are related to the scattered intensity by the following relations:

$$\langle F' \rangle = \iint_{\text{coherence area}} \langle I \rangle dA_R d\omega_s \quad [\text{watts}] \quad (1.50)$$

$$R_F'(t) = \iiint\limits_{\substack{\text{coherence} \\ \text{area}}} R_I(\vec{r}_s, \vec{r}_s', t) dA_R d\omega_s dA_R' d\omega_s' \text{ [watts]}^2$$

where dA_R and dA_R' are elements of a coherence area on the receiver surface and $d\omega_s$ and $d\omega_s'$ are elements of solid angle subtended by an element of the scattering volume at the receiver. Using (1.48), (1.49), and (1.50) it can be shown, similar to (1.42) and (1.43), that

$$\lim_{t \rightarrow 0} R_i(t) = \langle i^2 \rangle = (M^2 + M) \langle i' \rangle^2 + M \langle i' \rangle \frac{\mu e}{4(RC)_f} \quad (1.51)$$

$$\lim_{t \rightarrow \infty} R_i(t) = \langle i \rangle^2 = M^2 \langle i' \rangle^2$$

where the f subscript is dropped in some cases. Finally (1.51) yields the expressions

$$\langle i \rangle = \mu q \langle F \rangle$$

$$\sigma_i^2 = \langle i^2 \rangle - \langle i \rangle^2 = \underbrace{\frac{\mu e}{4(RC)_f} \langle i \rangle}_{\sigma_n^2} + \underbrace{\frac{\langle i \rangle^2}{M}}_{\sigma_s^2} \quad (1.52)$$

where $q = \alpha e \text{ [amperes/watt]}$, $\langle F \rangle = M \langle F' \rangle$ is the mean flux over the whole collector. The term denoted by σ_n^2 is the variance due to shot noise, and σ_s^2 is the variance due to fluctuations in the intensity of the scattered light. A general probability distribution for the photocurrent $\bar{p}(i)$

di see (1.44) has been developed (see 2.10.4) but is not presented here. However, for M large, the photocurrent becomes normally distributed with mean and variance given according to (1.52).

This then completes the calculation of the statistical properties of the scattered (laser) light from a continuous beam (laser). It should be noted that the calculations to this point have been sufficiently general to apply to any light scattering system. To this end and as an independent check on the work, the equations are evaluated for a typical radar system and the theoretical results discussed in light of actual reported measurements. A final example will be the application of the equations to a pulsed lidar system.

1.2.7 Results

1.2.7a Radar. Marshall et al. (1953) have shown by theory and experiment that the returned signal fluctuations from a collection of randomly moving scatterers are Rayleigh distributed when the receiver noise is below the signal noise from the scatterers ($\sigma_n^2 \ll \sigma_s^2$). For the typical radar system (Battan 1959) (see 3.3) the half-angle divergence of the receiver-transmitter antenna, θ_T , is related to the diameter of the receiver-transmitter antenna (d') and radar wavelength, λ , by

$$\theta_T = \frac{(0.85)\lambda}{2d'} \quad (1.53)$$

Employing (1.53) into (1.47) it can be shown that M (see 1.48) is close to 1.0. This implies that the received, radar energy is almost completely spatially coherent over the whole antenna so that the displayed signal, converted from the received energy, exactly follows the received energy fluctuation. The latter would be according to (1.44) which is the Rayleigh distribution which was found in actual measurements according to Marshall et al. (1953).

1.2.7b Pulsed, Bistatic System. The intensity correlation function for a pulse of light is somewhat different than the continuous bistatic system (see 1.8). The primary difference is the temporal correlation among the scatterers illuminated by the pulse of light at different times. In particular if the pulse length $\ell_p = ct_p$ (c is the speed of light), then for times $0 \leq t \leq t_p$ the pulse at time 0 and t have part of their volumes common, yet for $t > t_p$ the pulse at time 0 and t illuminates completely independent scatterers. The correlation function for the scatterers in the common volume will be exactly similar to that of the continuous case $\langle \bar{R}_I(\vec{r}_s, \vec{r}'_s, t) \rangle$, while the independent portions of the two pulses are equivalent to two independent samples of the continuous case $\langle \bar{R}_I(\vec{r}_s, \vec{r}'_s, \infty) \rangle$. Using these considerations the intensity correlation function for the pulsed system $\langle \bar{R}_I^P(\vec{r}_s, \vec{r}'_s, t) \rangle$ can be written (see 2.6.1) as

$$R_I^P(\vec{r}_s, \vec{r}'_s, t) = \{ \langle \bar{R}_I(\vec{r}_s, \vec{r}'_s, t) \rangle - R_I(\vec{r}_s, \vec{r}'_s, \infty) \}$$

$$\left(\frac{t_p - t}{t_p}\right) \} s(t) + R_I(\vec{r}_S, \vec{r}'_S, t) \quad (1.54)$$

where $s(t) = 1; 0 \leq t \leq t_p$
 $0; t > t_p$

It is easily shown that the statistical moments of intensity for the pulsed system are exactly the same as those for the continuous system.

A bistatic pulsed lidar system typical of those being used for studies of atmospheric aerosols is currently in operation at The University of Arizona. The most important result that the work in this paper reveals about the photocurrent fluctuations in this system is that they are shot noise limited (in contrast to the radar which is scatterer noise limited). The large light collector (collector radius = 15 cm) and small wavelength ($\lambda = 6943 \text{ \AA}$) both combine (see 1.47) to yield a very large number of coherence areas (M) for typical scattering volume-receiver geometries. M is so large, in fact, that the σ_s^2 term in (1.52) is at least two orders of magnitude below σ_n^2 . Further, because of this large spatial averaging of the light signal the probability distribution function of the photocurrent $\overline{p(i)di}$ is normally distributed according to

$$p(i)di = \frac{1}{\sqrt{2\pi}\sigma_i} \exp - \left[\frac{(i - \langle i \rangle)^2}{2\sigma_i^2} \right] di \quad (1.55)$$

where $\langle i \rangle$ and σ_i are given by (1.52) with $\sigma_s^2 = 0$.

Using (1.55) it can be shown that in order to obtain accurate estimates of $\langle i \rangle$ the signal from the pulsed system must be integrated in space and time over many independent values of i (the estimate of $\langle i \rangle$ from the integrated signal is improved by the square root of the number of independent values of i). These integration procedures are being used at the University of Arizona laser facility and, at least in principle, accurate estimates to within $\pm 1\%$ of $\langle i \rangle$ are routinely obtainable (see Chapter 3).

1.2.8 Attenuation Fluctuations

Equation (1.2d) represents the attenuation of the light from the source to receiver due to scattering and absorption (absorption is neglected in this work) along the light path. By calculating the volume of space through which the light beam passes, the number of scatterers which participate in the attenuation can be calculated. Employing relations for number density fluctuations of particles in a volume of space (Chandrasekhar 1943), expressions can be developed for the attenuation fluctuations in received intensity caused by Brownian and turbulent motion; similar relations can be developed for the molecules. It can be shown that these fluctuations can be neglected for lidar systems typical of the University of Arizona system

mentioned in Sec. 1.2.7. However, each system must be evaluated under its own particular operating conditions (see Appendix E).

1.2.9 Power Spectrum

Recent technical developments in lidar systems have allowed the detection of the frequency shifts in the scattered light due to the motion of scatterers. In addition to the raw, statistical characteristics of the fluctuations expressed by the correlation functions developed in this work, the correlation functions also contain Doppler shift and phase fluctuation information. A spectral analysis of the photocurrent correlation function is a means by which the frequency and phase information can be obtained. The complex photocurrent correlation function developed in this paper is particularly valuable because it includes a number of physical processes heretofore neglected. A brief summary includes number density fluctuations, Brownian and turbulent motion of scatterers, and the phase perturbations introduced by turbulent refractive inhomogeneities. The influence of these processes can be assessed by evaluating a power spectrum by means of the Fourier transform of the photocurrent correlation function.

1.2.10 Conclusions

An attempt has been made to analyze the fluctuations of scattered light by correlation functions. A generalized

relation has been developed which includes the effects of number density fluctuations of scatterers, Brownian and turbulent motion of scatterers, and phase perturbations introduced by refractive inhomogeneities. Particularly detailed work is presented for the turbulent motion of scatterers. The confidence of the results is shown by using radar as an example. Finally, the results are applied to a pulsed bistatic laser system. They show that systems similar to the University of Arizona bistatic laser system are shot noise dominated. Furthermore, the signal must be integrated to average out the noise in order to use the laser for accurate atmospheric probing. An additional value of the correlation functions developed in this work is that they immediately yield the power spectrum of the fluctuations.

CHAPTER 2

THE CAUSES OF THE FLUCTUATIONS OF SCATTERED LASER LIGHT

In general the fluctuations of scattered laser light from a collection of scatterers depend upon the temporal changes of the positions and number of the scatterers. The motion of the scatterers changes the relative phases of the components of the scattered light and, at the same time, varies the total concentration of the scatterers contributing to the scattered light at any one time. When the volume of space which contains the scatterers is distant from both the source of illuminating light and the receiver, the fluctuations of the scattered light which reach the receiver are not simply related to the scatterers within the distant scattering volume. The scattering medium along the source to receiver path modifies the fluctuations as well.

The purpose of this chapter is to describe and calculate the combined effects of all the important atmospheric scatterers and their influence on the fluctuations of the light which reaches the receiver. The first part of this chapter specifies the optical properties of the scatters and, concurrently, the types of motion the scatterers demonstrate. The concepts of temporal and spatial coherence are then

presented as a means to analyze the phase structure of the transmitted and scattered light in a semi-quantitative way. This information is the basis for a detailed development of the effects of the scatterers on the phase and amplitude structure of the light within three separate regions of the source to receiver path. Finally, a calculation of the method by which the received light from the atmospheric scatterers is converted to a measurable current is presented.

2.1 Optical Properties of Atmospheric Scatterers

2.1.1 Molecules

Simple electromagnetic scattering from objects in which the size of the scattering center is much smaller than the wavelength of the scattered light is called Rayleigh scattering. Each molecule which composes the earth's atmosphere satisfies the Rayleigh condition when illuminated by light in the visible region (the ruby laser emits radiation at 6943\AA).

The total scattered light field from a molecular medium is the sum of the singly and multiply scattered light fields from each molecule (with due regard for phase and amplitude). The singly scattered light is scattered out of the illuminating light field, while the multiply scattered light comes from the rescattering of the singly scattered light. In the earth's atmosphere there are about 10^6

molecules within a volume of λ^3 (where λ is the wavelength of visible light). Even under such high densities the amount of light singly scattered from each molecule is so small that multiple scattering is negligible. Therefore, the total scattered light field is simply the sum of the singly scattered light fields from each illuminated molecule. One way of summing the singly scattered fields is to group the molecular fields into regions of approximately constant phase. For example, all the molecules within a volume of $(\lambda/4)^3$ scatter the light with approximately constant phase. At the same time there exists a second, similar volume a certain distance away from the first whose molecules scatter light with a phase 180 degrees out of step with respect to the molecules of the first volume. If the number of molecules within these two volumes is equal, then the total resultant light field would be nearly zero. This last result implies that if the molecular medium is uniformly dense, then there is no resultant scattered field except in the forward direction of the illuminating light field. Nevertheless in the real atmosphere light is scattered in all directions from the molecular medium and must arise from the variations of the molecular density. In this connection a clear distinction between the individual scattered field from each molecule and the resultant scattered field from a group of molecules should be kept in mind. The individual scattered

fields always exist (when the molecules are illuminated), while the resultant field from a group may not. Finally, scattering from density variations is easier to visualize than the individual contributions to the resultant scattered field.

A graphical representation of the scales of molecular number density fluctuations helps to visualize the scattering problem. Along the direction which a light beam travels the molecular number density (at one instant of time), $N(r)$, within a volume $(\lambda/4)^3$ about the point r would appear similar to Fig. 2.1.

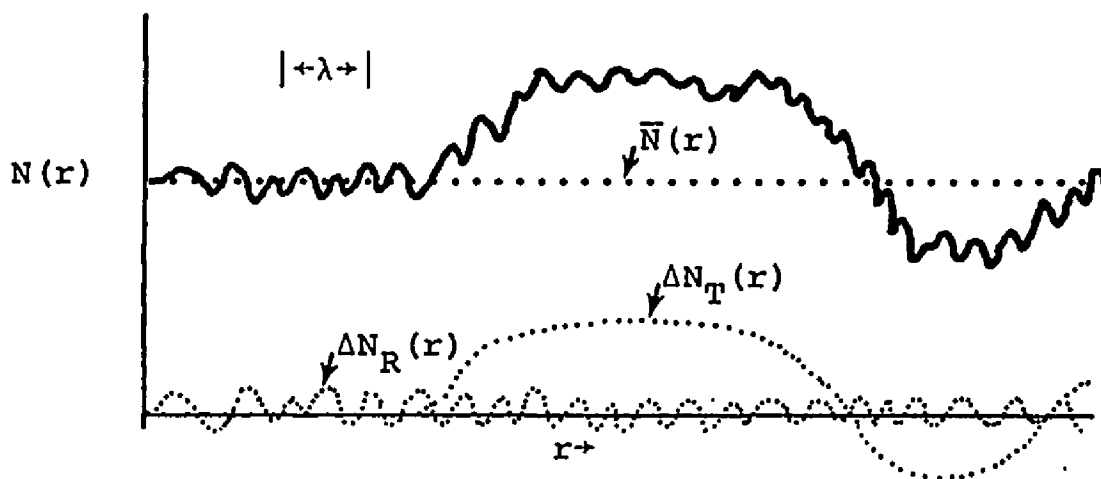


Fig. 2.1 The Number Density of Molecules, $N(r)$ (Solid Curve), and its Component Parts (Dotted Curves) Along the Path of the Light Beam.

The term $N(r)$ can be expressed as a sum of the component parts such that $N(r) = \bar{N}(r) + \Delta N_R(r) + \Delta N_T(r)$ (these terms are defined shortly). An expression for the resultant scattered field is found by multiplying $N(r)$ by the scattering phase-amplitude term $Ae^{i|\vec{k}| \cdot (\vec{r} - \vec{r}')} |$ (A is the scattering

amplitude, $|\vec{k}| = 2\pi/\lambda$, and $|\vec{r}-\vec{r}'|$ is the distance from the scattering event to the point where the resultant field is calculated, namely the receiver) for each molecule and finally summing over all r . The resultant scattered field can be discussed in terms of the components of $N(r)$. The $\bar{N}(r)$ term (mean number density) yields a component to the resultant scattered field only in the forward direction. This is caused by the phase terms canceling in all directions except the forward. Scattering of this type is commonly called dependent scattering. The $\Delta N_R(r)$ term yields a resultant field component (called the Rayleigh component) which appears in all directions. The Rayleigh component is attributed to the random number density fluctuations on a size scale $\leq \lambda$. Scattering of this type is commonly called independent scattering. Under these conditions the resultant field has a complicated pattern at any one time. Yet, an average performed over all the statistical realizations of $\Delta N_R(r)$ yields the well-known result that the average Rayleigh field component is $\propto (\bar{N}(r))^{1/2} A$. The $\Delta N_T(r)$ term yields a resultant field (called the turbulence component) whose characteristics are similar to both the $\bar{N}(r)$ and $\Delta N_R(r)$ field components. The reason is that $\Delta N_T(r)$ is correlated over scales of distance $> \lambda$, thus yielding partial dependency effects in the resultant field. The result is a negligible resultant field except near the forward direction. Further, as the distance scale becomes $\gg \lambda$, the results approach those for $\bar{N}(r)$.

In actuality there can be many causes of large scale (with respect to λ) density fluctuations. For example, the so-called Brillouin component to the scattered field can arise from density variations caused by sound waves. However, in this dissertation turbulence is considered the only cause of the large scale fluctuations. Finally, the detailed properties of the Rayleigh field component are thoroughly developed in Appendix B, while the properties of the turbulence component are discussed further in section 2.1.3.

The turbulence and Rayleigh components of the scattered light must be specially treated. It has been stated that the turbulence component appears almost entirely in the forward direction, while the Rayleigh component appears in all directions. Therefore, the energy of the laser beam, as it propagates through the medium, is essentially just redistributed within the beam by the turbulence component, while the Rayleigh component scatters the light permanently out of the beam (neglecting multiple scattering). For this reason the molecular attenuation is associated primarily with the Rayleigh component. In this connection, the molecular optical depth, which will be presently shown to be a measure of the molecular attenuation, is also associated with the Rayleigh component alone.

2.1.2 Particulates

The size range, number density, index of refraction and shape of particulate matter are extremely variable. The sensitivity of present laser-receiver systems is not sufficient to differentiate variations in some of the particulate properties. However, the laser, when used in conjunction with other direct measurement devices, can yield a great deal of useful information about particulate matter. Since this dissertation is concerned with the scattered light fluctuations caused in part by the particulate matter, it is sufficient to specify typical properties of the particulates as known and proceed to calculate the resultant scattered light fluctuations. To this end, the following paragraphs specify the properties of the particulates which are used throughout the rest of this dissertation.

The number of particulates per unit volume of size a and at position vector \vec{r} in space can be represented by $n(a, \vec{r})$. Since for the purposes of this dissertation a single model is sufficient to represent typical atmospheric particulate properties, a considerable simplification of $n(a, \vec{r})$ can be made. The first simplification is the assumption of uniformity of the size distribution (a) over all space (\vec{r}) so that $n(a, \vec{r})$ can be written in a separable form given by

$$n(a, \vec{r}) = N(a)N'(\vec{r}) \quad (2.1)$$

where $N(a)$ is the number of particulates per cm^3 at radius a

and $N'(\vec{r})$ is a multiplier (no units) adjusted to give the actual number density at position \vec{r} .

With regard to $N(a)$ Junge (1963) found the typical size range of radii of the atmospheric particulates extends from 10^{-2} μm to 10 μm ($\mu\text{m} = 10^{-6}$ meters). The actual values of $N(a)$ in the atmosphere are quite variable, but Junge has developed a mathematical number density distribution which on the average fits many independent observations of number density vs. size. This size distribution is given according to a power law and is expressed as

$$\frac{dN(a)}{da} = ca^{-(v^*+1)} \text{ [number/cm}^3 \text{ - size interval]} \quad (2.2)$$

where $N(a)$ is the number of particles per cm^3 of radius a , while c is a constant adjusted so that the integral of (2.2) yields the appropriate number density over a given size interval for a normalized distribution. For example, when c equals 3×10^{15} , there exists 1 particle per cm^3 in the size range $0.1 \leq a \leq 1.0\mu$ with a value of $v^* = 3.0$. The term v^* is a shape factor which typically ranges from 2.0 to 4.0; the value of $v^* = 3.0$ is chosen as an average. Finally, the assumption that $N(a)$ assumes the same form at all points in the typical atmosphere (away from sources and sinks) has not been proven, but for modeling purposes the assumption is convenient.

The second simplification of $n(a, \vec{r})$ is the assumption of particulate horizontal homogeneity. This assumption leads to the replacement of $N'(\vec{r})$ in (2.1) by $N'(z)$ where z is the position above the ground. Certainly many instances can be found in which this assumption is incorrect especially, for example, near sources and sinks of particulates. Yet the atmosphere tends to be horizontally homogeneous in many respects (wind and temperature field). For this reason the particulate density (far removed from sources and sinks) tends to be horizontally homogeneous. This is only a weak qualification for the expected horizontal homogeneity of the particulates. Nevertheless, experimental evidence has lead Elterman (1964) to calculate an average vertical distribution which adequately suits the purposes of this dissertation. This distribution, the so-called Air Force "clear atmosphere" model, is given as

$$N'(z) = N_0 \exp \left[(-0.8 \text{ km}^{-1}) z \right] \quad (2.3)$$

The term N_0 is a constant which can be adjusted to fit the total particulate optical depth, $\tau^P(0, \infty)$, as described in the following paragraphs.

Standard text books show that a monochromatic beam of radiation, $I_\lambda(\vec{r})$, at position \vec{r} is attenuated to $I_\lambda(\vec{r}) + dI_\lambda(\vec{r})$ after traveling a distance ds in the direction of $I_\lambda(\vec{r})$ according to

$$dI_{\lambda}(\vec{r}) = -[n(a, \vec{r}) Q_{t\lambda}^p(a) I_{\lambda}(\vec{r}) ds \quad (2.4)$$

where $Q_{t\lambda}^p(a) (\text{cm}^2)$ is the attenuation cross-section of each particle of size a at wavelength λ . Dropping the λ subscripts (for essentially monochromatic laser light) and using the separable form of $n(a, \vec{r})$, the particle size dependent terms in (2.4) are replaced with the relation

$$\gamma_p \beta_t = \int_{0.01 \mu\text{m}}^{10.0 \mu\text{m}} Q_t^p(a) dN(a) [\text{cm}^{-1}] = \int_a N(a) Q_{t\lambda}^p(a) \quad (2.5)$$

where $\gamma_p \beta_t$ is called the normalized volume attenuation coefficient and $dN(a)$ comes from (2.2). Using (2.5) and limiting (2.4) to a beam of radiation traveling in the vertical direction ($\vec{r} \rightarrow z$ and $ds \rightarrow dz$) yields

$$dI(z) = \gamma_p \beta_t N'(z) I(z) dz \quad (2.6)$$

From (2.6) a general definition of the particulate optical depth, $\tau^p(z_1, z_2)$, between any two levels z_1 and z_2 is given by

$$\tau^p(z_1, z_2) = \int_{z_1}^{z_2} N'(z) \gamma_p \beta_t dz \quad (2.7)$$

When z_1 is at ground level and z_2 is sufficiently high to include all of the particles [denoted by $z_2 = \infty$], (2.7) yields the total particulate optical depth, $\tau^p(0, \infty)$.

Using (2.3) and (2.7), it is easily shown that 99% of the light attenuation by the particles occurs within the first 5 kilometers ($z_1 = 0$; $z_2 = 5$ km). For this reason numerical calculations of scattered laser light which appear in Chapter 3 are not carried beyond 5 km; the region of interest is within the first 5 km. Furthermore, $\tau^P(0, \infty)$ can be set equal to $\tau^P(0, 5 \text{ km})$ with a high degree of accuracy and the term $\tau^P(0, \infty)$ can be inferred by independent measurements. For example, the directly transmitted solar flux which reaches the earth's surface depends on the total optical depth which, in turn, is just the sum of the particulate and molecular (Rayleigh component) optical depths in cloud free areas. The molecular optical depth, as a function of wavelength, is known and can be subtracted from the measured total optical depth, thereby yielding a reliable measurement of the particulate optical depth. This value can be used on the left hand side of (2.7) to scale the unknown N_0 which appears in $N'(z)$ (see 2.3). Therefore, the simplification previously discussed allows the attenuation properties of the particulates to be completely specified by $\tau^P(0, \infty) \underline{\underline{=}} \tau^P(0, 5 \text{ km})$ and v^* , the shape factor of the size distribution. The term $Q_t^P(a)$ is calculated for each size particle and depends on a number of other parameters yet to be discussed.

The attenuation properties of the molecules can be similarly defined as is done for the particles in the previous

paragraphs. In fact, molecular attenuation is much simpler for a number of reasons. In particular, the size of the molecules is much less than the wavelength of the light (allowing the Rayleigh condition to be used) and the density distribution depends only on the atmospheric density, $\rho(z)$, whose variation with z for the purposes of this dissertation can be well approximated by an isothermal atmosphere. Therefore, relations similar to (2.1) through (2.7) exist for molecules. In addition, molecular optical depths $\tau^m(z_1, z_2)$ and $\tau^m(0, \infty)$ have meanings and are used in Chapter 3.

In connection with (2.6) one final comment is in order. The relation (2.6) can be integrated along with (2.7) to yield

$$I(z_2) = I(z_1) e^{-\tau(z_1, z_2)} \quad (2.8)$$

where the superscript to $\tau(z_1, z_2)$ is dropped for generalizations to both molecules and particulates. From (2.8) it is easily seen that the fraction of the intensity transmitted from z_1 to z_2 is just $e^{-\tau(z_1, z_2)}$. This exponential term is commonly called the transmittance and is represented by the term $T(z_1, z_2)$. It will be recalled that variations in the light transmitted through a scattering medium is one of the three causes of light fluctuations mentioned in Chapter 1. An analysis of the fluctuations in $T(z_1, z_2)$ is performed in Appendix E for use later in this chapter.

The scattering properties of the particulates strongly depend on their index of refraction. The complete index of refraction of the particulates contains a real part, n , and an imaginary part, k . The real part is related to the dielectric constant of the particulate matter, while the complex part is related to the particulates' light absorptive properties. The index of refraction of particulate matter is discussed in a paper by Quenzel (1969). He produces considerable evidence that variations in n and k for spherical particulates cause significant differences in their scattering properties. This variability creates a great deal of uncertainty in the analysis of the scattered light from particulates. Yet, evidence indicates that a large percentage of the natural particulates are composed of silicates, ammonium sulfate, and sodium chloride (Junge 1963). Fortunately, these substances have a real index (n) near 1.5 in the visible; silicate quartz, for example, has $n = 1.54$ at the wavelength of the ruby laser ($\lambda = 6943\text{\AA}$). On the other hand the absorptive properties of the particles are difficult to specify (Eiden 1966, Fischer 1973). Furthermore, inclusion of these properties is not critical to the results of this dissertation. For the purpose of this dissertation, therefore, it is sufficient to consider the particulates as a non-absorbing ($k = 0$), silicate dust.

As if the uncertainties of the refractive index are not enough, the shape of the particulates causes an even

greater problem. Holland and Draper (1967) performed light scattering experiments with non-spherical, talc platelets. They concluded from these experiments that a collection of non-spherical, randomly oriented particles has scattering properties remarkably similar to an equivalent sized system of spherical particles. This conclusion is what everyone in scattering theory was silently hoping for. Then, new evidence by Holland and Gagne (1970) showed the shape of the particle has a critical influence on the scattering of light, not only from a single particle (as has been known for a long time), but also from a collection of randomly oriented particles of different sizes. Therefore, the simplifying assumption that light scattering from atmospheric particulates can be described by an equivalent distribution of spheres is questionable at best. Nevertheless, valuable inferences about the fluctuations in the scattered light can be made with the assumption of spherical particulates. Therefore, this dissertation uses the results for the spherical scatterer in lieu of a more viable alternative.

Hence, further discussions of particulate matter will assume that the number density vs. size (2.2), distribution with height (2.3), index of refraction ($n = 1.54$, $k = 0$), and the scattering phase functions (Mie 1908), spherical are known.

Recalling that fluctuations in the scattered light are ultimately a result of the motions of the scatterers, a

discussion of the relative motions of the scatterers is in order.

The simplest scale of atmospheric motion which influences the positions of the particulate matter is Brownian motion. This motion results from the fluctuations of molecular impaction on the surface of the particle. The molecular impaction is correlated over a distance very much smaller than the intra-particle separation; hence, the Brownian motion of each particle is independent. Yet, even though the motion is independent, the relative phases of the scattered light from the particles demonstrates dependency, if only for a very short time. Indeed, a finite amount of time is required for the particles to reshuffle themselves to new phase positions. Recall from Chapter 1 that during this reshuffle time two values of the relative phase components of the scattered light intensity are dependent, while after the reshuffle time the two phase components are independent. The difference between independence of motion of the particles and independence of the phase of the scattered light must be kept in mind. Further, the transition from dependence to independence in the relative phase is generally a smooth transition. Therefore, the point of transition from dependence to independence is a matter of choice. For example, the intensity correlation function of the scattered light from the particulates and the molecules, calculated in Appendix C, shows a critical dependence on the relative phases of the

scatterers. This dependence takes the form of an exponential time delay. When the delay time is sufficiently long so that the phase dependence reduces to 36.7% $[\exp(-1)]$ of its original value, independence is said to occur! These facts are important in the later development of the statistical theory of the fluctuations of the scattered laser light.

The next scale of motion that influences the particulate scatterers is turbulence. The principal concern is how the particle behaves by itself and among a collection of neighboring particles in a turbulent field. The turbulent motion of an individual particle depends on the inertial response to its turbulent fluid matrix. Hinze (1959) discusses the motion of a discrete particle in a homogeneous turbulent fluid.¹ Hinze begins his solution by calculating the equation of motion of a single spherical particle in a viscous fluid. He then simplifies the complete equation by order of magnitude calculations. The simplified equation is expanded into a Fourier representation. This allows a measure of the response velocity of the particle to the Fourier velocity components of the turbulent fluid. The results show that with typical atmospheric densities of air ($\rho_a = 10^{-3}$ gm/cm³) and particle ($\rho_p = 2.0$ gm/cm³), the actual motion of the particles is slightly different from the fluid elements for homogeneous turbulence. This difference is difficult to

1. Homogeneous turbulence is a random motion whose average properties are independent of position in the field.

incorporate and is not included, so it is assumed that the motion of the particle and the fluid coincide. Therefore, the motion of fluid elements (air) and particulates are referred to synonymously.

The relative motion among a collection of particles in a turbulent fluid is developed less adequately. To understand the physical principles involved, the turbulence field is considered as a collection of eddies which range from a minimum size (inner scale) to a maximum size (outer scale). If the distance r_{ij} between two particles is somewhere between the outer and inner scale of turbulence, then all eddies of size $s < r_{ij}$ (s is the eddy size) act independently on the relative motions of the particles, while those eddies of size $s \geq r_{ij}$ strongly correlate the relative motion (Fuchs 1964). This relationship continues until the particles are separated by a distance greater than the outer scale of turbulence at which point the motions show no correlation. Except for the longer correlation in the relative motion, the consequences of turbulent motion are analogous to those of Brownian motion. The correlation between the phase positions of different particles at different times leads to dependency in the scattered radiation from these particles. Similarly, when the relative motion of the particles show no correlation, the scattered radiation becomes independent.

In addition to the dependency of the phase positions of the scatterers, variations in the total number of particles within a scattering volume cause fluctuations in the scattered light. These total number fluctuations arise from two sources. First, the Brownian and turbulent motion move particles in and out of the volume. These variations are denoted as homogeneous fluctuations. Secondly, if the particles are distributed in inhomogeneous clumps, large variations in the total number of particles in the scattering volume at any time could occur by means of wind replacement; these non-stationary fluctuations, caused by the inhomogeneity, are not treated in this dissertation.

2.1.3 Turbulent Refractive Inhomogeneities

As was stated in section 2.1.1 the turbulence component of the scattered light is only a part of the resultant scattered field from the molecules. This turbulence component is associated with large scale molecular density variations which are commonly called turbulent refractive inhomogeneities. Unfortunately the spatial structure of these refractive inhomogeneities defies mathematical description. For this reason an exact calculation of the turbulence component of the molecularly scattered light remains unsolved. In addition, a light beam passing through a turbulent medium would encounter many randomly distributed refractive inhomogeneities whose spatial density structure changes with time.

This overwhelming complexity points to the statistical solution of the problem.

Tatarskii (1961) was one of the first to attempt a statistical solution for an electromagnetic wave passing through a refractively turbulent medium. Most of the subsequent work to this date is based on the ideas presented in Tatarskii's book, Wave Propagation in a Turbulent Medium. Tatarskii begins the solution by relating the macroscopic Maxwell's equations to the index of refraction of the air. He then uses Kolmogoroff's turbulence theory to relate the statistically averaged structure of the refractive index (spatial density structure) to the sizes of the turbulent eddies. His results are limited to weak scattering, but they demonstrate the perturbation of the phase and amplitude of a light beam which passes through a turbulent medium.

A physical description of the scattering process is as follows. The phase and amplitude structure of the light which reaches some distant field point are influenced by the magnitude and spatial structure of the refractive index variations. The larger the variation of refractive index of an inhomogeneity the greater the amount and angular spread of the scattered light. This result is generally apparent from Snell's laws. However, Tatarskii (1961) calculates a specific relation for the angular spread of the scattered light, given by

$$2 \sin^{-1} \frac{\lambda}{4\pi L_0} \ll \theta \ll 2 \sin^{-1} \frac{\lambda}{4\pi l_0} \quad (2.9)$$

where L_0 is the outer scale of turbulence and l_0 is the inner scale of turbulence associated with the averaged Kolmogoroff turbulent eddy spectrum, θ is the scattering angle, and λ is the wavelength of the light. Tatarskii states that typical values of L_0 and l_0 are 10m and 1.2 cm, respectively, for weak turbulence, and 1m and 0.3 cm, respectively, for strong turbulence. As shown by (2.9), a stronger turbulence results in larger scattering angles implying a wider spread to the scattering angles implying a wider spread to the scattering limits. The spatial structure of the refractive index relates the magnitude of the refractive index variations at two adjacent points. This association allows a calculation of the degree to which two adjacent scatterings remain correlated. In weak turbulence the spatial correlation of the refractive index is large while much smaller for strong turbulence. In the end the spatial correlation of the scatterings influences the spatial region over which the fluctuations in the transmitted light beam are correlated.

The temporal fluctuations of the transmitted light arise from the "motion" of the turbulence. Unfortunately, the motion of turbulent eddies is difficult to define since their physical structure cannot be well specified. Indeed, the mean wind can move one refractive inhomogeneity with respect to another. In addition, a refractive inhomogeneity

can decay through mixing and diffusion. All of these complexities have not provided any clear definition of the life time and motion of the refractive inhomogeneities. Consequently, very little can be said about the "speed" of the fluctuations in the transmitted light.

In conclusion, Tatarskii's work has allowed other researchers to make contributions more relevant to the needs of this dissertation. In particular, Ho (1969), as was mentioned in Chapter 1, has calculated the phase and amplitude changes of a laser beam passing through a turbulent medium. His work is outlined in the section discussing the effects of scatterers between the laser source and scattering volume.

The previous paragraphs were presented for acquaintance or review of the nature of atmospheric scatterers. Before magnitudes for each scattering process are calculated, it is important that two concepts associated with the phase structure of an electromagnetic wave be discussed. They are temporal and spatial coherence. Although specific examples and definitions are discussed in Chapter 1, a more generalized set of definitions are presented in the following sections.

2.2 Coherence

2.2.1 Temporal Coherence

Mandel and Wolf (1965) present the concepts of coherence in a good discussion. Temporal coherence is related to

the different frequency components which comprise a quasimonochromatic beam of light and the phase relationships among these components. It is recalled from Chapter 1 that a quasimonochromatic beam consists of a set of monochromatic beams differing very slightly in frequency. Assuming the phases of all the frequencies which form the light beam at some particular time, t , coincide, then at some later time, $t + \Delta t$, the phases of all the components become out of step with respect to a fixed point. The manifestation of temporal coherence is said to occur when the components of the beam at time t and $t + \Delta t$ can still be superimposed to form an interference pattern. The temporal coherence time (Δt) is related to the band width ($\Delta \nu$) of the frequency components comprising the light beam by the relation (2.10). The longitudinal coherence length is $c\Delta t$, where c is the speed of light.

$$\Delta t \Delta \nu \lesssim 1 \quad (2.10)$$

During the coherence time Δt or, equivalently, over the longitudinal coherence length the frequency components of the quasimonochromatic beam remain almost in step. Therefore, the phases between any two points within a coherence length can be related by $2\pi \nu t$, where ct is the separation of the two points and ν is the central quasimonochromatic frequency. Similarly, the relative phases of any scatterers which lie within a longitudinal coherence length of the

quasimonochromatic beam can also be calculated. This is an important step in defining the scattered light intensity from a collection of scatterers. For example, the University of Arizona ruby laser has a central wavelength of $\lambda = 6943 \text{ \AA}$ with a wavelength spread of $\Delta\lambda = 0.02 \text{ \AA}$. Using the wavelength-frequency relation $\lambda = c/\nu$ and (2.10), the temporal coherence time (Δt) and the longitudinal coherence length ($c\Delta t$) for the University of Arizona ruby laser are 8×10^{-10} seconds and 24 centimeters, respectively. Therefore, the relative phases among a collection of scatterers whose separations are beyond about 24 cm cannot be calculated and, furthermore, must assume random values. This conclusion is based on the original condition for the manifestation of temporal coherence applied to the laser beam. This condition states that when two portions of the laser beam, separated by a time delay greater than the temporal coherence time (Δt), are superimposed, no interference pattern occurs. No interference indicates a random phase relationship between the two portions of the laser beam.

The previous paragraphs have described a generalized condition (temporal coherence) which yields a measure of the degree to which phase surfaces of a light beam remain in step in the direction of beam propagation. Further, a knowledge of this condition facilitates the calculation of the relative phases among a collection of scatterers when illuminated by a light beam. However, because of the finite spread

of light beams the degree to which the phase surfaces of the light beam remain in step in a plane perpendicular to the beam's direction of propagation must also be calculated. This leads to the topic of spatial coherence.

2.2.2 Spatial Coherence

The concept of spatial coherence is related to an interference experiment of the Young's double slit design (Figure 2.2). The experiment involves a source, a double slit screen, and an observation plane (O) upon which an

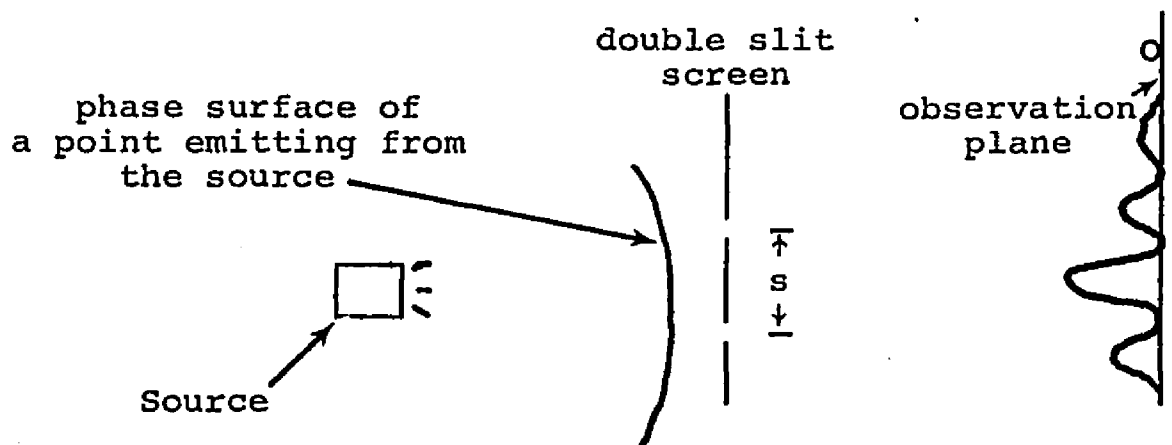


Figure 2.2. The Young's Double Slit Experiment

interference pattern is formed. Light from a source of any size and at any distance from the double slit screen is said to demonstrate spatial coherence over the width of the slit separation (s) provided the fringes on the observation screen (O) have a visibility (commonly denoted by the symbol δ) greater than 0.88. The choice of $\delta \geq 0.88$ is a condition that requires the phase surfaces of the light field to remain

almost in step, perpendicular to the direction of light propagation (Mandel and Wolf 1965).

The maximum separation of the slit (s), for which an interference pattern appears on a screen with $\delta \geq 0.88$ is denoted as the transverse coherence length. The transverse coherence length is synonymous with the far-field, Fraunhofer diffraction pattern of the source.

With regard to the double slit experiment, the visibility, δ , is determined by (2.11), where I_{\max} and I_{\min} are the adjacent maximum and minimum intensity of a fringe, respectively, which appear on the observation plane.

$$\delta = \frac{I_{\max} - I_{\min}}{I_{\max} + I_{\min}} \quad (2.11)$$

Mandel and Wolf show that (2.11) can be equivalently expressed in terms of the so-called light field correlation function. The general expression for the light field amplitude correlation function, $R_E(\vec{r}_1, \vec{r}_2, t)$, is

$$R_E(\vec{r}_1, \vec{r}_2, t) = \langle E(\vec{r}_1, 0) E^*(\vec{r}_2, t) \rangle \quad (2.12)$$

where \vec{r}_1 and \vec{r}_2 are two separate points in space at which the field amplitude, $E(\vec{r}_1, t_1) \langle \vec{t}_1 = \underline{0} \rangle$, and its complex conjugate, $E^*(\vec{r}_2, t_2) \langle \vec{t}_2 = \underline{t} \rangle$, exist. The brackets on the right hand side of (2.12) represent an average over all the possible values the light field amplitude samples at \vec{r}_1 and \vec{r}_2

with time delay t . Using (2.12) Mandel and Wolf show that the visibility expression, δ , is given by

$$\delta = \frac{R_E(\vec{r}_1, \vec{r}_2, 0)}{\sqrt{R_E(\vec{r}_1, \vec{r}_1, 0) R_E(\vec{r}_2, \vec{r}_2, 0)}} \quad (2.13)$$

The relation (2.13) is used throughout this dissertation to calculate the spatial phase structure of light sources; however, (2.13) is not always necessary for this purpose. For example, a laser emits a collimated spherical wave; the collimation is usually so narrow that the light wave is essentially plane parallel. In any case, the phase surfaces of the light field remain in step over the whole laser beam cross-section. Such a light field demonstrates complete spatial coherence in the same sense that a monochromatic light beam demonstrates complete temporal coherence. Further, if a Young's double slit experiment is performed with \vec{r}_1 and \vec{r}_2 at the slit positions, a visibility of $\delta = 1.00$ would be calculated both for the light intensity measurements of (2.11) and the light field amplitude measurements of (2.13). In the case of the laser, the spatial coherence of the light is reduced as the light beam passes through atmospheric scatterers. The amount of this reduction is discussed presently in this chapter.

Spatial coherence is not limited to a well behaved light source of laser quality. An extended thermal source

in which each point on the surface of the source emits an independent spherical wave can demonstrate spatial coherence on a double slit (in no way is this source to be confused with a point source). If the separation of the slits (s) (see Figure 2.2) is small enough, the spherical phase surfaces of all the independent emitters will have approximately the same phase relationship among them at the slits. At the same time the temporal phase of the light from all the emitters is almost completely out of step.

2.3 Interaction of the Laser Light with the Atmospheric Scatterers

The path over which the laser light passes (from laser to receiver) is divided into three parts. The parts are: laser to scattering volume, scattering volume, and scattering volume to receiver. A partition of this type is indicated since the atmospheric scatterers [molecules (Rayleigh and turbulence components) and particulates] are not uniformly important throughout the whole laser to receiver path. For example, the turbulence component of the scattered laser light appears primarily (see 2.9) in the forward direction, while the Rayleigh and the particulate components appear in all directions. Therefore, as long as the scattering angle, θ (see Figure 2.2), is not near the forward direction, the turbulence component of the scattered light from within the scattering volume can be neglected in comparison to the Rayleigh and particulate components. Yet, as the

laser light passes from laser source to the scattering volume and from the scattering volume to the receiver, the turbulent refractive inhomogeneities influence the phase and amplitude structure of the light. This partition, as such, appears to simplify the discussion of the many complex effects of the interaction of the laser light with the atmospheric scatterers between the laser source and receiver.

2.4 Effects of Scatterers between the Laser Source and Scattering Volume

2.4.1 The Effects of the Turbulence Component of the Scattered Light on the Transmitted Laser Light

A considerable amount of theoretical research has been done on the effects of refractive turbulence on the propagation of laser light. The nature of the turbulent refractive inhomogeneities has been previously discussed. As was stated, the works of T. L. Ho (1969, 1970) appear to be best suited for the purposes of this dissertation. Ho's works yield results comparable with other researchers (Asakura, Kinoshita and Suzuki 1969; Livingston, Deitz, and Alcaraz 1970; Brown 1971; Poirier and Korff 1972), but, more important, the physical basis for Ho's mathematical assumptions is clear. In addition his results can be immediately applied to the laser work at The University of Arizona.

The current mode of solution to the turbulent scattering problem used by most authors, including Ho, follows

Tatarskii (1961) and begins with Maxwell's Equation, suitably modified. No theory for the spatial and temporal refractive index structure, expressed by $n(\vec{r}, t)$, exists.

Therefore, a time independent, refractive index structure, $n(\vec{r})$, about which only a statistical average is known replaces $n(\vec{r}, t)$ in Maxwell's Equation. Consequently, the time independent form of Maxwell's Equation for a scalar electric field, $E(\vec{r})$, (also time independent), passing through a turbulent medium defined by $n(\vec{r})$, results and is expressed by

$$\nabla^2 E(\vec{r}) + k^2 n^2(\vec{r}) E(\vec{r}) = 0 \quad (2.14)$$

The simplified solution to (2.14) proceeds by assuming the refractive fluctuations about a mean are small and that the transmitted laser field is perturbed slightly. From these assumptions a generalized perturbation solution for the electromagnetic field which reaches a distant point is obtained.

For equation (2.14) $E^L(\vec{r})$ (the unperturbed laser field) is the unperturbed field, while $E^S(\vec{r})$ (the scattered field) is the perturbed field; the solution is just $E(\vec{r}) = E^L(\vec{r}) + E^S(\vec{r})$ as previously indicated. Furthermore, the requirement of small refractive index fluctuations about a mean is typically modeled as $n(\vec{r}) = n_0(\vec{r}) + n_1(\vec{r})$ where $n_0(\vec{r}) = 1$ (unperturbed atmosphere) and $n_1(\vec{r}) \ll 1$. With these requirements the perturbation solution to (2.14) actually

becomes two equations. The first equation has the same form as (2.14) except $E(\vec{r})$ is replaced by $E^L(\vec{r})$ and $n(\vec{r})$ is replaced by $n_0(\vec{r})$. The second equation is similarly defined except $E(\vec{r})$ is replaced by $E^S(\vec{r})$; however, on the right hand side of this equation a source term, $-2k^2 n_1(\vec{r}) E^L(\vec{r})$, appears instead of zero. This source term represents the interaction of the laser light, $E^L(\vec{r})$, with the turbulent refractive inhomogeneities, $n_1(\vec{r})$. As is discussed in an earlier portion of this chapter, $n_1(\vec{r})$ must be described by some statistical average structure. This in turn leads to only statistical solutions to the scattered light field. Nevertheless, a great deal of useful information can be obtained as will be shown.

Using the perturbation solution to (2.14) as outlined above, Ho calculates the product of the total transmitted field $\underline{E}(\vec{r}) = E^L(\vec{r}) + E^S(\vec{r})$ at the point $\vec{r} = \vec{r}_1$ with its complex conjugate $E^*(\vec{r})$ at the point $\vec{r} = \vec{r}_2$. This product, when statistically averaged $\underline{\langle E(\vec{r}_1) E^*(\vec{r}_2) \rangle}$ over all the realizations of the turbulent refractive index field, yields an expression which is analogous to the light field amplitude correlation function, (2.12). Recalling this correlation function $\underline{\langle R_E(\vec{r}_1, \vec{r}_2, t) \rangle}$ and realizing that $E(\vec{r})$ is time independent requires the expression be written as

$$R_E(\vec{r}_1, \vec{r}_2, 0) = \langle E(\vec{r}_1) E^*(\vec{r}_2) \rangle \quad (2.15)$$

This expression yields two pieces of useful information. When $\vec{r}_1 = \vec{r}_2$, then $R_E(\vec{r}_1, \vec{r}_1, 0) = \langle I(\vec{r}_1) \rangle$, where $I(\vec{r}_1)$ is the intensity at \vec{r}_1 . Therefore, information is obtained about the change in the statistical mean intensity at arbitrary points within the laser beam as it passes through the turbulent medium. Finally, (2.15) by itself can be used to calculate the spatial coherence of the light beam. In this connection, turbulent scattering causes adjacent phase surfaces of the composite laser field $[\vec{E}(\vec{r}) = E^L(\vec{r}) + E^S(\vec{r})]$ to become out of step. Since $E^S(\vec{r})$, is the bad actor with regard to the spatial phase uniformity of $E(\vec{r})$, the spatial coherence decreases as the beam penetrates the turbulent medium.

In the earlier section of spatial coherence it was pointed out that the visibility of the fringes, δ , from a Young's double slit is used to scale the spatial coherence of the light. The term δ is directly related to the field correlation function (2.15) through the expression (2.13). Before passing through the turbulent medium the laser beam is assumed to demonstrate perfect spatial coherence, represented by $\delta = 1.00$, for any double slit positions \vec{r}_1 and \vec{r}_2 within the beam cross-section. However, as soon as some turbulent scattering occurs δ never quite equals 1.00 again for any finite slit separation $|\vec{r}_1 - \vec{r}_2|$. Nevertheless, there exists a separation at which the light is almost spatially coherent, represented by $\delta = 0.88$; this separation is the

transverse coherence length. Further, a cross-sectional area of the beam within which any two slits can be chosen to demonstrate a fringe clarity of $\delta = 0.88$; is denoted as the spatial coherence area. Using Ho's (1970) expression for (2.15), modified for the University of Arizona laser system, the transverse coherence length and the corresponding spatial coherence area can be calculated as a function of range into a weak turbulent medium; this is done in the next section.

2.4.1a Magnitudes of the Turbulence Effects on the Spatial Phase Structure of the Transmitted Laser Light. The transverse coherence length (2.2.2) becomes smaller as the laser light passes through the weak turbulent medium. To calculate typical values of the transverse coherence length (TCL) as a function of range, $|\vec{r}|$, the results of Ho's 1970 paper were modified to fit the parameters of the University of Arizona ruby laser. To this end, the TCL for this laser was calculated by means of computer (University of Arizona CDC6400) for weak turbulent conditions $(C_n^2 = 10^{-16} \text{ m}^{-2/3})^2$ as a function of range, $|\vec{r}|$. In addition, two laser beam divergence angles were used where θ_T , the half angle beam width is used to express this divergence. These results are expressed in Table 2.1.

As an independent comparison, the results of Table 2.1 were compared with similar calculations made by Brown

2. C_n^2 is the Kolmogorov turbulence strength factor and typically varies from 10^{-16} to $10^{-14} \text{ m}^{-2/3}$ for weak to strong turbulence, respectively.

(1971). Brown calculated the TCL in a completely different manner and the results appear in a relatively simple closed form (his equation 61). The condition under which Ho's TCL was calculated was applied to Brown's developments. Ho's computed calculations were done for $\theta_T = 0.5$ mr. (mr. = 10^{-3} radians) and compared with Brown's results. The results compared so well that Brown's equation alone was used to calculate the TCL for $\theta_T = 1.5$ mr. The results of Table 2.1 clearly show the reduction of the TCL with increasing range. Finally the TCL serves as the diameter of a circular area which is called the spatial coherence area of the transmitted light.

2.4.1b Magnitude of the Turbulence Effects on the Temporal Phase Structure of the Transmitted Laser Light. A knowledge of the temporal phase of the composite laser field $\langle \vec{E}(\vec{r}) = \vec{E}^L(\vec{r}) + \vec{E}^S(\vec{r}) \rangle$ is required for two related reasons. First, the temporal phase, as expressed by the longitudinal coherence length, along with the spatial phase as expressed by the transverse coherence length discussed earlier, completes the three dimensional description of the phase of the composite laser field. This is necessary in order to approximately specify the relative phase relationships among the atmospheric scatterers contained in a volume of space illuminated by the laser beam. Secondly, the fluctuations in light intensity $\langle \vec{I}(\vec{r}) = |\vec{E}(\vec{r})|^2 \rangle$ are directly caused by the

TABLE 2.1 The Transverse Coherence Length, $TCL_{\vec{r}}$, of the Transmitted Laser Light as a Function of Range, $|\vec{r}|$, in Weak Turbulence. -- The term ρ_s is the effective laser beam radius, while θ_T is the half-angle beam width in milliradians (mr.).

$\theta_T = 0.5 \text{ mr.}$

$\theta_T = 1.5 \text{ mr.}$

$ \vec{r} $ (km)	ρ_s (cm)	TCL $\underline{[Ho]}$ (cm)	TCL $\underline{[Brown]}$ (cm)	TCL $\underline{[Brown]}$ (cm)
0.5	10.1	10.1	10.1	20.0
1.0	12.7	7.8	7.0	10.6
2.0	17.6	5.8	4.2	5.5
3.0	22.6	4.8	3.2	4.0
4.0	27.6	4.2	2.6	3.0
5.0	32.7	3.8	2.2	2.6

temporal phase shifts of the scattered light $\langle \bar{E}^S(\vec{r}) \rangle$ with respect to the unscattered light $\langle \bar{E}^L(\vec{r}) \rangle$.

Similar to the spatial phase, an exact knowledge of the temporal phase of the composite laser beam is not possible because the phase ultimately depends on the unknown temporal and spatial refractive index structure $\langle \bar{n}_1(\vec{r}, t) \rangle$. Nevertheless, the assumption of weak turbulence requires that the composite laser field, expressed as $E(\vec{r}) = E^L(\vec{r}) + E^S(\vec{r})$, satisfies the relation $|E^L(r)| \gg |E^S(r)|$. Therefore, the temporal phase as expressed by the longitudinal coherence length of the composite field is almost equal to the longitudinal coherence length of the unperturbed laser field $\langle \bar{E}^L(\vec{r}) \rangle$. The product of the longitudinal coherence length (24 cm) and the spatial coherence area $\langle \pi \times (TCL) / 4 \rangle$ defines the coherence volume of the transmitted light. It is within a coherence volume that the relative phases among a collection of scatterers can be calculated. This, in turn, allows the calculation of the phase of the scattered light incident on a receiver and the resultant fluctuations.

2.4.1c Fluctuations in the Transmitted Laser Light Caused by Turbulence. The statistical solution to Maxwell's equation (2.14) should yield information about the statistical distribution of the fluctuations in the transmitted laser light intensity. If all orders of statistical moments of the light intensity could be calculated, then the statistical (or probability) distribution of the transmitted laser light

intensity could be specified. Yet, the simplified solution to (2.14) yields only the first two moments of the transmitted light intensity for weak turbulence. Fortunately, the generally agreed upon intensity probability distribution, $p(I)dI$, for weak turbulence is log-normal for which only the first two moments are needed (see 2.16 below). For stronger turbulence scattering the solution for $p(I)dI$ is difficult and the proposed solutions by many researchers have caused a great deal of controversy. This controversy is well-described by deWolf (1969), so no further discussion of this subject will be made in this dissertation.

The log-normal intensity distribution valid for weak turbulence is given by

$$p(I)dI = (2\pi\sigma_L^2)^{-1/2} \exp \left\{ -\frac{[\log_e (I/\langle I \rangle)]^2}{2\sigma_L^2} \right\} \frac{dI}{I} \quad (2.16)$$

where $\langle I \rangle$ is the mean intensity of the transmitted laser light which reaches a point some distance from the source within the effective diameter of the laser beam, and σ_L^2 is a measure of the variance of the logarithmic intensity, L , given by $\log_e (I/\langle I \rangle)$. Both $\langle I \rangle$ and σ_L^2 have a range dependence not expressed in (2.16) for convenience.

Using some relationships given by deWolf (1969) and Ho (1969), a general expression for σ_L^2 , valid for the characteristics of the University of Arizona laser was calculated

and is given here by

$$\sigma_L^2 = 1.24 C_n^2 k^{7/6} |\vec{r}|^{11/6} \quad (2.17)$$

where C_n^2 is the Kolmogorov turbulence strength factor whose dimensions are $[m^{-2/3}]$ (where m is meters), k is the wave number of the laser light $[m^{-1}]$, and $|\vec{r}|$ is the distance from the source. For weak, homogeneous turbulence C_n^2 is typically taken as $10^{-16} m^{-2/3}$, while the wave number of the ruby laser is $[9.05 \times 10^{-6} m^{-1}]$.

Table 2.2 expresses some values of σ_L^2 as a function of range, $|\vec{r}|$.

TABLE 2.2 The Variance of the Transmitted Laser Light Log-intensity (σ_L^2) as the Light Passes Through a Weakly Turbulent Medium with Increasing Range, $|\vec{r}|$.

$ \vec{r} $ (km)	σ_L^2
0.5	0.14×10^{-2}
1.0	0.51
1.5	1.07
2.0	1.81
3.0	3.81
5.0	9.71

A well-known property of the normal distribution is that 68% of the spread of the distribution lies within one standard deviation on either side of the mean ($\langle I \rangle \pm \sigma_L$). Therefore, using (2.16) the upper (I_u) and lower (I_ℓ) bounds of the intensity about the mean which contain 68% of the spread can be calculated by setting

$$\log(I_u/\langle I \rangle) = \sigma_L; \log(I_\ell/\langle I \rangle) = -\sigma_L \quad (2.18)$$

At 5 km the solution to (2.18) using Table 2.2 yields $I_u = 1.1\langle I \rangle$ and $I_\ell = 0.9\langle I \rangle$. This solution indicates that 10% intensity fluctuations about the mean are fairly common even for weak turbulence. Yet, the weak turbulence condition insures that the energy is primarily redistributed and not lost from within the effective laser beam diameter. The spatial distribution of the intensity is the next important consideration in discussing the light fluctuations.

The intensity probability distribution functions are valid at a single point. Little mention is made in the literature regarding the spatial extent of these intensity fluctuations. This dissertation attempts to rectify this inadequacy through the logical assumption that the intensity fluctuations are correlated over a spatial coherence area, as has been previously discussed.

2.4.2 The Effects of the Rayleigh and the Particulate Components of the Scattered Light on the Transmitted Laser Light

The Rayleigh and particulate components of the scattered light reduce the temporal and spatial coherence in the same manner as the turbulence component, but there are some obvious differences. The scattering is not limited to the forward direction even for very weak scattering. The strength of the Rayleigh component is proportional only to the density of the molecules, while scattering from particles is related to the number density and size of the particles. Curran (1971) shows that for the University of Arizona laser facility multiple scattering contributions from the Rayleigh and particulate components can be neglected compared to single scattering.

A further calculation can be made to assess the magnitude of the transmitted laser field to the magnitudes of the Rayleigh and particulate components of the forward scattered light field (single scattered) as a function of range in the scattering medium. To this end a solution (Appendix B) to the radiative transfer equation is obtained for the mean flux density near the center of the transmitted laser beam. The solution, expressed as a ratio of the scattered to transmitted mean flux density, depends primarily on the total optical depth of the atmosphere and the half-angle beam width of the laser beam, θ_T . Now, for $\theta_T = 1.5$ mr. (milliradians) and the respective total particulate and molecular

optical depths of $\tau_T^P = 0.25$ and $\tau_T^m = 0.036$ (at the ruby wavelength of $0.6943\mu\text{m}.$), the mean flux density ratio is found to be of the order 10^{-4} for the vertically propagating laser beam at all ranges from 1 to 5 km. range into the medium. Therefore, since the ratio equals $\frac{|E^S(\vec{r})|}{|E^L(\vec{r})|} \approx 10^{-2}$ (E^S is the scattered field and E^L is the transmitted laser field), it is concluded that the molecules and particulates have a negligible effect, except for attenuation, on the laser light passing from the source to the scattering volume. With regard to this last statement the composite field ($= E^L + E^S$) remains essentially undisturbed and therefore its coherence properties are also virtually unchanged.

2.5 Effects of Atmospheric Scatterers at the Scattering Volume

Under the conditions of relatively weak scattering it is assumed that the laser light which reaches the scattering volume demonstrates some spatial and temporal coherence. It is then possible to relate the phase of the scattered light to the relative phase positions of the scatterers within the scattering volume.

2.5.1 Turbulence Component of the Scattered Light

The turbulence component of the scattered light appears near the forward direction of the transmitted laser light. Therefore, at the large scattering angles representative of the monostatic and bistatic laser facility at The

University of Arizona the turbulence component from the scattering volume is neglected.

2.5.2 The Rayleigh and Particulate Components of the Scattered Light

Molecules (Rayleigh component) and particulates scatter significant amounts of incident laser light at large scattering angles. Indeed, it is this very characteristic upon which the inference of their optical properties is based. The scattered light amplitude from all the molecules and particulates combines at the receiver surface to give some instantaneous intensity. This instantaneous intensity fluctuates about a statistical mean value. The statistical mean value contains information about the scatterers but is difficult to estimate because of the fluctuations. In order to calculate the fluctuations of the scattered light intensity about a mean, it becomes necessary to calculate the probability distribution of the scattered intensity. As stated earlier, if all the statistical moments of the scattered light intensity were known, then the probability distribution could be calculated exactly. In practice it is difficult, if not impossible, to calculate moments beyond the second order. Under certain conditions, such as Gaussian scattered light, the first and second moments of the scattered light intensity determine all the higher order moments. By means of the scattered intensity correlation function yet to be defined, the first and second moments of the

statistical distribution of the scattered intensity can be calculated. In addition, the intensity correlation function yields the correlation time of the scattered light. The intensity correlation function not only depends on the change of phase positions of the scatterers but also on the fluctuations in the total number density of scatterers within the scattering volume; Brownian and turbulent motion cause the changes in position and number density. Further, the loss of spatial and temporal coherence of the incident light reduces the temporal information about the relative phase positions of the scatterers at the receiver.

2.6 The Scattering Volume

2.6.1 The Scattering Volume for Pulsed and Continuous Illumination

The basic difference between a pulsed and continuous laser beam is the amount of time the laser is "turned on". For example, the typical pulsed ruby laser emits a pulse of light with pulse length about 30 nano-seconds or so, while the continuous laser emits light as long as desired. At the same time, the energy density of the pulsed laser is usually much higher than the continuous laser. Since the volume atmospheric scattering coefficient is so weak, the pulsed laser, because of its high energy density, must be used to obtain measurable amounts of scattered light from small scattering volumes. However, the very use of the pulsed laser results

in some special geometric conditions on the size and shape of the scattering volume.

For the statistical studies of the scattered light in this dissertation, it is necessary to calculate the number and position of the atmospheric scatterers which scatter light to the receiver arriving at the same time; the light from these scatterers composes the instantaneous intensity incident on the receiver. This requirement is satisfied by calculating the volume of space containing scatterers which are illuminated by the laser light and whose separate contributions to the scattered light arrive at the receiver at the same time; this volume is called the instantaneous scattering volume. In such a scattering volume all the scattering events do not occur at the same time. For example, a scattering event which occurs in a region with a given source-to-receiver path must occur later in real time with respect to a similar scattering event with a longer path in order for the light from both events to arrive at the receiver at the same time. Therefore, it is important to keep in mind that the scattering volume used in this dissertation for subsequent calculations is the instantaneous scattering volume.

The instantaneous scattering volume has been used by radar researchers in past studies. Since the radar system, which measures back-scattered energy from rain and clouds is in many ways similar to the monostatic lidar system, some useful comparisons can be made. First, the radar emits a

pulse of energy whose time length is on the order of a millisecond (10^{-3} sec), but this varies considerably. The pulse cross-section of energy widens as it propagates because of the beam spread determined by the radar antenna cross-section. The pulse of energy illuminates all the scatterers within the volume defined by the beam spread and the pulse length. However, only the scatterers within half the pulse volume scatter light which arrives at the receiver at the same time (directly back-scattered). The previously discussed scattering geometry is exactly the same for the monostatic lidar system.

When the bistatic laser-receiver system is considered, the dimensions of the instantaneous scattering volume are different. Curran (1971) has extensively studied the geometry of the instantaneous scattering volume for the pulsed bistatic system and it is left to interested readers to delve into the problem further; all that is needed in this dissertation is the size of the instantaneous scattering volume in terms of the measurable pulse volume, V_p , and scattering angle, θ .

From Curran's work it is shown that if l_p is the length of the pulse and A_p is its cross-sectional area, then the length of the instantaneous scattering volume, l_{ip} , is given by

$$l_{ip} = \frac{l_p}{2 \sin^2(\frac{\theta}{2})} \quad (2.19)$$

where Θ is the scattering angle; the cross-sectional area remains A_p . Therefore, the size of the instantaneous scattering volume, V_{ip} , is given by

$$V_{ip} = (\ell_{ip}) A_p \quad (2.20)$$

2.7 General Formulation of the Intensity Correlation Function of the Scattered Light

The basic goal of this dissertation, as has been often stated, is to study the fluctuations of the scattered light. A method which seems well-suited for this purpose is to calculate the intensity correlation function of the scattered light which arrives at the receiver. The correlation function as such has been discussed a number of times so far in this dissertation; recall the light field correlation function (2.15) used to calculate the spatial coherence of the light. The intensity correlation function (statistical) is similarly expressed as

$$R_I(\vec{r}_1, \vec{r}_2, t) = \langle I(\vec{r}_1, 0) I(\vec{r}_2, t) \rangle \quad (2.21)$$

where again, $R_I(\vec{r}_1, \vec{r}_2, t)$ is the intensity correlation function, $I(\vec{r}_2, 0)$ is the intensity (scattered) which arrives at the point \vec{r}_1 (on the receiver) from the instantaneous scattering volume at time 0, $I(\vec{r}_2, t)$ is similarly defined except the light arrives at \vec{r}_2 at time t . Finally, the brackets refer to the ensemble or statistical average. It will be

shown that (2.21) contains all the statistical information necessary to describe the fluctuations of the scattered light. First, (2.21) is employed to study the temporal correlation of the intensity at one point by setting $\vec{r}_1 = \vec{r}_2$; second, the spatial correlation is analysed by setting $t = 0$ and $\vec{r}_1 \neq \vec{r}_2$.

The intensity correlation function of the scattered light which arrives at one point on the receiver ($\vec{r}_1 = \vec{r}_2$) correlates two intensities after a time delay t . During this time delay the intensity can change from a number of causes. After a time delay, t , the instantaneous scattering length, ℓ_{ip} , moves a distance $\ell = t/c$. Now, if $\ell \geq \ell_{ip}$, the instantaneous scattering volume at time t , contains an entirely new set of scatterers with different numbers and relative phase positions than in the volume at time 0. On the statistical average, this condition is assumed to yield an intensity at time t , which is entirely independent (or uncorrelated) with the intensity at time 0. Yet, for $\ell < \ell_{ip}$ the instantaneous scattering volumes at time 0 and t have an overlapping portion. The non-overlapping parts of the instantaneous scattering volumes contribute a portion to the intensities which are uncorrelated, while the intensities from the overlapping portions are correlated. Further, the correlation of the intensities from the overlapping volume changes, not only because the overlapping volume becomes smaller with

time, but also because the scatterers may move between time 0 and t , however slightly. The motion causes a change in the relative phase positions and numbers of the scatterers contained within the overlapping volume which, in turn, reduces the correlation of the intensities between time 0 and t .

In order to include the effects of the changing instantaneous scattering volume in (2.21), it is found convenient to express (2.21) in terms of the intensity correlation function for a continuous beam laser, $R_I^C(t)$, (the condition $\vec{r}_1 = \vec{r}_2$ is implicit and is dropped; the c superscript denotes continuous beam) which illuminates a volume equivalent in size and shape to the instantaneous scattering volume of the pulsed laser, but remains fixed in space. For $R_I^C(t)$ the correlation in the scattered light intensity changes only by means of scatterer motion causing new relative phase positions and numbers of the scatterers within the fixed volume between time 0 and t . If the time t is sufficiently long, the scattered intensities become completely independent (or uncorrelated), this is denoted by $R_I^C(\infty) [\overline{t} = \infty]$. Therefore it seems logical to assume that $R_I^C(\infty)$, whose independence is caused by scatterer motion, is equivalent to that portion of $R_I(t)$ $[\vec{r}_1 = \vec{r}_2$ dependence is dropped] from the non-overlapping part of the instantaneous scattering volumes, while the overlapping portion of $R_I(t)$ is equivalent to $R_I^C(t)$.

Using the partial correspondence between $R_I(t)$ and $R_I^C(t)$ discussed in the previous paragraph, a mathematical relationship can be written for their complete correspondence. Figure 2.3 shows the instantaneous scattering volumes at time 0 and t ; the different cross-hatching denotes the overlapping and non-overlapping portions of the volumes. During the period when $l \leq l_{ip}$ or in terms of time $t \leq t_{ip}$, $R_I(t)$ is written as

$$R_I(t) = \left\{ R_I^C(t) \left(\frac{t_{ip} - t}{t_{ip}} \right) + R_I^C(\infty) \left(\frac{t}{t_{ip}} \right) \right\} s(t) \quad (2.22)$$

where the first term within the {} brackets is the contribution from the overlapping volume, while the second term is the contribution from the non-overlapping volume. Finally, the term $s(t)$ is a step function given by

$$s(t) = \begin{cases} 1 & ; 0 \leq t \leq t_{ip} \\ 0 & ; t > t_{ip} \end{cases} \quad (2.23)$$

Now when $t > t_{ip}$, $R_I(t)$ equals $R_I^C(\infty)$. In order for this solution to vanish for $t \leq t_{ip}$ we write

$$R_I(t) = R_I^C(\infty) [1 - s(t)] \quad (2.24)$$

Thus (2.22) is valid for $t \leq t_{ip}$ and vanishes for $t > t_{ip}$, while (2.24) is valid for $t > t_{ip}$ and vanishes for $t \leq t_{ip}$. A solution valid for all time is the sum of (2.22) and (2.24)

or,

$$R_I(t) = \{ \langle \bar{R}_I^C(t) - R_I^C(\infty) \rangle \left(\frac{t_{ip} - t}{t_{ip}} \right) \} s(t) + R_I^C(\infty) \quad (2.25)$$

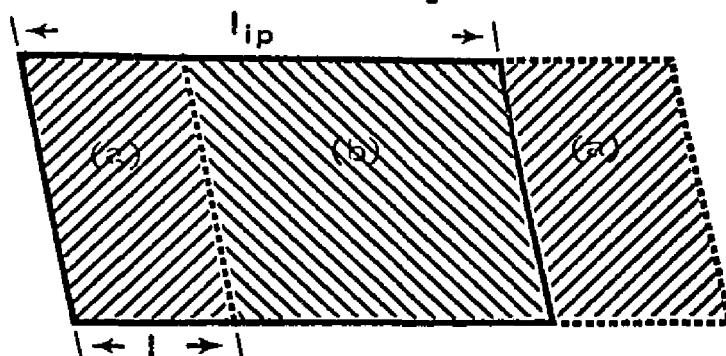


Figure 2.3 The Relative Position of the Instantaneous Scattering Volume at Time 0 (Solid Boundaries) and Time t (Dashed Boundaries). -- In the above figure the cross-hatching denotes the overlapping (b) and non-overlapping (a) portions of the volumes, while l_{ip} and l denote the distances which when divided by the speed of light correspond to the time t_{ip} and t

As a final note, if it is desired to correlate the scattered light between independent laser firings (denoted as pulse-to-pulse), then the correlation function $\langle \bar{R}_I(t) \rangle^{PP}$, coming from the same instantaneous scattering volume after a pulse delay time t , is

$$\langle \bar{R}_I(t) \rangle^{PP} = R_I^C(t) \quad (2.26)$$

and depends only on the motion of the scatterers as expressed by $R_I^C(t)$.

Therefore, the expressions (2.25) and (2.26) have separated the dependence of the intensity correlation

function, $R_I(t)$, on both the instantaneous scattering volume and the motions of the scatterers; $R_I^C(t)$ can now be separately analyzed for the effects of the scatterer motion.

2.7.1 The Intensity Correlation Function from the Continuously Illuminated Atmospheric Scatterers

2.7.1a Temporal Correlation. When the implicit range dependence (see 2.21) of $R_I^C(t)$ is expressed by writing, $R_I^C(\vec{r}, \vec{r}, t)$, the intensity correlation function of the scattered light from the molecules and particulates which arrives from a scattering volume a distance \vec{r} away is

$$R_I^C(\vec{r}, \vec{r}, t) = \langle I(\vec{r}, 0) I(\vec{r}, t) \rangle \quad (2.27)$$

The above expression is presently shown to yield the first two statistical moments of the probability distribution associated with the temporal fluctuations of $I(\vec{r}, t)$. Typically \vec{r} ends at some arbitrary point on the receiver surface. In order to include the phases of all the scatterers which contribute to (2.27), the expression must be written in terms of the light fields as

$$R_I^C(\vec{r}, \vec{r}, t) = \langle E(\vec{r}, 0) E^*(\vec{r}, 0) E(\vec{r}, t) E^*(\vec{r}, t) \rangle \quad (2.28)$$

The light field $E(\vec{r}, t)$ is the sum of all the scattered fields from the individual molecules and particulates within the scattering volume which arrives at some arbitrary point on the receiver at time t .

When the general field expression $E(\vec{r}, t)$ is written in terms of the sum of the molecular $\langle \vec{E}_m(\vec{r}, t) \rangle$ (Rayleigh component) and the particulate fields $\langle \vec{E}_p(\vec{r}, t) \rangle$ and placed into (2.28), the multiplication results in sixteen terms. Ten of these sixteen terms involve products of terms similar to $\langle E_m(\vec{r}, 0) E_p^*(\vec{r}, t) \rangle$; these terms must be zero because the motions of the molecules and particulates are independent. The six terms which are left boil down to the expression given by

$$R_I^C(\vec{r}, \vec{r}, t) = R_I^C(\vec{r}, \vec{r}, t)_p + R_I^C(\vec{r}, \vec{r}, t)_m \quad (2.29)$$

$$+ 2\text{Re}\{\langle \vec{R}_E^C(\vec{r}, \vec{r}, t)_p \rangle \langle \vec{R}_E^C(\vec{r}, \vec{r}, t)_p \rangle\} + 2\langle I_m \rangle \langle I_p \rangle$$

and, further, it can be shown that

$$R_E^C(\vec{r}, \vec{r}, t) = R_E^C(\vec{r}, \vec{r}, t)_p + R_E^C(\vec{r}, \vec{r}, t)_m \quad (2.30)$$

where the m and p subscripts on the right-hand side of (2.29) and (2.30) refer to the expressions involving the molecular or particulate fields only and the Re in front of the brackets {} denotes the real portion of the product. Also, it should be recalled that $R_E(\vec{r}, \vec{r}, t)$ (without the superscript) is generally written as

$$R_E(\vec{r}, \vec{r}, t) = \langle E(\vec{r}, 0) E^*(\vec{r}, t) \rangle \quad (2.31)$$

The * in both (2.29) and (2.31) denotes complex conjugate.

Finally, $\langle I_m \rangle$ and $\langle I_p \rangle$ are the mean scattered intensities from the molecules and particulates, respectively.

The forms of (2.29) and (2.30) have conveniently separated the joint correlation functions of the molecules and particulates into their separate correlation functions which can now be studied individually. However, since the light fields $E_m(\vec{r}, t)$ and $E_p(\vec{r}, t)$ are typically composed of a great number of contributions from the individual molecules and particulates, messy summation notation must be used. Further, since as many as four products of these summation terms appear in calculating the intensity correlation functions, an entirely unwieldy problem becomes manifest. Therefore, it was thought best to place these calculations in Appendix C, while the important features can be summarized here.

A discussion of the calculation of the intensity correlation function of the particulates, $R_I^C(\vec{r}, \vec{r}, t)_p$, will present all the factors necessary to calculate the additional correlation functions which appear in (2.29). The function $R_I^C(\vec{r}, \vec{r}, t)_p$ in terms of the field amplitudes $E_p(\vec{r}, t)$, is given by (2.28) with p subscripts on the field terms. Each field term, $E_p(\vec{r}, t)$, has a general form, calculated in Appendix A, which includes the phase and amplitudes of all the contributing scatterers; the expression is

$$E_p(\vec{r}, t) = e^{i\phi_R(t)} \left\{ \sum_{m=1}^{N(t)} A^m \int_{V_{ip}} e^{i(\vec{k} \cdot \vec{r}_1 + \gamma(\vec{r}_1))} \delta[\vec{r}_1 - \vec{r}_m(t)] dV(\vec{r}_1) \right\} \quad (2.32)$$

where $\phi_R(t)$ is the phase of the light which travels from the laser source to a fixed reference point within the instantaneous scattering volume and then to the arbitrary point on the receiver a distance \vec{r} away from the reference point, $N(t)$ is the number of particulates contained within the instantaneous scattering volume at time t , A^m is the scattered amplitude from the m th scatterer, the integral within the brackets seeks out the phase positions of all the scatterers, $\vec{r}_m(t)$, at time t with respect to the reference point within the scattering volume by integrating the dummy variable \vec{r}_1 over V_{ip} . The properties of the Dirac delta function $\delta[\vec{r}_1 - \vec{r}_m(t)]$, provide a useful simplification of notation. The term $\vec{k} \cdot \vec{r}_1$ is the general phase position of a particle located at \vec{r}_1 with respect to the reference point within V_{ip} . Further, $\vec{k} = \vec{k}_s - \vec{k}_0$, where \vec{k}_0 is the wave number of the laser light pointing in the direction of the incident light, while \vec{k}_s is the wave number pointing in the direction of the scattered light (from the scattering volume to the receiver). In addition

$$|\vec{k}| = \frac{4\pi}{\lambda} \sin\left(\frac{\theta}{2}\right) \quad (2.33)$$

where λ is the laser light wavelength, and θ is the scattering angle. Finally, $\gamma(\vec{r}_1)$ is the additional phase attributed to turbulence effects along the two-way optical transmission path.

The four products of the fields, expressed by (2.28), which comprise $R_I^C(\vec{r}, \vec{r}, t)_p$ contain four independent sums over the particulates within the scattering volume at time zero and time t . The details of these summations are carried out in Appendix C where it is shown that the correlations in the phase of the light arriving at the receiver depend on three main conditions.

The first condition concerns the temporal correlation of the incident laser light and the spatial correlation changes in the light attributed to turbulence effects along the two-way optical transmission path. The temporal correlation of the incident laser light has already been expressed by the longitudinal coherence length (or temporal coherence time), while the spatial correlation along the incident portion of the two-way optical path has been expressed by the transverse coherence length (TCL). Finally, the spatial correlation in the scattered portion of the two-way optical path, called the maximum transverse separation (MTS), is presently discussed. The three correlation lengths define a region within the scattering volume in which the relative phase relationships among the particulate scatterers remain

correlated at a point on the receiver when averaged over many statistical realizations of the turbulent medium. The defined region is called a mutual coherence volume (MCV). Particulates which become separated beyond the dimensions of the MCV between time zero and t change their relative phases to random values and thereby contribute to fluctuations in the received intensity.

The second condition concerns the changes in the relative phase positions among the particles between time zero and t as expressed through $\vec{k} \cdot \vec{r}_1(0)$ and $\vec{k} \cdot \vec{r}_1(t)$, respectively. Between time zero and t , $\vec{r}_1(t)$ changes by means of Brownian and turbulent motion. The Brownian motion moves each particle independently so that the relative phases among the particles demonstrate no correlation after a relatively short time. On the other hand, the turbulence tends to move groups of particles independently, while within any one group the particles show some dependent motion. Consequently, the relative phases among groups of particles demonstrate short correlation times, while relative phases of particles within one group demonstrate a longer correlation time. The combined Brownian and turbulent motion causes the received intensity fluctuations to demonstrate complex characteristics.

Finally, the third condition concerns the total number of particles within the scattering volume at time zero and t , denoted by $N(0)$ and $N(t)$, respectively. Again,

Brownian and turbulent motion move the particulates into and out of the scattering volume thus leading to differences between $N(0)$ and $N(t)$. These differences, in turn, cause fluctuations in the received intensity.

The molecules demonstrate the same effects on their correlation functions as previously outlined for the particulates; however, the results are much simpler.

The final results of Appendix C yield expressions in terms of measurables for the right-hand sides of (2.29) and (2.30). From these expressions it is shown that the first two statistical moments of the probability distribution are obtained in addition to the correlation time for the scattered light. The calculation of the correlation time is by far the most difficult because it is dependent on a complex interplay of (1) the turbulent and Brownian diffusion coefficients of the molecules and all the different sized particulates, (2) the correlation coefficient of the turbulent motion, (3) the size of the mutual coherence volume, and (4) the scattered intensity per molecule and per particulate for each different size. Expressions for the two statistical moments are now presented, while further discussion of the correlation time is presented in Chapter 3.

Recall that (2.25) gives the intensity correlation function for the pulsed laser illuminating a moving instantaneous scattering volume in terms of a continuous beam

illuminating a fixed instantaneous scattering volume. An important property of the correlation function written as

$$R_I(t) = \langle I(0)I(t) \rangle \quad (2.34)$$

is that

$$(1) \quad \lim_{t \rightarrow 0} R_I(t) = \langle I^2(0) \rangle = \langle I^2 \rangle \quad (2.35)$$

and

$$(2) \quad \lim_{t \rightarrow \infty} R_I(t) = \langle I(0)I(\infty) \rangle = \langle I(0) \rangle \langle I(\infty) \rangle = \langle I \rangle^2 \quad (2.36)$$

where $\langle I^2 \rangle$ is the mean square of the intensity and $\langle I \rangle$ is the mean intensity. The expression (2.36) is valid because it is assumed that the processes which correlate the intensity at time 0 with the intensity at time t vanish, if t is long enough ($t = \infty$); certainly, scattering from moving particulates and molecules eventually satisfies this condition. Now, employing (2.25) the results are

$$R_I(0) = R_I^C(0) \text{ and } R_I(\infty) = R_I^C(\infty) \quad (2.37)$$

Now from (2.29), the right-hand sides of (2.37) can be evaluated in terms of the molecules and particulates, so that

$$R_I(0) = R_I^C(0) = R_I^C(0)_p + R_I^C(0)_m + 2 R_E^C(0)_p R_E^C(0)_m + 2 \langle I_m \rangle \langle I_p \rangle \quad (2.38)$$

$$R_I(\infty) = R_I^C(\infty) = R_I^C(\infty)_p + R_I^C(\infty)_m + 2 R_E^C(\infty)_p R_E^C(\infty)_m + 2 \langle I_m \rangle \langle I_p \rangle$$

All the terms on the right-hand sides of (2.38) have been calculated in Appendix C in terms of measurables. The results are

$$\begin{aligned} R_I^C(0)_p &= 2 \langle I_p \rangle^2 ; R_I^C(0)_m = 2 \langle I_m \rangle^2 \\ R_E^C(0)_p &= \langle I_p \rangle ; R_E^C(0)_m = \langle I_m \rangle \\ R_I^C(\infty)_p &= \langle I_p \rangle^2 ; R_I^C(\infty)_m = \langle I_m \rangle^2 \\ R_E^C(\infty)_p &= 0 ; R_E^C(\infty)_m = 0 \end{aligned} \tag{2.39}$$

Therefore, using (2.35), (2.36), (2.38) and (2.39) yields after some simplification

$$\begin{aligned} \langle I^2 \rangle &= 2 (\langle I_p \rangle + \langle I_m \rangle)^2 \\ \langle I \rangle^2 &= (\langle I_p \rangle + \langle I_m \rangle)^2 \end{aligned} \tag{2.40}$$

where Appendix C additionally shows that

$$\langle I_p \rangle = \sum_{j=1}^J v_j I_p^j ; \langle I_m \rangle = v_m \bar{I}_m \tag{2.41}$$

where v_j is the total mean number of particulates within the instantaneous scattering volume of the j th size interval of which there are a total of J size intervals, I_p^j is the scattered intensity per particle of the j th size, v_m is the total

mean number of molecules in the instantaneous scattering volume and \bar{I}_m is the scattered intensity per molecule.

The results expressed by (2.40) and (2.41) are exactly the same results which are obtained for the first two statistical moments of Rayleigh distributed light for which the mean light intensity is the sum of the individual intensities from each scatterer. Although (2.40) and (2.41) do not prove the scattered light intensity is Rayleigh distributed the results do not contradict this conclusion. In this connection, the so-called Rayleigh distribution of the intensity is given by

$$P(I) dI = \frac{1}{\langle I \rangle} \exp \left(- \frac{I}{\langle I \rangle} \right) dI \quad (2.42)$$

where $\langle I \rangle$ is given by (2.40) and $p(I)$ probability density of the intensity.

Along with (2.42) and the correlation time of the intensity fluctuations, a complete picture of the intensity fluctuation of the scattered light which arrives at an arbitrary point on the receiver surface is obtained.

The next step is to investigate the spatial distribution of the intensity over the receiver surface.

2.7.1b Spatial Correlation. While Section 2.8.1a employed the intensity correlation function, written as

$$R_I(\vec{r}_1, \vec{r}_2, t) = \langle I(\vec{r}_1, 0) I(\vec{r}_2, t) \rangle \quad (2.43)$$

with the special condition $\vec{r}_1 = \vec{r}_2 = \vec{r}$ in order to analyze the temporal fluctuations of the scattered light at a point, this section employs the condition $t = 0$ and $r_1 \neq r_2$ to study the spatial distribution of the scattered light. The goal is to find the maximum region on a portion of the receiver surface over which an instantaneous value of the intensity remains relatively uniform (or constant); under such conditions, of course, the intensity at any two points within the region has a high spatial correlation. Rather than calculate this region, which will be referred to as the spatial coherence area, directly from (2.43), a better understanding of the principles involved can be obtained with a geometric approach.

From Figure 2.4 consider two scatterers at O and P scattering light to A and B on the receiver. The phase of the light which arrives at A from P is given by $\phi_P^A = \frac{2\pi}{\lambda} r_P^A + \gamma_P^A + \phi_S^P$, where λ is the wavelength, r_P^A is the geometric path from P to A, γ_P^A is the random phase factor attributed to turbulence along P to A, and ϕ_S^P is the phase of the light at P from the laser. Similar relations exist for the light traveling from P to B, O to A, and O to B. The relative phase difference of the light arriving at A from both P and O ($\Delta\phi_{PO}^A = (\phi_P^A - \phi_O^A)$) will have approximately the same relative phase difference at B ($\Delta\phi_{PO}^B = (\phi_P^B - \phi_O^B)$) provided

$$|\Delta\phi_{PO}^B - \Delta\phi_{PO}^A| \leq \pi/8 \quad (2.43a)$$

Under the conditions of (2.43a) the intensity of the light at both A and B is also approximately the same. Relation (2.43a) can be written as

$$\left| \frac{2\pi}{\lambda} \left[\overbrace{(r_P^B - r_P^A) - (r_O^B - r_O^A)}^X + \left(\overbrace{(\gamma_P^B - \gamma_P^A)}^Y - \overbrace{(\gamma_O^B - \gamma_O^A)}^Z \right) \right] \right| \leq \pi/8 \quad (2.43b)$$

(note: the ϕ_S^P and ϕ_S^O terms cancel). Using the Cauchy-Schwartz inequality (2.43b) can be written as

$$|X| + |Y| + |Z| \leq \pi/8$$

The terms $|X|$, $|Y|$, $|Z|$ become larger with increasing r (separation of O and P) and d (separation of B and A): the terms r and d are shown in Figure 2.4. For a fixed r , it will be shown that the point at which $|X| = \pi/8$ both $|Y|$ and $|Z|$ are $\ll \pi/8$. Therefore, $|X|$ dominates the expression (2.43b) which, consequently, simplifies to yield

$$\Delta = |(r_P^B - r_P^A) - (r_O^B - r_O^A)| \leq \lambda/16 \quad (2.43c)$$

Further, the path difference, Δ , in (2.43c) can be expressed in terms of the variables R , r , d , and ϕ as shown in Figure 2.4, so that the solution to (2.43c) becomes

$$\Delta = \left[\frac{d^2}{2R} - \left[(R^2 + r^2 + 2Rr \cos \phi + d^2 - 2rd \sin \phi)^{\frac{1}{2}} - (R^2 + r^2 + 2Rr \cos \phi)^{\frac{1}{2}} \right] \right] = \frac{\lambda}{16} \quad (2.44)$$

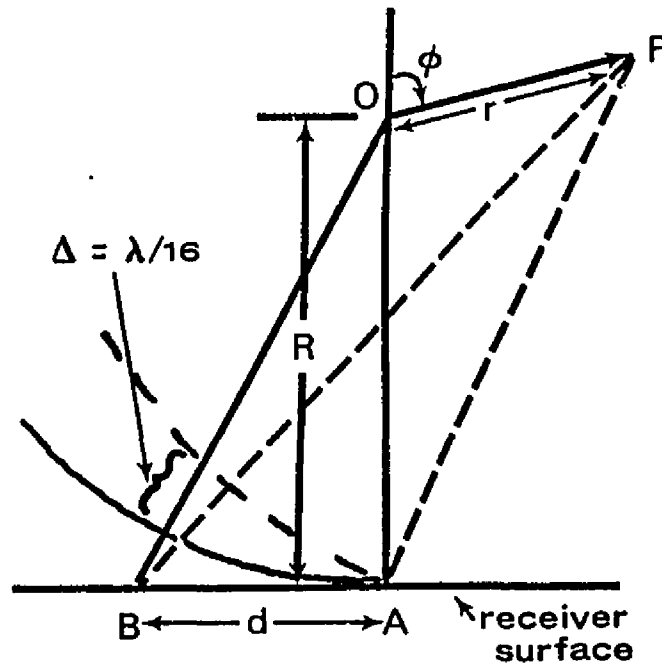


Figure 2.4 The Spherical Phase Surfaces of Two Scatterers at O and P have a Path Difference of $\Delta = \lambda/16$ at the Separation Length d on the Receiver Surface.

Further, since r at most will be limited by the dimensions of the instantaneous scattering volume, the condition $R \gg r$ applies. From this condition (2.44) simplifies to

$$\left| \frac{d^2}{2R} - \left| \frac{d^2 - 2 r d \sin \phi}{2(R^2 + r^2 + 2R r \cos \phi)^{1/2}} \right| \right| = \frac{\lambda}{16} \quad (2.45)$$

where further simplification yields

$$r = \frac{\lambda R^2}{8d} \frac{1}{(d \cos \phi + R \sin \phi)} \quad (2.46)$$

In (2.46) d is the radius of a circular area on the receiver surface, called the spatial coherence area, over which the phase surfaces of the scattered light fields from all the contributing scatterers between O and P remain almost in step. The scattered light comes from a volume a distance R away from the receiver and whose dimensions are given by r and ϕ ; this volume is a volume of revolution. When $(R \sin \phi) \gg (d \cos \phi)$ or $\phi \gg \tan^{-1} (d/R)$, then this volume is a cylinder whose central axis is aligned along \overline{OA} (see Figure 2.3) and whose radius $(= r \sin \phi)$ from (2.46) is given by

$$r \sin \phi = \frac{\lambda R}{8d} = \text{constant} \quad (2.47)$$

Now, for those angles $\phi < \tan^{-1} (d/R)$, the cylindrical volume tapers off, so that at $\phi = 0$, (2.46) reduces to

$$r = \frac{\lambda R^2}{8d^2} \quad (2.48)$$

In order to insure that all the scatterers within the instantaneous scattering volume are contained within this volume of revolution, the radius of this volume (2.47) is set equal to the maximum radius of the instantaneous scattering volume as observed from the receiver. For example, the receiver on the monostatic lidar system has a field of view sufficiently large to include the entire transmitted laser beam. Therefore, the radial dimension of the instantaneous scattering volume is defined strictly in terms of the geometry of the

transmitted beam. In this connection the radius of the effective transmitted beam, ρ_s , at a distance R from the laser head is given by

$$\rho_s = \theta_T (R^* + R) \quad (2.49)$$

where θ_T is the half-angle beam width and R^* is the radius of curvature of the phase surfaces of the laser light at the laser emitter. This radius, ρ_s , is set equal to (2.47). Therefore, the size of the coherence area on the surface, πd^2 , can be written entirely in terms of measurables, so that

$$\text{Spatial coherence area} = \pi d^2 = \pi \left| \frac{\lambda R}{8 \theta_T (R^* + R)} \right|^2 \quad (2.50)$$

Further, if P is the radius of the collecting aperture at the receiver surface, then the number of coherence areas, M , which are contained over this surface is

$$M = \frac{\pi P^2}{\pi d^2} = \left(\frac{8 \theta_T (R + R^*) P}{\lambda R} \right)^2 \quad (2.51)$$

The significance of all the calculations from (2.44) to (2.51) is as follows. The instantaneous value of the scattered light intensity from all the molecular and particulate scatterers which arrives at one point on the receiver depends on the temporal arrangement of all the phase surfaces which compose the scattered light. This temporal arrangement of phase remains almost the same (or in step) over a spatial

coherence area (2.50). Further, the light which arrives at two points on the receiver whose separation is greater than the diameter of a coherence area must necessarily have light arriving at these two points with a path difference, Δ , greater than $\lambda/16$. Therefore, the phase surfaces of the light are arriving with essentially a different temporal order at the two points. This, in turn, results in a different value of the instantaneous intensity at the two points. Yet, around each of these two points there is a region (spatial coherence area) over which the intensity is nearly uniform. From these relationships, it is seen that the receiver surface contains, on the average, M spatial coherence areas (2.51) over any one of which the instantaneous value of the intensity is nearly uniform, but between any two of which the instantaneous intensity values result from the different phase positions of the scatterers as calculated at the coherence areas on the receiver, the statistical values which the instantaneous intensity are most likely given by (2.42), the Rayleigh distribution. This then completes the temporal and spatial description of the probability distribution of the scattered light which arrives on the receiver surface.

Before the means by which the light is converted into a measurable current is discussed the effects of the scatterers between the scattering volume and the receiver must be considered.

2.8 Effects of the Atmospheric Scatterers between the Scattering Volume and Receiver

2.8.1 Turbulent Refractive Inhomogeneities

The turbulent refractive inhomogeneities cause a degradation of the phase structure of the light which reaches the receiver from the scattering volume.

The analysis of the degradation of the phase structure is similar to that done for the transmitted light. Recall the conclusion that the relative phases from a collection of scatterers within the same coherence volume can always be calculated; the relative phases are simply dependent on the relative separation of the scatterers in the direction of the transmitted laser light.

With regard to the scattered light to the receiver, the actual separation of any two scatterers can be divided into a transverse component, parallel to the receiver surface, and a longitudinal component, perpendicular to the receiver surface. An increase in the transverse separation causes the light from the two scatterers to pass through increasingly independent turbulent scatterers which results in a loss of the phase correlation of the received light. On the other hand, an increase in the longitudinal component within the boundaries of the coherence volume, defined by the transmitted laser light, causes only a slight difference in the relative phase at the receiver and, therefore, a negligible effect on the phase correlation of the received light.

The transverse separation of the scatterers acts as the effective separation of a double slit. When the visibility of the fringes (δ) is calculated by means of (2.12), (2.13), and the perturbation method for calculating the composite field reaching the receiver surface, an expression is obtained and written as

$$\delta = \sqrt{1 - K_1 F(|\vec{r}_1 - \vec{r}_2|)} \quad (2.52)$$

where K_1 is a factor related to the strength of the turbulence, and $F(|\vec{r}_1 - \vec{r}_2|)$ is a geometric factor related to the effective separation of the double slit (or the equivalent transverse separation of scatterers). When there is no turbulence K_1 equals 0 and consequently the visibility of the fringes equals 1.00, as it should.

The expression, (2.52), yields a means by which the phase effects of turbulence on the received laser light can be assessed. It is assumed that the maximum transverse separation ($|\vec{r}_1 - \vec{r}_2|$) up to the boundaries of the coherence volume defined by the transmitted laser light, at which the fringe visibility equals 0.88, is the point at which the turbulent inhomogeneities introduce a random factor into the relative phase of the light arriving from the two scatterers on the receiver surface. In this connection, a collection of scatterers will conserve their relative phase at a point on the receiver provided both the transverse component of

the particle separation between any two particles in the collection is less than the transverse separation ($|\vec{r}_1 - \vec{r}_2|$) and the collection of particles is in the same coherence volume defined by the transmitted laser light. These restrictions define a new coherence volume which will be called the mutual coherence volume (MCV). The final dimension of the MCV which must be specified is the maximum transverse separation; MTS will be used for brevity. To this end, Table 2.3 shows this dimension as a function of range from the receiver. In addition these values of the MTS in weak turbulence are always greater than the geometric spatial coherence length, d , as defined in (2.47) in the previous section, so that the definition of the spatial coherence area according to (2.50) is always valid.

Table 2.3 The Maximum Transverse Separation, MTS, of the Received Scattered Light as a Function of Increasing Range Through a Homogeneous, Weak ($C_n^2 = 1 \times 10^{-16}$) Turbulent Atmosphere.

RANGE	MTS
km	cm
0.5	34.4
1.0	20.6
2.0	15.1
3.0	11.9
4.0	10.1
5.0	8.8

2.8.2 Molecular (Rayleigh) and Particulate Effects

The results of Appendix B showed that the forward scattered light which arrives at some distant field point within the transmitted beam from the molecules and particulates is two orders of magnitude less than the directly transmitted laser light. Therefore, except for attenuation by the molecules and particulates, the laser light is transmitted essentially unaffected by these scatterers. For the same reasons, it is assumed that the light arrives at the receiver essentially unaffected by the molecules and particulates except for attenuation. Therefore, all that has been done regarding the probability distribution of the scattered light which arrives at the receiver remains unchanged except that the above mentioned attenuation must be included. This last point about attenuation leads into the next topic before the receiver effects are discussed.

2.9 Transmittance Fluctuations

This section discusses the second source of experimental error which hampers the measurement of the properties of the scattered light. The molecules and particulates change the transmittance of the light over two paths: (1) laser source to scattering volume and (2) scattering volume to receiver. These transmittance changes occur from greater and lesser numbers of scatterers occupying the transmission

paths (1) and (2). Further, these fluctuations cannot be differentiated from those caused by phase changes associated with scatterer motion within the instantaneous scattering volume (this is the first source of experimental error). Appendix E calculates the magnitude of these transmittance fluctuations caused by Brownian and turbulent motion along the two-way transmission path. Results are specifically calculated for the University of Arizona monostatic, laser-receiver system operating under normal atmospheric conditions. This result shows that these transmittance fluctuations are well below 1% about a mean transmittance assuming average number densities of molecules and particulates. In light of the results of Chapter 3, which show that the fluctuations in the scattered light about a mean, caused by scatterer motion within the instantaneous scattering volume, are much greater than 1%, the transmittance fluctuations are neglected.

2.10 Receiver Effects

Since the scattered laser light intensity from typical concentrations of atmospheric scatterers which arrives at the receiver is relatively weak, the light is usually collected by a large aperture in order to obtain a sufficiently strong signal for measurement. The collected light is then focused by an optical system onto a photosensitive surface to begin the conversion of the light to an electrical current.

At this point an important property of the optical focusing system must be mentioned. It should be emphasized that the interference pattern which appears on the receiver aperture also appears on the photosensitive surface; just the relative dimensions of the pattern are changed by the optical system. This point is important because it is the ratio of the receiver aperture area to the spatial coherence area of the interference pattern that partly determines the statistical nature of the electrical current associated with the collected light intensity.

The photosensitive surface which the collected and focused light strikes is just the photocathode surface of a photo-multiplier tube (PMT). Electrons are emitted from the photocathode surface in proportion to the light intensity, but only on the average. In actuality, the electrons are emitted in bursts according to a Poissonian probability distribution. This characteristic, therefore, requires the statistics of the photocathode current correlation function be coupled to the intensity correlation function.

An additional modification of the photocathode electron current occurs as the photocathode electron stream passes through the amplification dynodes of the PMT. A single photocathode electron becomes amplified into a pulse of electrons of ever increasing strength at each dynode stage. Upon leaving the amplification system the electrons arrive at the anode as a pulse of strength μe , where μ is the

amplification factor (gain) and e is the magnitude of the electronic charge. In addition, the pulse is broadened because of spread in the transit times of the electrons in the amplification system.

The characteristic of the conversion process outlined above is the addition of a fluctuating noise factor, called shot noise, to the photoanode current. This shot noise is the third source of experimental error outlined in Chapter 1.

In the following section, the correlation function of the photoanode current associated with the scattered light is calculated. This function is employed in the same manner as the scattered intensity correlation function; namely, the photoanode current correlation function yields the first two statistical moments of the current fluctuations, $\langle i \rangle$ and $\langle i^2 \rangle$, respectively, as well as the current correlation (or independence) time. From these parameters a complete statistical description of the photocurrent fluctuations associated with the scattered light fluctuations is obtained.

The calculations of the photocurrent correlation function are divided into a number of sub-sections. First, the photocurrent correlation function is calculated when the scattered light illuminates just one spatial coherence area, while the next section includes the effects of an arbitrary number of spatial coherence areas. This last subsection will

present the photoanode current correlation function in its most general form. The next sub-section treats the filtering of the photoanode current, while the last sub-section discusses the statistical properties of the filtered photoanode current.

2.10.1 Photocurrent Correlation Function for One Spatial Coherence Area

Greytak (1970) calculates the photoanode current correlation function for a photomultiplier tube illuminated by a spatially uniform intensity. His results apply to an area of any size and, therefore, in particular, to a spatial coherence area. In Appendix D, Part I, the steps similar to the method by which Greytak calculates the photocurrent correlation function are presented. Greytak made a number of errors in his original manuscript; these errors are corrected but not discussed. The final result for the photocurrent correlation function, $R_i'(t)$, in terms of measurables is

$$\begin{aligned} R_i'(t) &= \langle i'(0) i'(t) \rangle \\ &= \frac{\mu e}{2RC_s} (\alpha \mu e \langle F' \rangle) e^{-t/RC_s} + (\alpha \mu e)^2 R_F'(t) \end{aligned} \quad (2.53)$$

where $i'(0)$ and $i'(t)$ are the photoanode currents at time 0 and t , respectively, μ is the gain factor of the photomultiplier tube, α is the electron conversion efficiency of the photoanode (electrons/joules), e is the magnitude of the electronic charge, the product, RC_s , is the response time of

the PMT and represents the spread in transit time of the photoelectrons $\left[\overline{RC}_s \sim 10^{-9} \text{seconds} \right]$, $\langle F' \rangle$ is the mean flux of the scattered light collected by the one coherence area, while $R_F'(t)$ is the flux correlation function, written as

$$R_F'(t) = \langle F'(0) F'(t) \rangle \quad (2.54)$$

where $F'(0)$ and $F'(t)$ are the fluxes of the scattered light collected by one coherence area at time 0 and t , respectively. Both $\langle F' \rangle$ and $R_F'(t)$ are related to the scattered intensity by the following relations:

$$\begin{aligned} \langle F' \rangle &= \iint \langle I \rangle dA_R d\omega_s \left[\overline{\text{watts}} \right] \\ R_F'(t) &= \iint \iint R_I(t) dA_R d\omega_s dA_R' d\omega_s' \left[\overline{\text{watts}}^2 \right] \end{aligned} \quad (2.55)$$

where dA_R and dA_R' are elements of a coherence area on the receiver surface and $d\omega_s$ and $d\omega_s'$ are elements of solid angle subtended by an element of the instantaneous scattering volume at the receiver. Now, the dA_R 's are integrated over the coherence area, while the $d\omega_s$'s are integrated over the solid angle subtended by the instantaneous scattering volume at the receiver. Finally, it should be pointed out that the first expression on the right-hand side of (2.53) is the contribution to $R_i'(t)$ from shot noise (the third and final source of experimental error), while the second term is the contribution of the scattered intensity fluctuations via (2.55) (The first contribution to the experimental error).

2.10.2 Photocurrent Correlation Function for Many Spatial Coherence Areas

If the light incident on the photomultiplier tube contains M spatial coherence areas, then the photoanode current can be thought of as the independent sum of M photoanode currents each coming from one coherence area. Consequently, the photoanode current correlation function, $R_i(t)$, from M coherence areas is written as

$$R_i(t) = \langle i(o) i(t) \rangle = \left\langle \sum_{p=1}^M i'_p(o) \sum_{q=1}^M i'_q(t) \right\rangle \quad (2.56)$$

Since the contribution to the photocurrent from each coherence area is independent of another (since the illuminating intensities over each coherence area are independent); terms such as $\langle i'_p(o) i'_q(t) \rangle$ for $p \neq q$ must become $\langle i'_p(o) \rangle \langle i'_q(t) \rangle = \langle i' \rangle^2$, while terms for $p = q$ must become $\langle i'_p(o) i'_p(t) \rangle = R'_i(t)$. From these relations (2.56) becomes

$$R_i(t) = (M^2 - M) \langle i' \rangle^2 + M R'_i(t) \quad (2.57)$$

where M is the number of coherence areas and $\langle i' \rangle$ is the mean photoanode current from one coherence area, while $R'_i(t)$ is the photocurrent correlation function from one coherence area and is given by (2.53). The expression (2.57) is the most general form of the photoanode current correlation function.

2.10.3 Filtering the Photoanode Current

The University of Arizona laser-receiver has a post detection circuit which integrates the raw photoanode current from the PMT. Along with this integration the circuit filters the shot noise contribution to the photoanode current, while passing the fluctuations associated with the scatterers. The filtering circuit acts as an equivalent RC_f (f subscript denotes filter) filter (resistor-capacitor in series) with a time constant, $(RC)_f \sim 2.5 \times 10^{-8}$ seconds, (equivalent to 40 MHz band pass). Appendix D, Part 2 shows that the filtering modifies the shot noise portion of the photoanode current correlation function (see 2.53), so that (2.57) becomes

$$R_i(t)_f = (M^2 - M) \langle i' \rangle^2 + M R_i'(t)_f \quad (2.58)$$

where

$$R_i'(t)_f = \frac{\mu e}{4RC_f} (\alpha \mu e \langle F' \rangle) e^{-t/RC_f} + (\alpha \mu e)^2 R_p'(t)$$

where the f subscript denotes the filtered values. One notes that the shot noise portion of the filtered photocurrent is reduced to $\frac{1}{2}$ of that associated with the unfiltered shot noise expressed by (2.53). However, since $(RC)_f \sim 2.5 \times 10^{-8}$, the filtering increases the correlation time of the

shot noise. This has some important consequences which are discussed in Chapter 3.

2.10.4 The Statistical Properties of the Filtered, Photoanode Current

Employing the properties of the filtered, photoanode current correlation function, (2.58), as is done for the intensity correlation function (see 2.35 and 2.36), the first two moments of the filtered photocurrent probability distribution can be found, yielding

$$\lim_{t \rightarrow 0} R_i(t)_f = \langle i^2 \rangle \quad (2.59)$$

$$\lim_{t \rightarrow \infty} R_i(t)_f = \langle i \rangle^2$$

Using (2.58), (2.59) becomes

$$\begin{aligned} \langle i^2 \rangle &= (M^2 - M) \langle i' \rangle^2 + M R_i'(0)_f \\ \langle i \rangle^2 &= (M^2 - M) \langle i' \rangle^2 + M R_i'(\infty)_f \end{aligned} \quad (2.60)$$

Now,

$$\begin{aligned} R_i'(0)_f &= \langle i'^2 \rangle = \frac{\mu e}{4RC_f} (\alpha \mu e \langle F' \rangle) + (\alpha \mu e)^2 R_F'(0) \\ R_i'(\infty)_f &= \langle i' \rangle^2 = (\alpha \mu e)^2 R_F'(\infty) \end{aligned} \quad (2.61)$$

Now combining (2.60) to (2.61) and simplifying yields

$$\begin{aligned} \langle i^2 \rangle &= (M^2 + M) \langle i' \rangle^2 + M \langle i' \rangle \left[\frac{\mu e}{4RC_f} \right] \\ \langle i \rangle^2 &= M^2 \langle i' \rangle^2 \end{aligned} \quad (2.63)$$

Now since $M\langle F' \rangle$ is the total mean flux density, $\langle F \rangle$, over the whole receiver surface, it is easily shown that the mean and the variance of the filtered, photoanode current are

$$\begin{aligned} \langle i \rangle &= \mu q \langle F \rangle \\ \sigma_i^2 &= \langle i^2 \rangle - \langle i \rangle^2 = \underbrace{\frac{\mu e}{4RC_f}}_{\sigma_n^2} \langle i \rangle + \underbrace{\frac{\langle i \rangle^2}{M}}_{\sigma_s^2} \end{aligned} \quad (2.64)$$

where $q = \alpha e$ and has the units of amperes per watt. The above expression shows that the mean photoanode current is directly related to the mean flux from the scatterers collected by the receiver surface which, in turn, is directly related to the mean scattered intensity. The variance on the other hand is dependent on the shot noise fluctuations, σ_n^2 , and the fluctuations in the intensity of the scattered light as expressed by σ_s^2 .

The next step is to attempt a calculation of the most likely probability distribution associated with (2.64). It will be recalled that this was done for the intensity distribution of the scattered light (see 2.42). However, the task in attempting to calculate $p(i)di$ (probability distribution of the current) is more complicated.

Rice (1954) has made an extensive study of shot noise. He showed that, if the mean photocurrent is sufficiently strong, the shot noise is normally distributed about the mean according to

$$p(i)di = (2\pi\sigma_n^2)^{-\frac{1}{2}} \exp \left\{ -\frac{(i - \langle i \rangle)^2}{2\sigma_n^2} \right\} di \quad (2.65)$$

from shot
noise only

where, of course, $\langle i \rangle$ is the mean and σ_n^2 is given in (2.64).

With regard to that portion of the photocurrent associated with scattered light fluctuations, it seems logical to assume that the photocurrent distribution would be analogous to the intensity distribution, but with some modifications. First, the photocurrent distribution from one spatial coherence area $\int p(i') di'$ would follow the Rayleigh distribution of the scattered intensity according to

$$p(i') di' = \frac{i'}{\langle i' \rangle} \exp \left\{ -\frac{i'}{\langle i' \rangle} \right\} di' \quad (2.66)$$

from light
fluctuations
only

where $\langle i' \rangle = \mu q \langle F' \rangle$

However, the photocurrent probability distribution associated with M independent spatial coherence areas is a little more complicated, but standard probability texts show how the distribution can be easily calculated, so that

$$p(i)di = \frac{1}{\langle i' \rangle} \frac{M}{(M-1)!} \left(\frac{i}{\langle i' \rangle} \right)^{M-1} \exp \left(\frac{-i}{\langle i' \rangle} \right) di \quad (2.67)$$

from light
fluctuations
only

From this distribution it is easily shown that

$$\langle i \rangle = M \langle i' \rangle$$

$$\langle i^2 \rangle = (M^2 + M) \langle i' \rangle^2$$

which implies that $\sigma_i^2 = \frac{\langle i \rangle^2}{M}$ and is equivalent to σ_s^2 in (2.64). The expression for (2.67) simplifies even further when M is large, i.e., it approaches the normal distribution equivalent to (2.65), so that

$$p(i)di = (2\pi\sigma_s^2)^{-\frac{1}{2}} \exp\left\{-\frac{(i - \langle i \rangle)^2}{2\sigma_s^2}\right\} di \quad (2.68)$$

from light
fluctuations
only

If the probability distributions associated with the shot noise and light fluctuations are independent, the same probability texts (Uspensky 1937, in particular) show that the joint probability distribution of both the shot noise and light fluctuations can be found by taking the Fourier transforms of (2.65) and (2.68), consolidating them, and calculating the inverse Fourier transform; the result is

$$p(i)di = (2\pi\sigma_i^2)^{-\frac{1}{2}} \exp \left\{ -\frac{(i - \langle i \rangle)^2}{2\sigma_i^2} \right\} di \quad (2.69)$$

where $\langle i \rangle$ and σ_i^2 are given by (2.64). This distribution seems to be the most likely probability distribution of the filtered photoanode current. The conditions require that $\langle i \rangle$ must be reasonably large with respect to σ_i and that M be fairly large. It will be shown in the next chapter that the conditions of large M are well-satisfied by the University of Arizona laser system operating under normal conditions, while $\langle i \rangle$ being reasonably large with respect to σ_i is satisfied most of the time. If $\langle i \rangle \leq 2\sigma_i$, then (2.65) and, therefore, (2.69) cannot be used. This is also obvious from (2.69) since such a condition would cause $p(i)di$ to be positive in the region $i < 0$ which is not physically realizable.

Therefore, the probability distribution (2.69) completely specifies all the information obtainable about the magnitude of the photoanode current fluctuations associated with the fluctuations in the scattered light. However, the photocurrent correlation function (2.58) provides the correlation time for the photocurrent to assume an independent value. The correlation time and probability distribution are necessary in order to make an estimate of the true mean photocurrent associated with the true mean intensity of the scattered light which is the main goal of this dissertation. In the next chapter (2.58) and (2.69) are used to analyze

the ability of the University of Arizona monostatic laser receiver system to estimate the true mean photocurrent, $\langle i \rangle$ associated with the true mean intensity of the scattered light.

2.11 Chapter Summary

Only the important results are summarized here. The scattered light which arrives on the receiver surface fluctuates because of the motions of the molecular and particulate scatterers. The fluctuations are most likely distributed about a mean according to the Rayleigh distribution (see 2.42). The mean intensity of this distribution is the independent sum of the intensities from each scatterer (see 2.40) which, on the average, occupies the scattering volume. The fluctuations in the transmittance of the light, because of molecules and particulate number density fluctuations along the laser source - scattering volume - receiver path, are negligible (see Section 2.9). The fluctuating light field which is collected by the receiver optics is focused onto a photomultiplier tube where the light is converted into a measurable current (see Section (2.10)). The fluctuating current (photoanode current) is composed of the fluctuations associated with the light and some additional fluctuations associated with the light conversion process, shot noise (see 2.53). In order to reduce the shot noise, the photocurrent is filtered (see 2.65). Finally, the

fluctuations in the filtered photoanode current about a mean are shown to be distributed, most likely, according to a normal distribution (see 2.69). The mean photoanode current is proportional to the mean intensity, while the variance is proportional to the shot noise and light fluctuations (see 2.69). The correlation time between independent values of the filtered photoanode current is obtained from the photoanode current correlation function (see 2.58). All of the previous is necessary for the calculations of Chapter 3.

CHAPTER 3

RESULTS

3.1 The Photoanode Current Fluctuations for the University of Arizona Monostatic Lidar

Using the mathematical relationships developed in Chapter 2, the ability of the University of Arizona monostatic laser-receiver to estimate the true mean photoanode current associated with the true mean intensity of the scattered light can be calculated. To achieve this purpose the parameters associated with the probability distribution of the photoanode current must be evaluated in terms of measurables. The photocurrent probability distribution has been shown to be

$$p(i)di = \frac{1}{\sqrt{2\pi}\sigma_i} \exp \left\{ -\frac{(i - \langle i \rangle)^2}{2\sigma_i^2} \right\} di \quad (3.1)$$

where

$$\begin{aligned} \langle i \rangle &= \mu q \langle F \rangle \\ \sigma_i^2 &= \sigma_n^2 + \sigma_s^2 = \frac{\mu e}{4(RC)_f} \langle i \rangle + \frac{\langle i \rangle^2}{M} \end{aligned}$$

In (3.1), i is the instantaneous value of the filtered photoanode current. The mean photocurrent, $\langle i \rangle$ (amperes), depends upon the mean flux from the atmospheric

scatterers $\langle F \rangle$ (watts) collected by the receiver optics, the conversion factor, q (amperes/watts), and the amplification factor, μ . The variance, σ_i^2 , consists of the sum of the shot noise (σ_n^2) and the variance of the current associated with light intensity fluctuations caused by the motions of the atmospheric scatterers (σ_s^2). The term e is the magnitude of the electronic charge and $(RC)_f$ is the time constant of the circuit which filters the raw photoanode current, while M is the number of spatial coherence areas the instantaneous scattering volume projects on the receiver surface.

For the monostatic lidar system, the laser source and receiver are as coaxial as is physically permitted. Therefore, the laser light which illuminates the scatterers within the instantaneous scattering volume is directly back-scattered to the receiver. Consequently, the scattering angle, θ , is virtually 180° ; this condition eliminates a number of cumbersome problems. For example, the size and shape of the instantaneous pulse volume V_{ip} becomes simply related to size and shape of the laser pulse volume, V_p . The exact relationship is given as

$$V_{ip} = \frac{V_p}{2 \sin^2(\frac{\theta}{2})} = \frac{V_p}{2} \quad (\text{at } \theta = 180^\circ) \quad (3.2)$$

Further, since the light paths from the source to receiver

coincide, the attenuation of the light over the whole path can be calculated in terms of the properties of just one path.

The first step in specifying the parameters of (3.1) is to calculate the mean instantaneous flux of the scattered light collected by the receiver optics, $\langle F \rangle$. The expression for $\langle F \rangle$ in terms of the physical parameters can be written as

$$\langle F \rangle = \underbrace{\left(\frac{E_T c}{V_p} \right)}_{\leftarrow A \rightarrow} \underbrace{(\ell_s)}_{\leftarrow B} \underbrace{(V_{ip} \beta_s(180, R))}_{\rightarrow C \rightarrow} \underbrace{\left(\frac{A_R}{R^2} \right)}_{\leftarrow D \rightarrow} \underbrace{\langle T_1(O, R) T_2(O, R) \rangle}_{\rightarrow} (\ell_R) \quad (3.3)$$

In (3.3) the term A is the normal flux density of the laser light (energy/unit normal area, time) which arrives at the instantaneous scattering volume a distance R away. Specifically, E_T is the total energy (joules) initially contained in the laser pulse and V_p is the volume of the laser pulse at range R, while c is the speed of light. The term ℓ_s is the fraction of the available light transmitted by the source optics. The second term, B, is the product of the instantaneous scattering volume, V_{ip} , and the volume back-scattered coefficient per unit solid angle $(\text{km str})^{-1}$ at range R. Term C is the solid angle subtended by the collecting area of the receiver at the scattering volume (str) written as the ratio of the normal receiver area, A_R , to the square of the range, R^2 . Term D expresses the amount of

light transmitted as the light passes to the scattering volume $T_1(O,R)$, and back to the receiver, $T_2(O,R)$, respectively. When the two paths coincide, as for the backscattered light, $T_1(O,R)$ equals $T_2(O,R)$. Finally, the last term in (3.3), ℓ_R , is the fraction of the available light transmitted by the receiver optics to the surface of the photomultiplier tube. The transmittance factors can be expressed in terms of the volume scattering coefficients of all the scatterers encountered along a vertical path in the atmosphere. In Appendix E such a relationship is calculated in order to study the fluctuations in the transmittance. The result shows that the total transmittance associated with the particulate scatterers is given by

$$\langle \bar{T}_1(O,R) T_2(O,R) \rangle_p = T_1^2(O,R)_p = e^{-2\tau_p(O,R)} \quad (3.4)$$

where $\tau_p(O,R)$ is the particulate optical depth (see 2.7, Chapter 2) from the ground to a range position, R , along a vertical ($z=R$) path and for the model of the vertical distribution used here is given by

$$\tau_p(O,R) = \tau_T^p \{1 - \exp[-(0.8 \text{ km}^{-1})R]\} \quad (3.5)$$

where τ_T^p is the total particulate optical depth of the atmosphere.

Expressions equivalent to (3.4) and (3.5) exist for the molecules which have not been needed in the development

up to this point. Rather than make a detailed calculation, the form suggests itself by analogy to (3.4) and (3.5). First, it is obvious that

$$\overline{T_1(O,R)T_2(O,R)}_m = T_1^2(O,R)_m = e^{-2\tau_m(O,R)} \quad (3.6)$$

where $\tau_m(O,R)$ is molecular optical depth over the vertical path from zero to R . The exponential within the brackets of (3.5) is exactly the height-number density relationship for the particulates for the Air Force "clear atmosphere" model (see 2.3, Chapter 2). Similarly, the functional decrease of molecular density with height is available in the Smithsonian Meteorological Tables (1958). For the purposes of this dissertation, the simple isothermal atmosphere yields an adequate functional dependence (since we are dealing with a narrow height range); this relation is given by

$$\frac{\rho(z)}{\bar{\rho}_s} = \exp\left(-\frac{z}{H}\right) \quad (3.7)$$

where $\rho(z)$ is the molecular density at height z , $\bar{\rho}_s$ is the density at sea level, and H is the scale height of the isothermal atmosphere. Using (3.7) the molecular optical depth $\tau_m(O,R)$ may be expressed as

$$\tau_m(O,R) = \tau_T^m \{1 - \exp[-(H)^{-1}R]\} \quad (3.8)$$

Since Tucson is not at sea level, $\bar{\rho}_s$ must be adjusted slightly. With this adjustment, a value of $H = 8.5$ km seems to give the best approximation to the actual density-height relationship. The combined transmittance, $T_1^2(O,R)$, of the molecular and particulate atmosphere is given by the product of (3.4) and (3.6), so that

$$\begin{aligned} T_1^2(O,R) &= [\bar{T}_1^m(O,R) T_1^p(O,R)]^2 \\ &= \exp \{-2[\bar{\tau}_m(O,R) + \tau_p(O,R)]\} \end{aligned} \quad (3.9)$$

The volume backscattering coefficient, $\beta_s(180,R)$ expressed in (3.3) is the sum of the separate volume backscattering coefficients from the molecules, $\beta_s^m(180,R)$ and the particulates, $\beta_s^p(180,R)$. This follows from a conclusion of Chapter 2 (see 2.41) which shows that the mean scattered intensity from a collection of molecules and particulates is the sum of the separate scattered intensities from each scatterer. Appendix B shows that the $\beta_s^p(180,R)$ at any height can be related to the particulate density of the Air Force "clear atmosphere." This relation, in turn, is related to the particulate optical depth (Appendix B) so that

$$\beta_s^p(180,R) = \frac{(0.8 \text{ km}^{-1})}{S} \tau_T^p \exp [(-0.8 \text{ km}^{-1})R] / \text{km str}^{-1} \quad (3.10)$$

where S is the ratio of the normalized volume attenuation coefficient, $\tilde{\beta}_t^p / \text{km}^{-1}$, to the normalized volume

backscattering coefficient, $\tilde{\beta}_S^P(180) \text{ [km str]}^{-1}$. For a Junge distribution with $v^* = 3.0$, for which the calculations in this dissertation are done, $S = 19 \text{ str}$.

A relation analogous to (3.10) exists for the molecules. Again, by similarities this relation is

$$\beta_S^m(180, R) = \frac{(H)^{-1} \tau_T^m}{S'} \exp \left[-(H)^{-1} R \right] \quad (3.11)$$

where S' is the ratio of the molecular volume attenuation coefficient to the volume backscattering coefficient. The work of Appendix C indicates that S' is equal to $8\pi/3 \text{ (str)}$.

The equations (3.4) through (3.11) have completely specified the scattering properties of the molecular and particulate atmosphere in terms of their respective total optical depth--a great convenience.

A certain number of parameters associated with the characteristics of the University of Arizona monostatic laser receiver facility remain to be specified before $\langle i \rangle$ and σ_i^2 in (3.1) can be calculated as a function of range. Some of these parameters have already been mentioned, but will be presented again for the immediately following calculations. The parameters which apply to (3.1) and (3.3) are:

$$\begin{aligned} \theta_T &= 1.5 \times 10^{-3} \text{ radians} & \ell_S &= 0.80 \\ R^* &= 7.5 \text{ cm}/\theta_T = 0.5 \text{ km} & \ell_R &= 0.65 \\ \mu &= 10^7 & E_T &= 1 \text{ joule} \end{aligned}$$

$$\begin{aligned}
 e &= 1.6 \times 10^{-19} \text{ (coul)} & A_R &= \pi P^2 \\
 (RC_f)^{-1} &= 40 \text{ MHz} & P &= 15 \text{ cm} \\
 q &= 0.02 \text{ amperes/watt} & \theta_R &= 3 \times 10^{-3} \text{ radians} \\
 & & \lambda &= 6943 \text{ \AA}
 \end{aligned}$$

where θ_T is the half-angle divergence of the laser beam as it leaves the collimation optics, R^* is the ratio of the radius of the laser beam cross-section as it leaves the source optics (7.5 cm) to θ_T , μ is the gain of the PMT, e is the magnitude of the electronic charge, $(RC_f)^{-1}$ is the filter band width of the post detection circuit employed to reduce shot noise, q is the PMT sensitivity, ℓ_s is the fraction of available light transmitted by the source optics, while ℓ_R is the fraction of the available light transmitted by the receiver optics, E_T is the total energy contained in one laser pulse, A_R is the area of the receiver lens, while P is its radius, and finally θ_R is the half-angle field of view of the receiver optics and λ is the wavelength of the ruby laser light.

When these constants are applied to (3.1) through (3.10) for a vertically propagating beam (where the total molecular and particulate optical depths for typical operating conditions are $\tau_T^m = 0.036$ and $\tau_T^p = 0.25$, respectively), the results are given in Table 3.1

Before $\langle i \rangle$ and σ_i^2 are calculated, the number of spatial coherence areas, M , over the receiver surface associated

with the instantaneous scattering volume must be calculated. Chapter 2 (2.51) gives this number in terms of measurables and is rewritten below. This specific form requires that $\theta_T < \theta_R$ as indicated in the parameter listing, so that

$$M \sim \frac{\text{Area of receiver}}{\text{Coherence area}} = \left(\frac{8\theta_T (R+R^*) P}{\lambda R} \right)^2 \quad (3.12)$$

Expression (3.12) completes all the relations needed to calculate $\langle i \rangle$, σ_i^2 , and $S_N = \langle i \rangle / \sigma_i$, commonly called the signal-to-noise ratio. Therefore, using the results of Table 3.1 and all necessary relations, Table 3.2 is calculated.

From Table 3.2 it is quite apparent that the variance in the photocurrent caused by the shot noise (σ_n^2) is about three to six orders of magnitude greater than the variance associated with the light fluctuations (σ_s^2) caused by the motions of the molecular and particulate scatterers. The reason is the overwhelming number of coherence areas (M) on the receiver surface.

3.2 Estimating the True Mean Photocurrent

The importance of knowing the probability distribution of the photocurrent is related to the degree of confidence in estimating the true mean value of the photocurrent from a fluctuating signal. For the University of Arizona monostatic lidar the photocurrent appears to be normally distributed (3.1) with a variance dependent only on the shot

TABLE 3.1 The Total Flux Collected by the Receiver ($\langle F \rangle$) as a Function of Range (R) for the University of Arizona Monostatic Laser Propagating Vertically. -- The total particulate and molecular optical depths are $\tau_T^P = 0.25$ and $\tau_T^M = 0.036$.

R (km)	$\beta_B^P(180, R)$ (km str) ⁻¹	$\beta_B^M(180, R)$ (km str) ⁻¹	$[\bar{T}_1^P(O, R)]^2$	$[\bar{T}_1^M(O, R)]^2$	A_R/R^2 (str)	$\langle F \rangle$ (watts)
1	47.3 x 10 ⁻⁴	4.49 x 10 ⁻⁴	.759	.9960	70.7 x 10 ⁻⁹	332. x 10 ⁻⁹
2	21.3	4.00	.671	.9925	17.7	35.8
3	9.55	3.55	.635	.9893	7.85	7.75
4	4.91	3.16	.619	.9866	4.42	2.61
5	1.93	2.81	.612	.9841	2.83	0.969

Table 3.2 The Photoanode Current ($\langle i \rangle$), Variance (σ_i^2), and Signal-to-Noise Ratio (S_N) as a Function of Range for the University of Arizona Monostatic Lidar.

R (km)	M	$\langle i \rangle$ (amperes)	σ_n^2 (amperes)	σ_s^2 (amperes)	σ_i^2 (amperes)	$S_N = \frac{\langle i \rangle}{\sigma_i}$
1	149×10^5	43.2×10^{-3}	69.2×10^{-8}	125×10^{-12}	69.2×10^{-8}	50.2
2	37.2	4.65	7.44	5.81	7.44	17.1
3	16.5	1.09	1.61	0.618	1.61	7.95
4	9.30	0.339	0.54	0.124	0.54	4.61
5	5.95	0.126	0.20	0.0267	0.20	2.80

noise. However, it will be recalled from Chapter 2 that (2.69) is not accurate for $\langle i \rangle \leq 2\sigma_i$. Specifically, with this limitation in mind, it is found that for $S_N = 2$ (i.e., $\langle i \rangle = 2\sigma_i$), (3.1) predicts that 2.3% of the current is negative, while for $S_N = 1$, 16% of the current is negative. Consequently, as long as $S_N \geq 2$, an insignificant error is made in assuming (3.1) valid.

The procedure for estimating the true mean photocurrent begins by setting arbitrary limits about the true mean value of the photocurrent as expressed in the probability distribution. These limits are adjusted, taking advantage of the symmetry of the probability distribution, so that the amount of area between the limits is equal to the fraction of the time that the photocurrent remains within the limits.

The limits, i_1 and i_2 , within which 95% of the photocurrent fluctuation is contained, are expressed mathematically by

$$\int_{i_1}^{i_2} p(i) di = 0.95 \quad (3.13)$$

In this connection, if it is desired that the estimate of $\langle i \rangle$, called $\langle i \rangle_{\text{est}}$, be within $\pm 1\%$ of $\langle i \rangle$ with 95% certainty, then

$$\langle i \rangle_{\text{est}} = \langle i \rangle \pm 0.01 \langle i \rangle \quad (3.14)$$

where from (3.13) and (3.14), the limits of i_1 and i_2 must

be

$$\begin{aligned} i_1 &= \langle i \rangle - 0.01 \langle i \rangle \\ i_2 &= \langle i \rangle + 0.01 \langle i \rangle \end{aligned} \quad (3.15)$$

If Δi is defined to be the error spread about the mean ($\Delta i = i_2 - i_1$), and, if f is defined as $\frac{\Delta i}{\sigma_i}$ where σ_i is the variance given in (3.1), then Δi may be written as a function of the instantaneous signal-to-noise ratio, S_N , and the mean photocurrent, $\langle i \rangle$, and f , as

$$\Delta i = \frac{\langle i \rangle f}{S_N} \quad (3.16)$$

This expression may seem somewhat redundant at first, yet it provides a convenient form for the analyses to follow. The 95% confidence interval for the normal distribution, (3.1), requires that $f = 3.92$. In addition, if the tolerated error of $\langle i \rangle_{\text{est}}$ is $\pm 1\% \langle i \rangle$ as expressed by (3.14), then the error spread, Δi , defined by (3.15) must be $0.02 \langle i \rangle$. Therefore, from (3.16)

$$\frac{f}{S_N} = \frac{3.92}{S_N} = 0.02 \quad (3.17)$$

From (3.17) it is easily seen that the instantaneous signal-to-noise ratio, S_N , must assume values on the order of 200! Clearly to achieve such a condition is next to impossible from back-scattered ($\theta = 180$) laser light in typical

scattering atmospheres. At best, as shown by Table 3.2, typical values for the instantaneous signal-to-noise ratio are around 50. Since an estimate of the true mean ($\langle i \rangle_{\text{est}}$) with error limits of $\pm 1\%$ about $\langle i \rangle$ (the true mean) at 95% confidence may be too restrictive, Table 3.3 lists the values that S_N may assume as a function of $\pm X\%$ about $\langle i \rangle$ at $Y\%$ confidence level.

Table 3.3 The Values of S_N as a Function of the Error Spread About the Mean, $\pm X\%$, and the Confidence Level, $Y\%$.

	Y%	
	95	85
$\pm X\%$	± 1	196
	± 2	98
	± 3	49
	± 4	25
	± 5	13
		9

From Table 3.3 it is seen that even for greatly relaxed restrictions on the quality of $\langle i \rangle_{\text{est}}$, the values of S_N are still too large. For this reason, the photoanode current signal must be integrated over many independent values of the signal in order to achieve accurate estimates of $\langle i \rangle$. Since the variance in the photocurrent caused by the scatterers (σ_s^2) is negligible compared to that of the shot noise (σ_n^2) an independent value of the photocurrent appears after

the shot noise correlation time, RC_f (see 2.58, Chapter 2). This value is the $1/e$ time for the current correlation function and is shown from the parameters of the receiver system for the monostatic lidar to be about 2.5×10^{-8} seconds. Since the typical signal fluctuations from the University of Arizona lidar are dominated by shot-noise, the independent signal values occur only after the shot-noise correlation time.

In order to calculate the improvement in the estimate of the mean signal by spatial and temporal averaging of the signal, the probability distribution of the integrated signal must be specified. In this connection probability texts show that a random variable, t , which consists of a sum of K independent values of i , each of which is distributed with mean $\langle i \rangle$ and variance σ_i^2 , is also normally distributed according to

$$P(t)dt = \frac{1}{\sqrt{2\pi} \sigma_t} \exp - \left(\frac{t - \langle t \rangle}{2\sigma_t^2} \right)^2 dt \quad (3.18)$$

where $\langle t \rangle = K \langle i \rangle$

$$\sigma_t^2 = K \sigma_i^2$$

From (3.18) the probability that the integrated photocurrent, t , is within $\pm X\%$ of $\langle t \rangle$ at the $Y\%$ confidence level can be calculated as was done for instantaneous photocurrent.

The result shows that all the values of S_N which appear in Table 4.3 may be reduced by the value \sqrt{K} when applied to estimating $\langle i \rangle_{est}$ from K independent values of the photocurrent.

Now, if a single laser pulse is spatially integrated over a distance ΔR in space (vertically), then the corresponding time length of the current record, T_1 , is $\Delta R/c$. The number of independent values of the photocurrent contained in this record is $K_1 = T_1/(RC)_f$. Further, if the scattering medium remains locally stationary over this region for a length of time, T_2 , and during this time a laser is fired once every $\overline{\Delta t}$ seconds, then the number of independent pulses, K_2 , is $T_2/\overline{\Delta t}$ ($\overline{\Delta t} \geq (RC)_f$). Finally, if the photocurrent is integrated spatially and temporally over all these pulses, then the total number of independent photocurrent values, K , is $K_1 \times K_2$; then,

$$K = K_1 K_2 = \left(\frac{\Delta R}{c(RC)_f} \right) \left(\frac{T_2}{\overline{\Delta t}} \right) \quad (3.19)$$

For a particular example applied to the monostatic system which is typical of normal operations, let $\Delta R = 90\text{m}$, $T_2 = 100$ seconds, and $\overline{\Delta t} = 5$ seconds ($(RC)_f = 2.5 \times 10^{-8}$ seconds). The result shows that $K = 240$, while $\sqrt{K} = 15.5$. Now, dividing all the terms in Table 3.3 by 15.5 shows that the highest value of S_N is 12.6 ($\pm 1\%$ at the 95% level), while the lowest value of S_N is ~ 1 ($\pm 5\%$ at the 85% level). Looking back at

Table 3.2 shows that the actual values of S_N obtainable from the University of Arizona monostatic system can yield very accurate estimates of $\langle i \rangle$ by means of integrating the signal; this is currently being done.

3.3 Photocurrent Fluctuations for the Monostatic System when the Scatterer Noise is Greater than the Shot Noise

In section 3.1 the spatial averaging of the receiver is the primary cause of the scatterer noise (σ_s^2) being less than the shot noise (σ_n^2). In this section the conditions which lead to $\sigma_s^2 \gg \sigma_n^2$ are discussed.

The results at the end of Chapter 2 are general enough to predict the signal fluctuation characteristics of other measurement systems. Using the radar, Marshall et al. (1953) have shown both by theory and experiment that the returned signal fluctuations from a collection of randomly moving scatterers are Rayleigh distributed when the receiver noise is below the signal noise from the scatterers. For the typical radar system (Battan 1959) the half-angle divergence of the transmitter antenna, θ_T , which coincides with the receiver is related to the diameter of the receiver-transmitter antenna, (d') and radar wavelength, λ , by

$$\theta_T = \frac{(0.85)\lambda}{2d'} \quad (3.20)$$

When (3.20) is substituted into (3.12) with $d' = 2P$ and $R^* = 0$, (3.12) becomes

$$M(\text{radar}) \sim 3.0 \quad (3.21)$$

From (3.21) and (2.67), the results show that, when $\sigma_s^2 > \sigma_n^2$ (where σ_n^2 here is noise in the radar receiver system), the signal fluctuations, in accordance with the findings of Marshall, et al. are very nearly Rayleigh distributed. These results give further support to the generality and correctness of the conclusions of Chapter 2.

Perhaps the greatest motivation for creating conditions where $\sigma_s^2 > \sigma_n^2$ is that a spectral analysis of the signal fluctuation can yield the Doppler spectrum associated with the motions of the scatterers. The Doppler-lidar spectrum has the potential to yield information on meteorological phenomena such as wind speeds in the upper atmosphere, clear air turbulence, and circular air motion from small scale vortices such as dust devils and water spouts.

For the monostatic lidar, the ratio (R_a) of σ_s^2 to σ_n^2 can be written in terms of previously mentioned parameters according to

$$R_a = \frac{\sigma_s^2}{\sigma_n^2} = \frac{(RC)_{f^q}}{32e(A_p)} (E_T) c (\ell_s \ell_R) \beta_s (180, R) \pi^2 \lambda^2 T_1^2(0, R) \quad (3.22)$$

where $A_p = \pi(\theta_T(R + R^*))^2$ is the cross-sectional area of the laser beam at the scattering volume. Inspection of (3.22) shows that the most easily adjustable variable would be A_p . If the laser source for the University of Arizona lidar is

collimated so that $A_p = \text{constant} = \pi C^2$ for all ranges, then the new value of R_a in terms of the old value (everything else being equal) is given by

$$(R_a)_{\text{new}} / (R_a)_{\text{old}} = (A_p)_{\text{old}} / (A_p)_{\text{new}} = (\theta_T (R + R^*) / C)^2 \quad (3.23)$$

If C is chosen as 2 cm., then, using Table 3.2, $(R_a)_{\text{new}} \sim 2.5$ at $R=1$ km. Under these conditions a meaningful Doppler spectrum could be obtained, but greater ranges yield conditions where $(R_a)_{\text{new}} \leq 1$. There are many addition effects which are interesting, but the length of this dissertation curtails such discussions.

CHAPTER 4

CONCLUSIONS

It has been shown that the photocurrent signal fluctuations for the University of Arizona monostatic laser operating under conditions in which the mean properties of the atmospheric scatterers are stationary depend only on the receiver noise (shot noise)--the third source of experimental error mentioned in the introduction.

The signal fluctuations caused by the motions of the particles, the first source of experimental error, are suppressed because of receiver averaging, while the second source, transmittance fluctuations, are negligible.

In order to obtain accurate measurements of the true mean signal, the photocurrent must be averaged spatially and temporally. In addition, it is found that even for the relatively clear atmospheres through which the University of Arizona monostatic laser system typically operates, estimates of the true mean photocurrent associated with the true mean intensity from the molecular and particulate scatterers can be routinely obtained to a high accuracy. In particular, it can be concluded that even the desired accuracy of estimating the true mean photocurrent to within $\pm 1\%$ at the 95% confidence level is within reason. If indeed the scattering

medium does not have stationary mean properties (less than 1% variation in the mean) during the measurement period, a true mean would not exist. Under these conditions the statistical estimate of the scattering properties of the medium is modified. What is desired then is an estimate of the fluctuation of the true mean. It is not the purpose of this dissertation to elaborate on this particular problem. Suffice to say that fluctuations in the true mean on the order of a few percent could not be discerned from the shot noise. Of course all of this depends on the time scales of the measurements with respect to the fluctuating true mean, which, again, is another problem. Certain modifications such as reducing the diameter and half angle divergence of the laser beam can "bring out" the scatterer noise. The usefulness of such a venture is not directly apparent, until it is realized that the scatterer noise contains information about the scatterers. As an example, the Brownian diffusion coefficient, related to the particulate scatterers, can be obtained from Fourier analysis of the noise fluctuations when the shot noise is very low (Clark, Lunacek and Benedek 1970). The Brownian diffusion coefficient, in turn, can be related to the size of the particle. More general applications lead to information concerning a wide range of atmospheric motion. Consequently, while "noise" by itself hampers the measurement of any direct quantity, a proper analysis of the noise

fluctuations can lead to additional information about the scattering medium.

Finally, the length of this dissertation curtails a detailed study of the fluctuations of laser signals for the University of Arizona bistatic system. However, the accuracies should be comparable with the vertically pointing monostatic system, perhaps even more accurate. For example, an increased accuracy is associated with the slant paths of the bistatic system. In particular, the laser pulse traveling over a slant path takes longer to pass through a vertical section of the atmosphere over which the vertical number density of the scatterers can be assumed constant. Therefore, the longer the time, the better the estimate of $\langle i \rangle$. Of course, the monostatic laser may be employed over slant paths as well. All of this points to a bright future for laser studies and the eventual development of the laser as a reliable meteorological tool.

In conclusion, it should be emphasized that some of the original work in this dissertation was placed in the Appendices to maintain the continuity of the main text.

APPENDIX A

THE FIELD AMPLITUDE OF THE SINGLE SCATTERED LASER LIGHT

Consider the transmitted laser light arriving at some point within its effective beam diameter at distance \vec{r} away from the equivalent point source (O') from which the laser effectively emits as depicted in Figure A.1. The effective distance at which the equivalent point source emits is given by R^* and equals the ratio of the beam diameter as it leaves the collimation optics to twice the half-angle beam divergence, θ_T .

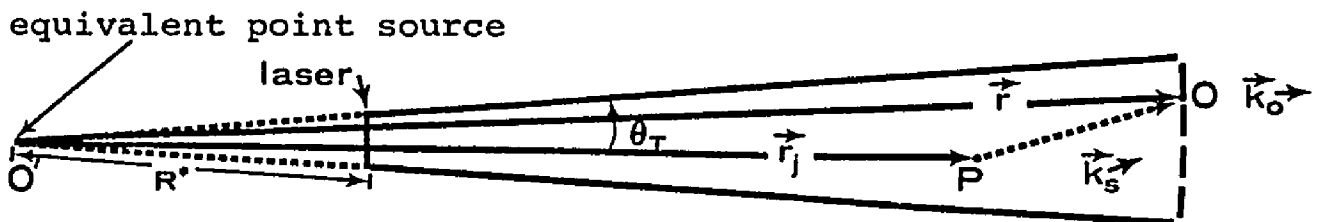


Figure A.1 The Geometry of the Transmitted Laser Beam and the Forward Scattered Light.

Radiation which is scattered from point P to position O will be out of phase with respect to the unperturbed laser light. If \vec{k}_o is the wave vector in the direction of the unperturbed laser light and \vec{k}_s is the wave vector in the direction of the scattered light, then the relative phases with

which the unperturbed and scattered light arrive at O are respectively, $\phi_L(t)$ and $\phi_j(t)$, given by

$$\begin{aligned}\phi_L(t) &= \omega t - \vec{k}_O \cdot \vec{r} \\ \phi_j(t) &= \omega t - \{\vec{k}_O \cdot \vec{r}_j(t) + \vec{k}_s \cdot [\vec{r} - \vec{r}_j(t)]\}\end{aligned}\quad (\text{A.1})$$

The expression for $\phi_j(t)$ in (A.1) becomes more compact if $\vec{k}_O \cdot \vec{r}$ is added and subtracted from the right-hand-side of (A.1) yielding

$$\phi_j(t) = \phi_L(t) - \vec{k} \cdot [\vec{r} - \vec{r}_j(t)] \quad (\vec{k} = \vec{k}_s - \vec{k}_O) \quad (\text{A.2})$$

Therefore, the light which reaches point O at a distance \vec{r} away from the equivalent point source O' can be considered as the sum of the unperturbed laser light $\underline{\vec{E}^L(\vec{r}, t)}$, with time dependence expressed and the perturbed or scattered light from all the scatterers $\underline{\vec{E}^S(\vec{r}, t)}$ with the following expressions

$$\begin{aligned}\vec{E}^L(\vec{r}, t) &= A^L e^{i(\omega t - \vec{k}_O \cdot \vec{r})} \\ \vec{E}^S(\vec{r}, t) &= e^{i(\omega t - \vec{k}_O \cdot \vec{r})} \times \\ &\left\{ \sum_{j=1}^{N(t)} A_j \int_{V(\vec{r}_1)} e^{-i\vec{k} \cdot (\vec{r} - \vec{r}_1)} \delta[\vec{r}_1 - \vec{r}_j(t)] dv(\vec{r}_1) \right\}\end{aligned}\quad (\text{A.3})$$

where ω denotes the frequency of the laser light, A^L is the field amplitude of the unperturbed laser light appropriately adjusted for attenuation, laser characteristics, and the

$|\vec{r}|^{-1}$ drop off with range, $N(t)$ is the total number of scatterers which single scatter light to point O at time t , A^j is the field amplitude of the scattered light from scatter j , $V(\vec{r}_1)$ is the total single scattering volume, and \vec{r}_1 is a dummy variable which seeks out the actual positions of the scatterers $[\vec{r}_j(t)]$, via the Dirac delta function $\delta[\vec{r}_1 - \vec{r}_j(t)]$, when integrated over $V(\vec{r}_1)$.

A.1 The Scattered Light to the Receiver

If the point O in Figure A.1 is now chosen as a reference point within the instantaneous scattering volume which contains the scatterers, then an expression similar to $E^S(\vec{r}, t)$ in (A.3) can be obtained for the field amplitude of the scattered light which arrives on a receiver surface a distance \vec{r} away from O. Figure A.2 depicts the geometry of the scattered light with respect to the source-receiver system and the reference point at O.

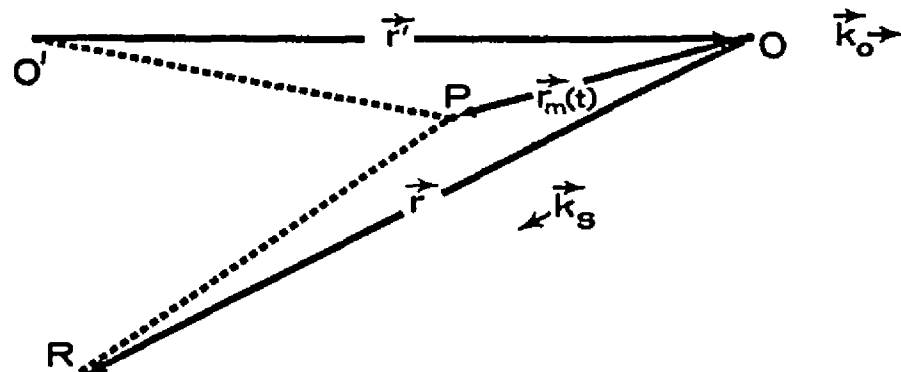


Figure A.2 The Geometry of the Scattered Light Arriving at a Point on the Receiver (R).

In the above figure O' is the laser source, O is a reference point within the scattering volume, $\vec{r}_m(t)$ is the position of the m th scatterer from O to P , and the point R is at the receiver.

The phase of the scattered light which travels along the path from O' to O to R is $\phi_R(t)$ and the phase from O' to P to R is $\phi_m(t)$; these phases are easily seen to be

$$\begin{aligned}\phi_R(t) &= \omega t - (\vec{k}_O \cdot \vec{r}' + \vec{k}_s \cdot \vec{r}) \\ \phi_m(t) &= \phi_R(t) - [\vec{k}_O \cdot \vec{r}_m(t) - \vec{k}_s \cdot \vec{r}_m(t)]\end{aligned}\quad (A.4)$$

The last term of ϕ_m comes from the path difference of the light from the m th scatterer with respect to the reference path (O' to O to R). It is easily seen, therefore, that the total light field from $N(t)$ scatterers which arrives at a point on the receiver can be written similar to (A.3) as

$$E_R^s(\vec{r}, t) = e^{i\phi_R(t)} \left\{ \sum_{m=1}^{N(t)} A_m \int_{V(\vec{r}_1)} e^{+i\vec{k} \cdot \vec{r}_1} \delta[\vec{r}_1 - \vec{r}_m(t)] dV(\vec{r}_1) \right\} \quad (A.5)$$

In some applications in this dissertation the s superscript and R subscript are dropped and replaced with other symbols, while the essential form of (A.5) remains the same. For example, the scattered light from the molecules and particulates which arrives at a point on the receiver will be written as $E_m(\vec{r}, t)$ and $E_p(\vec{r}, t)$, respectively.

Finally, the turbulent medium changes the two-way optical transmission path and its effect on the light is accounted for by adding a random phase factor $\gamma_m(t)$ (m subscript denotes dependence on $\vec{r}_m(t)$), to $\phi_m(t)$ in (A.4). As a result, the exponential within the integral of (A.5) becomes

$$e^{i(\vec{K} \cdot \vec{r} + \gamma(\vec{r}_1))} \quad (\text{A.6})$$

where $\gamma_m(t)$ is replaced by $\gamma(\vec{r}_1)$ so that (A.6) is commensurate with the delta-function expressed in (A.5).

APPENDIX B

MAGNITUDE OF THE SINGLE SCATTERED LIGHT FROM MOLECULES (RAYLEIGH COMPONENT) AND PARTICULATES IN THE TRANSMITTED LASER BEAM

In this section the magnitude of single scattered light from a typical distribution of molecules and particulates which contributes to the total transmitted laser beam is calculated. First, the amount of light scattered from the particulates in the forward direction ($\Theta = 0$) is calculated in terms of the amount of backscattered light which will be used in other parts of this dissertation. Then, the ratio of the single scattered light from the particulates to the unperturbed (except for attenuation) laser light is calculated as a function of range. The square root of this ratio yields a measure of the ratio of $|E^S(\vec{r})|$ from the particulates to $|E^L(\vec{r})|$, the desired goal of this section. Finally, the results for the particulates are easily extended to the molecules without further calculation.

B.1 Scattering and Attenuation

Let a scattering volume (size dAd_s) be located about position \vec{r}_j in which there are many scatterers (Figure B.1); the scatterers are assumed to be molecules and particulates.

The rate at which a energy of one polarization is scattered out of the volume (no absorption considered) at

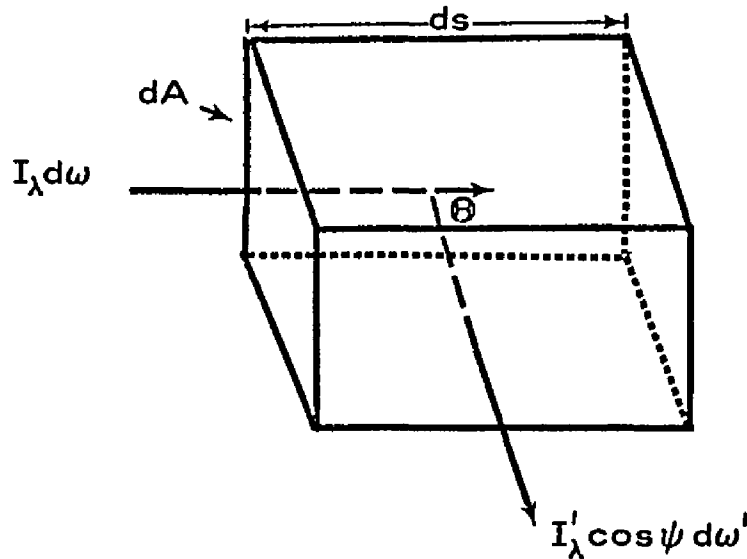


Figure B.1. A Volume Containing Many Scatterers Upon Which is Normally Incident a Differential of Monochromatic Flux Density $I_\lambda d\omega$. -- A differential of the normal flux density (energy/unit normal area, time) is scattered into a direction θ amounting to $I'_\lambda \cos \psi d\omega'$.

some height z in a direction θ into an element of solid angle $d\omega'$ from the incident beam $I_\lambda d\omega$ is

$$\left[\sum_{a_i} Q_{\lambda s}^p(a_i) p(a_i, \theta) \rho(a_i, z) ds dA \cos \psi d\omega' \right] / \left[I_\lambda d\omega \right] \quad (B.1)$$

where $Q_{\lambda s}^p(a_i) / [\text{CM}^2]$ is the scattering cross-section per particle of size a_i at wavelength λ , $p(a_i, \theta) / [\text{str}^{-1}]$ is the normalized scattering phase function for the i th particle size and, when multiplied by $d\omega'$, yields the fraction of the light scattered into $d\omega'$ at the scattering angle θ . With no absorption, the amount of light scattered in all directions must be such that

$$\int_0^{4\pi} p(a_i, \theta) d\omega' = 1 \quad (B.2)$$

The expression $\rho(a_i, z)$ is the number of scatterers per unit volume of size a_i at height z , while $ds dA$ is the scattering volume at height z . Finally, $I_\lambda d\omega$ [energy/time, unit normal area, wavelength (λ)] is a differential of the monochromatic normal flux density of the incident laser light.

To simplify (B.1), the expression is summed over the Junge size distribution (Section 2.1.2) to yield

$$\int \tilde{\beta}_s^p(\theta) N'(z) ds dA \cos \psi d\omega' / \int I_\lambda d\omega' \quad (B.3)$$

where $\tilde{\beta}_s^p(\theta)$ is the normalized volume angular scattering coefficient and, under the condition of no absorption, is related to the normalized volume attenuation coefficient, $\tilde{\beta}_t^p$ (see 2.5, Chapter 2), by

$$\tilde{\beta}_t^p = \int_0^{4\pi} \tilde{\beta}_s^p(\theta) d\omega' \quad [\text{cm}^{-1}] \quad (B.4)$$

where $\cos \psi = 1$. Finally, $N'(z)$ is a multiplier (no units) and is given by the Air Force "clear atmosphere" model, written as

$$N'(z) = N_0 \exp [(-0.8 \text{ km}^{-1})z] \quad (B.5)$$

The value of N_0 must be fixed by the total particulate optical depth, $\tau^p(0, \infty)$, (see 2.7, Chapter 2), by

$$\tau^P(o, \infty) = \int_0^{\infty} \tilde{\beta}_t^P N'(z) dz \quad (B.6)$$

Further, it is shown in Chapter 2, that $\tau^P(o, \infty) \sim \tau^P(o, 5 \text{ km})$ which indicates most of the particulates reside within the first 5 km of the ground. Using (B.6) and the previous statement yields

$$\tau^P(o, \infty) = \frac{\tilde{\beta}_t^P N_o}{(0.8 \text{ km}^{-1})} \sim \tau^P(o, 5 \text{ km}) \quad (B.7)$$

B.2 Forward Scattered Light

Expression (B.3) can be used to calculate the magnitude of the forward scattered light reaching some distant point within the effective, unperturbed, laser beam. In summing up the contributions from all scatterers between the laser source and the distant point, the variations of $\tilde{\beta}_s^P(\theta)$ with θ must be included. Yet, an upper bound to the actual solution can be obtained by assuming $\tilde{\beta}_s^P(0)$ and $\tilde{\beta}_s^P(180)$ apply in all cases of $\tilde{\beta}_s^P(\theta)$ with θ near 0 or 180. Finally, it is convenient to express the forward scattered light in terms of the backscattered light for which a ratio of $\tilde{\beta}_s^P(0)$ to $\tilde{\beta}_s^P(180)$ is useful.

In an unpublished work by Herman and Browning, the total scattering phase functions for a Junge distribution (see 2.1.2, Chapter 2) with particulates ranging from 0.1 μm . to 5.01 μm in size with power coefficients of $v^* = 2.0, 2.5,$

3.0 were calculated at a wavelength 0.5 μm . Although the calculations were not done at the ruby laser wavelength ($\lambda = 0.7 \mu\text{m}$), the exact results are not needed; an order of magnitude calculation is sufficient. From these results, values of the ratio of $\tilde{\beta}_s^P(0)$ to $\tilde{\beta}_s^P(180)$ are presented in Table B.1 for selected powers of v^* ; the power of the Junge distribution.

Table B.1 The Ratio of the Volume Scattering Coefficients in the Forward and Backward Directions. v^* is the power of the Junge distribution.

v^*	$\tilde{\beta}_s^P(0)/\tilde{\beta}_s^P(180)$
2.0	1000
2.5	500
3.0	167

B.3 Attenuation on a Slant Path

A final generalization is made for obtaining the attenuation along a slant path at an angle θ with respect to the vertical. A simple transformation of height, z , to the same height on a slant path, R , yields the appropriate number density of particulate scatterers, $N(R)$, in terms of $N(z)$ for a horizontally homogeneous atmosphere. Therefore, for a non-vertically traveling laser beam passing through the atmosphere defined above, the optical depth for any penetration

distance, R , and any angle away from the zenith, θ , is given by

$$\frac{\tau^P(o, R)}{\tau^P(o, \infty)} = \frac{\int_0^R \exp \left[(-0.8 \text{ km}^{-1}) R' \bar{\mu} \right] dR'}{\tau^P(o, \infty)} \quad (\text{B.8})$$

$$(\bar{\mu} = \cos \theta)$$

which simplifies to

$$\tau^P(o, R) = \frac{\tau_T^P}{\bar{\mu}} \{ 1 - \exp \left[(-0.8 \text{ km}^{-1}) R \bar{\mu} \right] \} \quad (\text{B.9})$$

$$\tau_T^P = \tau^P(o, \infty)$$

B.4 Calculation of the Forward Scattered Light

From (B.3), the differential of energy scattered in the forward direction per unit time per unit scattered solid angle per wavelength (the wavelength dependence is dropped for the monochromatic laser light) is

$$\frac{\text{differential scattered energy}}{\text{time, unit scattered solid angle}} = \tilde{F}_L(R') \tilde{\beta}_S^P(0) N(R') dV \quad (\text{B.10})$$

$$\left[\int I_\lambda \cos \xi d\omega, \cos \xi = 1 \text{ in this case} \right]$$

where $\tilde{F}_L(R')$ is the normal flux density of the laser light which reaches the position of the scattering volume at R' (see Figure B.2), $\tilde{\beta}_S^P(0)$ is the volume scattering coefficient in the forward direction, $N(R')$ is the multiplier at

position R' and $dV \sqrt{ds dA}$ is an element of scattering volume.

From data presented by MacKinnon (1969) it is found that the volume scattering coefficient, $\tilde{\beta}_S^P(180)$, for a $v^* = 3.0$ and the associated volume attenuation coefficient, $\tilde{\beta}_t^P$, are

$$\begin{aligned}\tilde{\beta}_S^P(180) &= \frac{1.2 \times 10^{-4} \text{ km}^{-1}}{4 \pi \text{ str}} = 9.52 \times 10^{-6} \sqrt{\text{km str}}^{-1} \\ \tilde{\beta}_t^P &= 1.8 \times 10^{-4} \text{ km}^{-1} \\ S &= \tilde{\beta}_t^P / \tilde{\beta}_S^P(180) = 19 \text{ str}\end{aligned}\tag{B.11}$$

The ratio S has since been verified by Fernald (1972) for an identical Junge distribution.

Using this last relation it can be shown that

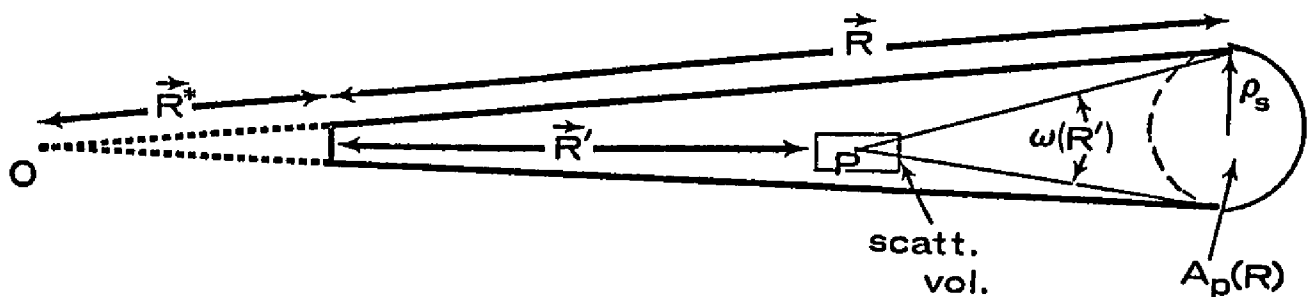
$$\tilde{\beta}_S^P(0) N(R') = \overline{\beta}_S^P \frac{(0.8 \text{ km}^{-1})}{S} \tau_T^P \exp \sqrt{(-0.8 \text{ km}^{-1}) R \mu} \tag{B.12}$$

where $\overline{\beta}_S^P = \tilde{\beta}_S^P(0) / \tilde{\beta}_S^P(180)$ for simplicity of notation. Also the normal flux density of the laser light which reaches the position, R' , is

$$\tilde{F}_L = \frac{E_T}{A_P \Delta t} \tag{B.14}$$

Here E_T is the total energy contained in the laser pulse of effective beam cross-sectional area, A_P , and length (time) Δt . Typically, E_T is 1 joule and $\Delta t \sim 30$ nanoseconds, while

A_p depends on the collimation optics. The exponential attenuation in (B.13) should include the molecular optical depth $\tau^m(O, R')$, but, since $\tau^p(O, \infty) \sim 0.25$ and $\tau^m(O, \infty) \sim 0.036$, the effects of molecules in this calculation are neglected.



(Note: $\vec{r}_j = \vec{R}^* + \vec{R}'$ and $\vec{r} = \vec{R}^* + \vec{R}$ when compared to Figure A.1 in Appendix A)

Figure B.2 Description of the Laser Beam and Scattering Volume. -- The term $A_p(R)$ is the effective beam cross sectional area at R .

Now referring to Figure B.2, the normal flux density of the scattered light passing through the effective beam cross-sectional area at a distance R , due to all scatterings occurring at R' , is given approximately by

$$\tilde{F}_S^p(r) \sim \frac{1}{A_p(R)} \int_{V_T} \tilde{F}_L(R') \tilde{\beta}_S^p(0) N(R') \omega(R') e^{-\tau^p(R', R)} dV(R') \quad (B.15)$$

where $A_p(r)$ is the effective beam normal cross-sectional area ($\cos \psi = 1$) at distance R , $\omega(R')$ is the solid angle subtended by the effective beam cross-sectional area at R from R' , and $dV(R')$ is an element of the total scattering volume, V_T . Finally, the last term in (B.15) is the amount of attenuation the single scattered light incurs between the scattering volume at R' and the position R .

The solid angle $\omega(R')$ can be easily shown to be

$$\omega(R') = 2\pi \left\{ 1 - \frac{(R-R')}{\sqrt{(R-R')^2 + \rho_s^2}} \right\} \underline{\text{str}} \quad (\text{B.16})$$

A ratio of $\tilde{F}_S^P(R)$ to $\tilde{F}_L(R)$ yields

$$Q(R) = \frac{\tilde{F}_S^P(R)}{\tilde{F}_L(R)} = \frac{1}{A_p(R)} \int_0^R \tilde{\beta}_S^P(0) N(R') \omega(R') dV(R') \quad (\text{B.17})$$

where $e^{-\tau^P(R')} - \tau^P(R-R') \sim e^{-\tau^P(R)}$ is assumed for forward scattering. Because of the nature of $\omega(R')$, a far field (f) and near field (n) solution to (B.17) must be calculated.

The conditions are

$$\begin{aligned} \underline{\text{Far field}} \quad \omega_f(R') &= \frac{\pi \rho_s^2}{(R-R')^2} \underline{\text{str}} \quad \text{for } R-R' \geq \sqrt{10} \rho_s \\ \underline{\text{Near field}} \quad \omega_n(R') &= (\text{B.16}) \quad \text{for } R-R' < \sqrt{10} \rho_s \end{aligned} \quad (\text{B.18})$$

Consequently the total solution, as expressed by (B.17), is

$Q(R) = Q_f(R) + Q_n(R)$ in which

$$Q_f(R) \sim \frac{1}{A_p(R)} \int_0^{R_f} \tilde{\beta}_s^p(0) N(R') \omega_f(R') dV(R') \quad (B.19a)$$

$$Q_n(R) \sim \frac{1}{A_p(R)} \int_{R_f}^R \tilde{\beta}_s^p(\Theta) N(R') \omega_n(R') dV(R') \quad (B.19b)$$

where $R_f = R - \sqrt{10} \rho_s$, $\rho_s = \angle(R^* + R) \theta_T$, $A_p(R) = \pi \rho_s^2$, and the full expression for $\tilde{\beta}_s^p(\Theta)$ must be used in the near field (B.19b) so that $Q_n(R)$ is not grossly overestimated. Employing previously defined expressions (B.19a) is simplified to

$$Q_f(R) \sim \overline{\beta_s^p} \frac{0.8}{S} \tau_T^p \pi \theta_T^2 \int_0^{R_f} \frac{(R^* + R')^2}{(R - R')^2} \exp\{ \angle(-0.8) \mu R' \} dR' \quad (B.20)$$

For the particulates defined by Table B.1, the far-field, normal flux density ratio as a function of range is expressed by

$$Q_f(R) \sim \overline{\beta_s^p} \frac{0.8}{S} \tau_T^p \pi \theta_T^2 \{I_1 + I_2 + I_3\} \quad (B.21)$$

where

$$I_1 = e^{-W} X^2 a \left\{ \frac{e^Y}{Y} - \frac{e^W}{W} + E_i \angle \overline{W} - E_i \angle \overline{Y} \right\}$$

$$I_2 = 2e^{-W} X \{E_i \angle \overline{Y} - E_i \angle \overline{W}\}$$

$$I_3 = \frac{e^{-W}}{a} \{ e^W - e^Y \} \sim \frac{1}{a} \{ 1 - e^{-W} \}$$

$$W = aR, X = R^* + R, Y = a \sqrt{10} X \theta_T, a = 0.8 \text{ (km}^{-1}\text{) and}$$

$$E_i \langle \bar{X}' \rangle = \int_{-\infty}^{X'} \frac{e^u}{u} du$$

$$\overline{\beta_S^P} = \beta_S^P(0) / \beta_S^P(180)$$

Integration of $\tilde{\beta}_S^P(\theta)$ in (B.19b) can be accurately done only by computer. Yet, an upper bound to the forward scattered energy can be calculated by taking the energy scattered out of the laser beam in the near-field zone and concentrating it into the forward direction. Using this expression an upper bound to (B.19b) can be expressed as

$$Q_n(R) < \frac{\langle \tilde{F}_L(R_f) - \tilde{F}_L(R) \rangle A_p(R)}{\tilde{F}_L(R) A_p(R)} = \frac{\text{energy-scattered out}}{\text{energy transmitted}}$$

$$< \tau_p(0, R) - \tau_p(0, R_f) \quad (\text{B.19c})$$

$$< \tau_T^P \exp \langle -0.8 \text{ km}^{-1} R \rangle / \langle 0.8 \text{ km}^{-1} \sqrt{10} (R^* + R) \theta_T \rangle$$

\langle An integration of (B.19b) was performed and the above expression was verified as an upper bound. \rangle

An upper bound (sum of B.19a and B.19c) to the normal flux density ratio, $Q(R)$, for a vertically propagating beam ($\bar{\mu} = 1$) as a function of range (R) and with $\tau_T^P = 0.25$ and $v^* = 3.0$ is presented in Table B.2

Table B.2. The Normal Flux Density Ratio, $Q(R)$, as a Function of Range For a Vertically Propagating Laser Beam With Particulates.

(Optical depth $\tau_T^P = 0.25$, $\theta_T = 1.5$ milliradians and $v^* = 3.0$).

$R(\text{km})$	$(I_1 + I_2 + I_3) (\text{km})$	$Q(R)$	$\angle \bar{Q}(R) \angle^{1/2}$
1	145.5	25.5×10^{-4}	5.06×10^{-2}
2	106.2	18.8	4.32
3	64.1	8.05	2.84
4	34.4	5.87	2.43
5	18.3	3.36	1.83

In addition, Table B.2 presents $\angle \bar{Q}(R) \angle^{1/2}$ which is directly related to the field strength ratio of the singly scattered to transmitted laser light, the desired goal of this section.

$$\angle \bar{Q}(R) \angle^{1/2} \geq \frac{|E^S(\vec{r})|}{|E^L(\vec{r})|} \quad (\text{evaluated at } |\vec{r}| = R) \quad (\text{B.22})$$

where the time dependent forms of $E^S(\vec{r})$ and $E^L(\vec{r})$ are given in Appendix A.

As a conclusion, it can be firmly stated that $|E^S(\vec{r})|$ is typically two orders of magnitude below $|E^P(\vec{r})|$ for the University of Arizona laser light passing through a representative turbid particulate atmosphere.

Similarly, the molecular atmosphere, whose total optical depth over Tucson is τ_T^m (molecules) ~ 0.036 , would scatter relatively insignificant amounts of light in the forward direction compared to $|E^L(\vec{r})|$.

APPENDIX C

CALCULATION OF THE INTENSITY CORRELATION FUNCTION OF THE MOLECULES AND PARTICULATES

The scattered intensity correlation function from the instantaneous scattering volume (the \vec{r} dependence of $R_I^C(\vec{r}, \vec{r}, t)$ is dropped for notation convenience) is written as

$$R_I^C(t) = \left\langle \sum_{i=1}^{N(0)} \sum_{j=1}^{N(0)} \sum_{k=1}^{N(t)} \sum_{\ell=1}^{N(t)} A^i A^{j*} A^k A^{\ell*} \exp \{i[\bar{\phi}_i(0) - \phi_j(0) + \phi_k(t) - \phi_\ell(t)]\} \right\rangle \quad (C.1)$$

where $N(0)$ is the number of scatterers within the instantaneous scattering volume (V_{ip}) initially and $N(t)$ is the number at a later time, t . The term A^k is the scattered amplitude of the light of one polarization from the k th scatterer, while $\phi_k(t)$ is the phase position of the k th scatterer at time t and is expressed by

$$\exp \{i[\bar{\phi}_k(t)]\} = \int_{V_{ip}} \exp \{i(\vec{K} \cdot \vec{r} + \gamma(\vec{r}_1))\} \delta(\vec{r}_1 - \vec{r}_k(t)) dV(\vec{r}_1) \quad (C.2)$$

where the terms of (C.2) are explained in Appendix A. Similarly, $\phi_j(0)$ is the phase position of the j th scatterer initially.

The instantaneous scattering volume, V_{ip} , is considered to be continuously illuminated by a beam of light which is temporally and spatially coherent only over the dimensions of an MCV with respect to the receiver.

C.1 Particulates

Beginning with (C.1), the correlations in the scattered light intensity arise from the manner in which the indices i, j, k , and l are summed. All summation terms are included as the sum of three independent summations of (C.1). Each of the three independent summations within the ensemble average of (C.1) are

$$R_I^C(t)_p = (1) + (2) + (3) \quad (C.3)$$

where

(1) $i = j; k = l$, yields

$$\left\langle \sum_{i=1}^{N(0)} |A^i|^2 \sum_{j=1}^{N(t)} |A^j|^2 \right\rangle$$

(2) $i = l; j = k; i \neq j$, yields

$$\left[\begin{aligned} & \left\langle \sum_{i=1}^{N'(t)} |A^i|^2 \sum_{j=1}^{N'(t)} |A^j|^2 \right\rangle \times \\ & \exp \{ i[\bar{\phi}_i(0) - \phi_i(t)] - i[\bar{\phi}_j(0) - \phi_j(t)] \} \end{aligned} \right]$$

$$(3) \quad i = k; \quad j = l; \quad i \neq j$$

$$0$$

The terms of (1) in (C.3) denote the products of the individual intensities from each particle of which there are $N(0)$ at time 0 and $N(t)$ at time t contained within the instantaneous scattering volume. The variations of $N(0)$ and $N(t)$ account for the motions of particles into and out of the instantaneous scattering volume.

Term (2) accounts for the changes in phase of the scattered light which reaches the receiver. In (2) $N'(t)$ is the number of particles from the original $N(0)$ which remain within the instantaneous scattering volume after time t ; only the particles that remain can have a correlated phase. The $\langle \rangle$ brackets refer to an ensemble average over all the positions the particles may assume and all the realizations the turbulent medium along the two-way transmission path. Using (C.2), the exponential in term (2) can be written as $\exp\{i\vec{k} \cdot [\Delta\vec{r}_i(t) - \Delta\vec{r}_j(t)] + i[\bar{\gamma}_{ij}(0) - \gamma_{ij}(t)]\}$ where $\Delta\vec{r}_i(t) = \vec{r}_i(0) - \vec{r}_i(t)$ and $\gamma_{ij}(t) = \gamma_i(t) - \gamma_j(t)$ $\{\gamma(\vec{r}_i(t)) \equiv \gamma_i(t)\}$. The $\gamma_{ij}(t)$ terms express the relative phase added to the received light from the turbulent medium along the two-way transmission path; $\gamma_{ij}(t)$ depends on the strength of the turbulence and $|\vec{r}_i(t) - \vec{r}_j(t)|$, the separation between the particles. If the separation between any two particulate scatterers is less than the dimensions of the mutual coherence volume (MCV),

then on the average the turbulent medium adds a very small relative phase to the light which arrives at any one point on the receiver. Mathematically it can be stated that if $u_k = |\underline{\vec{r}}_i(t) - \underline{\vec{r}}_j(t)| \cdot \underline{\vec{d}}_k < d_k^2$ ($k=1,2,3$), then $\langle \exp(i\gamma_{ij}(t)) \rangle \approx 1$, where $\underline{\vec{d}}_k$ = longitudinal coherence length, transverse coherence length, and maximum transverse separation for $k=1,2$, and 3, respectively, and $\langle \rangle$ denotes an ensemble average over many realizations of the turbulent medium along the two-way transmission path. For $u_k > d_k^2$, $\langle \exp(i\gamma_{ij}(t)) \rangle \approx 0$.

It would be difficult to account for every relative phase addition among the particles. Yet, if the scattering volume is divided up into separate mutual coherence volumes, then all the particles which remain within any one MCV both at time 0 and t will approximately satisfy $\langle \exp\{i(\gamma_{ij}(0) - \gamma_{ij}(t))\} \rangle \approx 1$. Therefore, averaging over the statistical realizations of the turbulent medium along the two-way transmission path, (2) becomes

$$\left(\frac{V_{ip}}{MCV} \right)^2 < \sum_{i=1}^{N''(t)} |A^i|^2 \sum_{j=1}^{N''(t)} |A^j|^2 \exp\{i\vec{k} \cdot [\underline{\vec{r}}_i(t) - \underline{\vec{r}}_j(t)]\} >$$

(2a)

(2b)

where $N''(t)$ is the number of the original particulates, $N''(0)$, which remain within their respective mutual coherence volumes during time 0 to t . The $\langle \rangle$ brackets now refer to a statistical average over all the positions the particles may assume within an MCV. To simplify the above expression a

separate average over (2a) and (2b) is taken, so that

$$\langle (2a)(2b) \rangle = \langle (2a) \rangle \langle (2b) \rangle$$

All the remaining terms which are expressed by (3) in (C.3) contain factors which involve the initial phase positions of the particles. When the ensemble average is taken over the initial phase positions of the particles, the result yields

$$\langle e^{-i\phi_j(0)} \rangle = 0, \text{ for } \phi_j(0) \text{ random} \quad (\text{C.4})$$

As a consequence, all the terms which would have been expressed by (3) in (C.3) are zero. Further analysis of (C.3) is divided into separate analyses of (1), (2a), and (2b).

C.2 Analysis of Term (2b)

If Δz_i is denoted as the component of $\Delta \vec{r}_i(t)$ in the direction \vec{K} and if K is the absolute value of \vec{K} , then (2b) becomes

$$\langle \exp \{i K [\Delta z_i - \Delta z_j] \} \rangle \quad (\text{C.5})$$

As mentioned in Chapter 1 the Brownian (B) and turbulent (T) motion are independent. Hence, if

$$\Delta z_i = \Delta z_i^B + \Delta z_i^T \quad (\text{C.6})$$

then, placing (C.6) into (C.5) yields the product of the two

independent exponential terms

$$\langle \exp \{iK (\Delta z_i^B - \Delta z_j^B)\} \rangle \langle \exp \{iK (\Delta z_i^T - \Delta z_j^T)\} \rangle \quad (C.7)$$

A separate analysis of the Brownian and turbulent motion can now be done.

C.3 Brownian Motion

Chandrasekhar(1943) calculates the probability of a displacement of a Brownian particle from its initial position as a function of time. Wang and Uhlenbeck (1945) provide a generalized probability relationship for the displacement of two particles in terms of their correlation coefficient. Combining the results of Chandrasekhar, and Wang and Uhlenbeck, an expression for the probability density, $G_B(\Delta z_i, \Delta z_j, t)$, of a displacement Δz_i and Δz_j in time can be given by

$$G_B(\Delta z_i, \Delta z_j, t) = \frac{1}{\pi \bar{\sigma}_i \bar{\sigma}_j (1 - \bar{\rho}^2)^{1/2}} \exp \frac{-1}{(1 - \bar{\rho}^2)} \times \left(\frac{\Delta z_i^2}{\bar{\sigma}_i^2} + \frac{\Delta z_j^2}{\bar{\sigma}_j^2} - \frac{2\bar{\rho}\Delta z_i \Delta z_j}{\bar{\sigma}_i \bar{\sigma}_j} \right) \quad [\text{cm}^{-2}] \quad (C.8)$$

where $\bar{\sigma}_i^2 = \langle \Delta z_i^2 \rangle$ and $\bar{\rho} \bar{\sigma}_i \bar{\sigma}_j = \langle \Delta z_i \Delta z_j \rangle$. In addition,

$$\bar{\sigma}_i^2 = \frac{4k_B T}{m_i \beta_i^2} \{ \exp [-\beta_i |t|] + \beta_i |t| - 1 \} \quad (C.9a)$$

$$\beta_i = \frac{k_B T}{m_i D_i} \quad (\text{C.9b})$$

In (C.9a) and (C.9b), k_B is Boltzmann's constant, T is the Kelvin temperature of the gas in which the particles are embedded, m_i is the mass of the particles, D_i is the diffusion coefficient of the particle in the air [cm^2/sec] (or water or whatever). Therefore,

$$\begin{aligned} \langle \exp \{iK(\Delta z_i^B - \Delta z_j^B)\} \rangle &= \iint_{\text{MCV}} G_B(\Delta z_i, \Delta z_j, t) \\ &\quad \exp \{iK(\Delta z_i - \Delta z_j)\} d(\Delta z_i) d(\Delta z_j) \end{aligned} \quad (\text{C.10})$$

The mutual turbulent coherence volume (MCV) is usually sufficiently large and $G_B(\Delta z_i, \Delta z_j, t)$ usually drops off sufficiently fast with Δz_i and Δz_j that the limits to (C.10) can be extended equivalently to $\pm\infty$. The integral of (C.10) with these limits yields,

$$\langle \exp \{iK(\Delta z_i^B - \Delta z_j^B)\} \rangle = \exp \left[-\frac{K^2}{4} (\overline{\sigma}_i^2 + \overline{\sigma}_j^2 - 2\overline{\rho}\overline{\sigma}_i\overline{\sigma}_j) \right] \quad (\text{C.11})$$

It is important to recall from Chapter 1 that the motion of a Brownian particle is uncorrelated at all times with the motion of any other Brownian particle (on the average). Consequently, $\overline{\rho}$ in (C.11) is zero.

C.4 Turbulent Motion

The diffusion of particulates in a turbulent field has a great many similarities to Brownian motion. Indeed most probability of displacement distributions are Gaussian (Hinze 1959), as expressed by (C.8). However, there does appear to be some correlated movement of two separated particles, as explained in Chapter 1. The assumptions for turbulent motion are exactly the same as presented in the previous section on Brownian motion with a few exceptions. Since all the particles move along with the turbulent field, the displacements are independent of the scatterer size and mass, so that

$$\bar{\sigma}_i = \bar{\sigma}_j = \bar{\sigma}_T \quad (C.12)$$

Further, the rate of mean separation $\langle \Delta r_{ij}(t) \rangle = \langle |\vec{r}_i(t) - \vec{r}_j(t)| \rangle$ is proportional to $\langle \Delta r_{ij}(t) \rangle$, so that $\langle \Delta r_{ij}(t) \rangle = \Delta r_{ij}(0) \exp(\Gamma t)$ where $\Delta r_{ij}(0)$ is the initial separation and Γ is a constant.

Hinze (1959) states that for small diffusion times in homogeneous turbulence, the correlation function of the position components of two fluid elements (synonymous with the particles' positions) is

$$\bar{C} = \frac{\langle \Delta z_i \Delta z_j \rangle}{\bar{\sigma}_T^2} = \left[1 - \frac{11}{9} \frac{\bar{A}}{u'^2} (\epsilon \langle \Delta r_{ij}(t) \rangle)^{2/3} \right] \quad \Delta r_{ij}(t) \leq \Lambda_0$$

$$\bar{C} = 0 \quad \Delta r_{ij}(t) > \Lambda_0 \quad (C.13)$$

where \bar{A} is some absolute constant, $\overline{u'^2}$ is the mean square fluctuation velocity of the turbulent air, ϵ is the eddy dissipation by turbulence per unit mass, and Λ_0 is the integral scale of turbulence. Equation (C.13) is modified slightly, for the purposes of this dissertation, to extend the correlation relation to longer periods of time.

$$\begin{aligned}\bar{C} &= \left[\bar{1} - \left(\frac{\langle \Delta r_{ij}(t) \rangle}{\Lambda_0} \right)^{2/3} \right] & \langle \Delta r_{ij}(t) \rangle \leq \Lambda_0 \\ \bar{C} &= 0 & \langle \Delta r_{ij}(t) \rangle > \Lambda_0\end{aligned}\quad (C.14)$$

The relation (C.14) must now be averaged over all the possible initial separations of the particulates within the mutual coherence volume. In this connection it is equally probable that the particles may assume any initial separation. Consequently, the turbulent correlation function which is equivalent to $\bar{\rho}$ in (C.11) is

$$\frac{\bar{\rho}}{\rho_T} = \langle \bar{C} \rangle = \frac{\langle \langle \Delta z_i \Delta z_j \rangle \rangle}{\bar{\sigma}_T^2} = \frac{1}{(\text{MCV})} \int_{\text{MCV}} \bar{C} \, dV(\Delta r_{ij}(0)) \quad (C.15)$$

The solution to (C.15) is quite difficult for odd shaped, mutual coherence volumes. When (C.15) is integrated for a spherical MCV of diameter D , the result is

$$\begin{aligned}\bar{\rho}_T &= 1 - \frac{9}{11} \left(\frac{D}{\Lambda(t)} \right)^{2/3} & \Lambda(t) \geq D \\ \bar{\rho}_T &= \left(1 - \frac{9}{11} \right) \left(\frac{\Lambda(t)}{D} \right)^3 & \Lambda(t) < D\end{aligned}\tag{C.16}$$

where $\Lambda(t) = \Lambda_0 \exp(-\Gamma t)$. Even though (C.16) is an approximation to the actual $\bar{\rho}_T$, it seems quite reasonable. If D is taken as the average dimension of the MCV, (C.16) can apply well enough to the actual problem. Finally, the probability distribution of the displacements, $G(\Delta z_i, \Delta z_j, t)$, caused by turbulence is written as

$$\begin{aligned}G_T(\Delta z_i, \Delta z_j, t) &= \frac{1}{\pi \bar{\sigma}_T^2 (1 - \bar{\rho}_T^2)^{1/2}} \exp \left\{ \frac{-1}{(1 - \bar{\rho}_T^2)^{1/2}} \right. \\ &\quad \left. \frac{(\Delta z_i^2 + \Delta z_j^2 - 2\bar{\rho}_T \Delta z_i \Delta z_j)}{\bar{\sigma}_T^2} \right\} [\text{cm}^{-1}]\end{aligned}\tag{C.17}$$

where the form of (C.17) is suggested by (C.8) and (C.12).

Now, integration of $\exp \{iK(\Delta z_i - \Delta z_j)\}$ over (C.17) as is done in (C.10) yields

$$\langle \exp \{iK(\Delta z_i^T - \Delta z_j^T)\} \rangle = \exp \left\{ -\frac{K^2}{4} (2 \bar{\sigma}_T^2 (1 - \bar{\rho}_T)) \right\} \tag{C.18}$$

Finally, the phase correlation term, (C.5), for a distribution of particulate scatterers moving by Brownian and turbulent motion is given by (C.7) which, in turn, is the product of (C.11) and (C.18); the final form of term

(C.5) is

$$\langle \exp \{ iK(\Delta z_i - \Delta z_j) \} \rangle = \exp \left\{ -\frac{K^2}{4} \left[\bar{\sigma}_i^2 + \bar{\tau}_j^2 + 2\bar{\sigma}_T^2(1 - \bar{\rho}_T) \right] \right\} \quad (C.19)$$

In (C.19), $\bar{\sigma}_i^2$ and $\bar{\tau}_j^2$ refer to the Brownian diffusion coefficients of different sized particles i and j and do not refer, per se, to the positions of the particles. All other terms are previously defined.

C.5 Analysis of Term (1) and Term (2a)

The particulate number densities are uniformly distributed according to the Junge power distribution within size interval increments over which a mean intensity $|\bar{A}^i|^2 = I^i$ is calculated. Let f_i be the fraction of the total number of particles in the i th increment. For a well-mixed, stationary distribution $f_i = v_i/v_p$ where v_i is the total mean number of particles in the i th interval and v_p is the total mean number of particles of all sizes within the instantaneous scattering volume. Any sub volume, such as a mutual coherence volume, will contain the same fractional ratio f_i . Let $N''(t)$ be the total number of particles in an MCV after time t , and let f_i' be the fractional ratio of the original f_i that remain after time t . This notation is used since smaller particles will escape from the MCV faster than the larger ones, thereby, the fractional ratio of the particles

remaining does not resemble f_i . Finally, if $N(0)$ and $N(t)$ are the total number of particles within the instantaneous scattering volume initially and at some later time respectively then term (1) and term (2a) are written

$$(1) \quad = \langle N(0) N(t) \rangle \sum_{i=1}^J \sum_{j=1}^J f_i f_j I^i I^j$$

$$(2a) \quad = \left(\frac{v_{ip}}{MCV} \right)^2 \{ \langle \bar{N}''(t) \rangle^2 \} \left[\sum_{i=1}^J \sum_{j=1}^J f_i' f_j' I^i I^j - \sum_{j=1}^J (f_j^i)^2 (I^j)^2 \right] \quad (C.20)$$

In (C.20) J denotes the number of size intervals of particulates represented.

It is recalled that number density fluctuations are caused by turbulence and Brownian motion moving the particulates in and out of the instantaneous scattering volume (for term 1) and the mutual coherence volume (for term 2a). In order to calculate probability distributions for the number density fluctuations, considerable use is made of a landmark work done by Chandrasekhar (1943). Through his work it can be shown that the mean probability of escape of a particle in the i th size interval out of a volume V in time t is given by $P_i(t)$, where

$$P_i(t) = 1 - \int_V G_{BT}(r_i, t) dV(r_i) \quad (C.21)$$

and $G_{BT}(r_i, t)$ is the combined probability of a displacement r_i in time t per unit volume for a particle under Brownian and turbulent motion (the combined expression is an extension of Chandrasekhar's work), given by

$$G_{BT}(r_i, t) [\text{cm}^{-3}] = \frac{1}{[\pi(\bar{\sigma}_i^2 + \bar{\sigma}_T^2)]^{3/2}} \exp \left\{ -\frac{r_i^2}{\bar{\sigma}_i^2 + \bar{\sigma}_T^2} \right\} \quad (\text{C.22})$$

Finally, V in (C.21) is either the instantaneous scattering volume for use in (1) or the MCV for use in (2a).

In the same landmark work Chandrasekhar shows the probability that there exist $(n-k)$ particulates within the volume V after time t from an original number n is given by

$$W(n; n-k) = e^{-vP} \sum_{j=k}^n \frac{n!}{j!(n-j)!} P^j (1-P)^{n-j} \frac{(vP)^{j-k}}{(j-k)!} \quad (\text{C.23})$$

where the expression holds for any collection of particles so that $v = v_i$, the total mean number of particulates in the i th size interval and $P = P_i(t)$, already defined. An expression similar to (C.23) exists (not given here), denoted by $W(n; n+k)$, for the probability that k particles are added to the original n after time t . One other useful relation is the probability of finding n particulates occupying the volume V at any one time, given by

$$W(n) = \frac{e^{-v} v^n}{n!} \quad (C.24)$$

where v in this case is the mean number of particulates in the volume V .

Now, the relations (C.21) to (C.24) yield the means necessary to calculate $\langle N(0) N(t) \rangle$ and $\langle \overline{N}''(t) \rangle^2$ which appear in (C.20). It should be emphasized that in calculating these relations the associated statistics require $v \gg 1$. After lengthy calculations, it can be shown that

$$\begin{aligned} \langle N(0) N(t) \rangle &= v_p^2 + \langle \overline{1} - \overline{P}(t) \rangle v_p \\ \langle \overline{N}''(t) \rangle^2 &= v_p'^2 \langle \overline{1} - \overline{P}'(t) \rangle^2 + v_p' \langle \overline{1} - \overline{P}'(t) \rangle \end{aligned} \quad (C.25)$$

where v_p has already been defined and v_p' is the mean of particles of all sizes within a mutual coherence volume. In addition, $\overline{P}(t)$ is the particle weighted mean probability of escape and is written as

$$\overline{P}(t) = \sum_{i=1}^J f_i P_i(t) \quad (C.26)$$

where $P_i(t)$ is given by (C.21) and the volume over which $P_i(t)$ is integrated is the instantaneous scattering volume, V_{ip} . Similarly, $\overline{P}'(t)$ is given by

$$\overline{P}'(t) = \sum_{i=1}^J f_i P_i'(t) \quad (C.27)$$

where $P'_i(t)$ is given by (C.21) integrated over a mutual coherence volume, MCV. The term v'_p is related to v_p simply by

$$v'_p = \left(\frac{MCV}{V_{ip}}\right) v_p \quad (C.28)$$

The terms which remain to be defined in (C.20) are the fractional ratios, f_i and f'_i . The term f_i is fixed and remains so for all time (the ratios are defined by the Junge distribution, while f'_i is a function of time, denoted by $f'_i = f'_i(t)$). The fraction ratio, $f'_i(t)$, is simply the ratio of the number of the i th size remaining after time t to the number of the i th size originally there; this relation must be given by

$$f'_i(t) = f_i \frac{[1 - P'_i(t)]}{[1 - P'_i(0)]} \quad (C.29)$$

where f_i is the original fractional ratio and $P'_i(t)$ has been previously defined. Since $P'_i(0) = 0$, then $f'_i(0) = f_i$; using this correspondence all the fractional ratio terms appearing in (C.20) can be written in terms of (C.29).

The final expressions then, for (1) and (2a) are

$$\begin{aligned} (1) &= \{v_p^2 + [1 - \bar{P}(t)]v_p\} A^*(0) \\ (2a) &= \left(\frac{V_{ip}}{MCV}\right)^2 \{v_p'^2 [1 - \bar{P}'(t)]^2 + v_p' [1 - \bar{P}'(t)]\} \end{aligned} \quad (C.30)$$

$$\{A^*(t) - B^*(t)\}$$

$$\text{where } A^*(t) = \sum_{i=1}^J \sum_{j=1}^J f'_i(t) f'_j(t) I^i I^j$$

$$B^*(t) = \sum_{j=1}^J \left[\bar{f}'_j(t) I^j \right]^2$$

$$C^*(t) = \exp \left\{ -\frac{K^2}{4} \left[\bar{\sigma}_i^2 + \bar{\tau}_j^2 + 2\bar{\tau}_T^2(1-\bar{\rho}_T) \right] \right\}$$

C.6 Complete Expression for $R_I^C(t)_p$

Since it is required that v_p and $v'_p \gg 1$, as stated before, for the statistics to apply, the complete expression for $R_I^C(t)_p$ can be written as

$$R_I^C(t)_p = \{v_p^2 + [\bar{I} - \bar{F}(t)]v_p\} A^*(0) + v_p^2 [\bar{I} - \bar{F}'(t)]^2 \{A^*(t) - B^*(t)\} C^*(t) \quad (C.31)$$

C.7 Molecules

The properties of the Rayleigh component of the scattered light are well known. Substituting the expression for the scattered field into the intensity correlation function yields

$$R_I(t)_m = \bar{I}^2 \langle B(0) B^*(0) B(t) B^*(t) \rangle \quad (C.32)$$

where $\bar{I} = \frac{3Q_s}{16\pi} \{1 + \cos^2\theta\} \tilde{F}_L$ (scattered intensity per molecule)

$$Q_s = \frac{8\pi}{3} \alpha^2 \frac{\omega_0^2}{c^4} \text{ (total scattering cross section per molecule)}$$

θ = scattering angle

$$\alpha = \frac{1}{4\pi} \left(\frac{\partial \epsilon}{\partial \rho} \right)_{\rho=\rho_0} \quad (\text{polarizability})$$

$$F_L = I^i d\omega^i \quad (\text{incident normal flux density})$$

$$B(t) = \frac{1}{V_{ip}} \int_{V_{ip}} \exp \{-i\vec{k} \cdot \vec{r}_i\} \left\{ \sum_{k=1}^{N(t)} \delta[\vec{r}_1 - \vec{r}_k(t)] - \rho_0 V_{ip} \right\} dV(\vec{r}_1)$$

At this stage the solution proceeds exactly as that for the particulates. The molecules move by thermal and turbulent motion, and can be influenced by soundwaves (the latter not discussed). Specification of $G(\Delta z_i, \Delta z_j, t)$ for the various types of motion along with the initial random position of the molecules yields all the statistical information. The results are

$$R_I^C(t)_m = \bar{I}^2 \{v_m^2 + v_m^2 [\bar{I} - P'(t)]^2 \exp \left\{ \frac{-K^2}{2} [\bar{\sigma}_m^2 + \bar{\sigma}_T^2 (1 - \bar{\rho}_T)] \right\} \quad (C.33)$$

where

$$P'(t) = 1 - \int_{MCV} \frac{1}{\sqrt{\pi} (\bar{\sigma}_m^2 + \bar{\sigma}_T^2)^{3/2}} \exp \left\{ \frac{-r_i^2}{\bar{\sigma}_m^2 + \bar{\sigma}_T^2} \right\} dV(\vec{r}_i)$$

In (C.33), $\bar{\sigma}_m^2$ is the mean square displacement for the molecules by Brownian motion and is given by (C.9) in which the particulate terms are replaced by the molecular terms.

C.8 Calculation of the Field Correlation Function of the Particulates and Molecules

Again, the range dependence of $R_E^C(\vec{r}, \vec{r}, t)$ is dropped for notation convenience, so that $R_E^C(\vec{r}, \vec{r}, t) \rightarrow R_E^C(t)$. Now, this function consists of a double sum and its evaluation is made much simpler by employing the results of the previous section. In general, $R_E^C(t)$ is given by

$$R_E^C(t) = \left\langle \sum_{j=1}^{N(0)} \sum_{k=1}^{N(t)} A^j A^{k*} \exp \{i[\phi_j(0) - \phi_k(t)]\} \right\rangle \quad (C.34)$$

The general expression, (C.34) is evaluated by dividing the general sum into two sub-sums. These sums are: (1) $j=k$, and (2) $j \neq k$ whose specific evaluation is given below.

C.8.1 Particulates

$$R_E^C(t)_p = (1) + (2)$$

- (1) $j=k$ The correlation occurs only for those particulates of the original $N(0)$ which remain phase correlated after time t ; i.e., $N''(t)$ within an MCV.

$$= \left(\frac{V_{ip}}{MCV} \right) \left\langle \sum_{j=1}^{N''(t)} |A^j|^2 \right\rangle \langle \exp \{i[\phi_j(0) - \phi_j(t)]\} \rangle \quad (C.35)$$

- (2) $j \neq k$ These terms are zero since the phases, $\phi_j(0)$ and $\phi_k(t)$, which the j th and k th scatterers may assume are completely random and independent so that

$$\exp \{i[\bar{\phi}_j(0) - \phi_k(t)]\} = 0$$

for all $j \neq k$.

The evaluation of (1) proceeds by simplification of (C.35) to

$$(1) = \left[\frac{V_{ip}}{MCV} \right] \langle N'(t) \sum_{j=1}^J f'_j(t) I^j \rangle \langle \exp \{i[\bar{\phi}_j(0) - \phi_j(t)]\} \rangle \quad (C.36)$$

The results of the previous section show that

$$R_E^C(t)_p = v_p \langle \bar{I} - \bar{P}'(t) \rangle \sum_{j=1}^J f'_j(t) I^j \exp \left\{ \frac{-K^2}{4} \langle \bar{\sigma}_j^2 + \bar{\sigma}_T^2 \rangle \right\} \quad (C.37)$$

where all the terms in (C.37) have been previously defined.

C.8.2 Molecules

The form of this equation suggests itself by first comparing (C.37) with (C.31) so that $R_E^C(t)_m$, given below, compares with (C.33). Therefore, $R_E^C(t)_m$ is given as

$$R_E^C(t)_m = \bar{I} \{ v_m \langle \bar{I} - \bar{P}'(t) \rangle \exp \left\{ \frac{-K^2}{4} \langle \bar{\sigma}_m^2 + \bar{\sigma}_T^2 \rangle \right\} \} \quad (C.38)$$

where all the terms in (C.38) have been previously defined.

C.9 The Statistical Moments of the Intensity Distribution

The intensity and field correlation functions for the molecules and particulates and their respective expressions in terms of the measurables are given below

$$R_I^C(\vec{r}, \vec{r}, t)_p = (C.31) ; R_I^C(\vec{r}, \vec{r}, t)_m = (C.33)$$

$$R_E^C(\vec{r}, \vec{r}, t)_p = (C.37) ; R_E^C(\vec{r}, \vec{r}, t)_m = (C.38)$$

where the dependence on range, \vec{r} , is explicitly expressed. By applying the condition $t=0$, the left-hand sides of the above expressions become the statistical moments, while the right-hand sides become simple forms in terms of measurables. The results are

$$\begin{aligned} \langle \underline{I}(\vec{r}, 0)_p^2 \rangle &= 2 \underline{v}_p \sum_{j=1}^J f_j'(0) \underline{I}_p^i{}^2 \\ \langle \underline{I}(\vec{r}, 0)_m^2 \rangle &= 2 \underline{v}_m \underline{I}_m^i{}^2 \\ \langle \underline{I}(\vec{r}, 0)_p \rangle &= \underline{v}_p \sum_{j=1}^J f_j'(0) \underline{I}_p^i \\ \langle \underline{I}(\vec{r}, 0)_m \rangle &= \underline{v}_m \underline{I}_m^i \end{aligned} \tag{C.39}$$

The interesting and, perhaps, expected results of (C.39) show that the mean scattered intensities from the collection of molecules and particulates are the sums of the mean intensities from each scatterer alone. Further, mean square intensities are just twice the square of the means. The expressions of (C.39) can be placed in a simpler form for use in Chapter 2.

$$\langle I_p^2 \rangle = 2(\langle I_p \rangle)^2 ; \langle I_p \rangle = \sum_{j=1}^J v_j I^j$$

(C.40)

$$\langle I_m^2 \rangle = 2(\langle I_m \rangle)^2 ; \langle I_m \rangle = v_m \bar{I}_m$$

The limits of the correlation functions at $t=\infty$ are easily formed by realizing σ_i^2 and $\tau_j^2 \rightarrow \infty$ as $t \rightarrow \infty$, so that

$$R_I^C(\infty)_p = \left(\sum_{j=1}^J v_j I^j \right)^2 ; R_I^C(\infty)_m = (v_m \bar{I}_m)^2$$

(C.41)

$$R_E^C(\infty)_p = 0 ; R_E^C(\infty)_m = 0$$

APPENDIX D

CONVERSION OF LIGHT TO CURRENT

Light strikes a photocathode surface for a length of time T . During this time the light causes photoelectrons to be emitted from the cathode. Each photocathode electron enters an amplification system. This amplification system consists of a stage of dynodes. An electron accelerated between any two dynodes gains sufficient energy to knock a number of electrons off a dynode surface after impact. Thus, a single photoelectron becomes amplified into a pulse of electrons of ever increasing strength at each dynode stage. Upon leaving the amplification system the electrons arrive at the anode as a pulse of strength, μe , where μ is the amplification factor (gain), and a broadened width related to the spread in the transit times of the electrons in the amplification system.

Following Papoulis (1965) and Greytak (1970) it can be shown that the photocurrent correlation function, $R_i(t)$, at the anode for a stationary signal is given by

$$R_i(t) = \langle i(0)i(t) \rangle = \frac{\mu e}{2RC_s} (\alpha \mu e \langle F \rangle) e^{-t/RC_s} + (\alpha \mu e)^2 R_F(t) \quad (D.1)$$

The first term on the right-hand side of (D.1) is the contribution associated with the shot noise, while the second term is the contribution from the correlation function of the received flux, $R_F(t)$. Specifically, RC_s (sec) is the time constant of the dynode system and represents the spread in the transit times of the electrons, α is the conversion efficiency of the photocathode (electron/joule), $\langle F \rangle$ (watts) is the average light flux collected by the receiver, and finally $R_F(t) = \langle F(0)F(t) \rangle$ is the average correlation in the light flux at times 0 and t .

D.1 Filtering the Photoanode Current

When the photoanode current is passed through a filter, the statistical characteristics of the current are modified. The filter contains a frequency band pass chosen so that those frequencies associated with the shot noise are reduced, while those associated with the signal from the scattered light are passed or transmitted. However, even though this filtering reduces the magnitude of the fluctuations associated with the shot noise, these current fluctuations demonstrate a longer correlation time. In this connection a longer correlation time requires a longer record of the photocurrent signal in order to obtain confident estimates of the mean value of the photocurrent associated with the scattered light. So in effect, the reduced noise magnitude is

traded off for the longer correlation time. The net result however is an improvement in the measurement of the true mean photocurrent.

The University of Arizona laser-receiver system has a post detection circuit which passes the raw photoanode current through an effective RC (resistor-capacitor in series) filter. Papoulis (1965) shows that the filter response function for such a circuit is given by

$$H(t') = \frac{1}{2RC_f} e^{-|t'|/RC_f} \quad (D.2)$$

where RC_f is the time constant of the filter.

If RC_f is sufficiently long in order to pass the fluctuations of the scattered light as expressed through $R_F(t)$ in (D.1), then only the shot noise portion of $R_i(t)$ is affected. Therefore, the filtered portion of $R_i(t)$, denoted by $R'_i(t)$ is found by using

$$R'_i(t) = \int_{-\infty}^{\infty} R_i(t-t')H(t')dt' \quad (D.3)$$

which, in turn, yields

$$R'_i(t) = \frac{\mu e \langle i \rangle}{4(RC_f - RC_s)} \left[e^{-t/RC_f} - \frac{2RC_s}{RC_f - RC_s} e^{-t/RC_s} \right] \quad (D.4)$$

For the post-detection filter in the University of Arizona lidar system, $RC_f \approx 2.5 \times 10^{-8}$ seconds, while $RC_s \approx 1.0$

$\times 10^{-9}$ seconds (Greytak 1970). Therefore,

$$R_i'(t) \text{ [filtered shot noise portion]} = \frac{\mu e \langle i \rangle}{4RC_f} e^{-t/RC_f} \quad (D.5)$$

APPENDIX E

TRANSMITTANCE FLUCTUATIONS

This dissertation has been primarily occupied in discussing the fluctuations in the scattered light caused just by the motions of the scatterers within the instantaneous scattering volume. These same scatterers cause additional fluctuations indirectly through fluctuations in the transmitted light (transmittance). The transmittance of the scattered light which arrives at the receiver is directly related to the attenuation of the light by the scatterers (molecules and particulates) along two light paths. The first path, of course, is from the laser source to the scattering volume, while the second is from the scattering volume to the receiver. Fluctuations in the amount of attenuation may arise by variations in the numbers of scatterers along these two paths. A fewer number of scatterers along a path causes less attenuation and therefore increased transmittance of the light, while larger numbers cause a corresponding decrease in transmittance. These fluctuations in transmittance cause fluctuations in the light intensity which arrives at the receiver and are essentially indiscernible from those caused by scatterer motion within the instantaneous scattering volume. Consequently, it is important

that the magnitude of these transmittance variations be analyzed.

In Section 2.1.2, Chapter 2, it is shown that the transmittance, $T(z_1, z_2)$, along a vertical path between any two levels z_1 and z_2 in a horizontally homogeneous atmosphere is related to the optical depth, $\tau(z_1, z_2)$, between those levels by

$$T(z_1, z_2) = e^{-\tau(z_1, z_2)} \quad (\text{E.1})$$

Now, $\tau(z_1, z_2)$ generally includes a separate optical depth for the molecules and particulates such that $\tau(z_1, z_2) = \tau^m(z_1, z_2) + \tau^p(z_1, z_2)$ where m and p superscripts refer to the molecules and particulates, respectively. For simplicity only vertical paths with the condition $z = \bar{\mu}R$ and $\bar{\mu} = 1$ (see Appendix B) are considered, so that $z \equiv R$ in the following. Therefore, by setting $z_1=0$ and $z_2=R$, and from (2.7) in Chapter 2, the transmittance for the particulates alone along one transmission path (denoted by subscript 1) is given by

$$T_1^p(0, z) = T_1^p(0, R) = e^{-\tau^p(0, R)} \quad (\text{E.2})$$

where

$$\tau^p(0, R) = \tau_T^p \{1 - \exp[-(0.8 \text{ km}^{-1})R]\}$$

A similar expression exists for the molecules but its discussion is deferred to the end of this Appendix. It is easily shown that the total attenuation for the two-way path in the monostatic system yields a transmittance given by

$$T^P(0,R) = (T_1^P(0,R))^2 \quad (E.3)$$

Since the flux of the light, F_T , collected by the receiver of the monostatic system is proportional to $\sqrt{T_1^P(0,R)}$, then a 1% variation in the received flux caused by a corresponding variation in the transmittance is

$$\left| \frac{F_T' - F_T}{F_T} \right| = 0.01 = \left| \frac{e^{-2\tau^{P'}(0,R)} - e^{-2\tau^P(0,R)}}{e^{-2\tau^P(0,R)}} \right| \quad (E.4)$$

where (E.2) is used to obtain (E.4). This expression simplifies further to yield

$$|\tau^P(0,R) - \tau^{P'}(0,R)| \approx 0.005 \quad (E.5)$$

The choice of a 1% variable in F_T caused by the transmittance fluctuations equals a desirable upper limit for the F_T fluctuations. From (2.7) in Chapter 2

$$\tau^P(0,R) = \int_0^R \tilde{\beta}_t^P N'(R) \, dR \quad (E.6)$$

Therefore, variations in $\tau^P(0,R)$, as expressed by (E.6), can occur both from variations in $\tilde{\beta}_t^P$ and $N'(R)$. Variations in $\tilde{\beta}_t^P$ arise from changes in the relative number of particulates in each size interval described on the average by the Junge distribution, while variations in $N'(R)$ arise from fluctuations in the total number of particulates encountered along the two way path with the relative numbers remaining constant. The $\tilde{\beta}_t^P$ variations would be very difficult to calculate and the author has not developed a method to calculate such variations. However, based on the results of allowing $N'(R)$ to vary appears to indicate that variations in $\tilde{\beta}_t^P$ would be insignificant compared to the $N'(R)$ variations. Be that as it may, the $N'(R)$ variations are much easier to calculate. Therefore, from (E.6) let us assume that $\tau^{P'}(0,R)$ is given by

$$\tau^{P'}(0,R) = \tau^P(0,R) \pm \int_0^R \tilde{\beta}_t^P \Delta N'(R) dR \quad (E.7)$$

where $\Delta N'(R) = \Delta N_0 \exp[-(0.8 \text{ km}^{-1})R]$, then substitution of (E.7) into (E.5) yields

$$\left| \frac{\Delta N_0}{N_0} \int_0^R \tilde{\beta}_t^P N'(R) dR \right| = \left| \frac{\Delta N_0}{N_0} \tau^P(0,R) \right| \approx 0.005 \quad (E.8)$$

Expression (E.8) yields a measure of the variation in the total fraction of the particulates in all size intervals,

ΔN_0 , which would yield a 1% variation in the mean received flux.

Chandrasekhar (1943) shows that the fluctuations in the total numbers of a collection of particles contained in a volume, V , whose surface area is A can be calculated. If $\bar{N}(a)$ is the total mean number of particulates contained within a size range between a and $a + \Delta a$, then the mean life of a state of fluctuation which consists of a total of $N(a)$ particulates $\langle \bar{N}(a) \pm \bar{N}(a) \rangle$ is given by T_N , and is related to $N(a)$ and $\bar{N}(a)$ by

$$T_N = \frac{1}{\langle \bar{N}(a) + \bar{N}(a) \rangle P_0} \quad (E.9)$$

where $P_0 (\text{sec}^{-1})$ is the probability that a particle will escape from V per unit time. The term P_0 is simply found by calculating the number of particles which pass through the surface area of the containing volume and dividing this number by the total number of particles contained in V ; simply stated

$$P_0 = \frac{(\text{particle flux})(\text{surface area of } V)}{(\text{number of particles in } V)} \quad (E.10)$$

Although the particulates move under Brownian motion, they instantaneously behave as free particles in thermal equilibrium with their surroundings. Therefore,

$$\text{particle flux} = \frac{\bar{n}(a)\bar{v}}{4} \quad (\text{E.11})$$

where $\bar{n}(a) = \bar{N}(a)/V$ and \bar{v} is the Maxwellian velocity given by $\bar{v} = (8kT/\pi m)^{1/2}$; the term k is Boltzmann's constant, T is the temperature in the region containing the particles and m is the mass of the particles of size a . Therefore, using (E.10) and (E.11) P_0 becomes $\frac{A}{V} = \text{surface area of } \underline{V}$

$$P_0 = \frac{A}{V} \left(\frac{kT}{2\pi m} \right)^{1/2} \quad (\text{E.12})$$

Chandrasekhar goes on to show that the average time between the occurrence of a state of fluctuation consisting of $N(a)$ particulates, given by Θ_N , when $\bar{N}(a)$ is large is expressed as

$$\Theta_N = \left[\frac{\pi}{2\bar{N}(a)} \right]^{1/2} \frac{1}{P_0} \exp \left[-\frac{(N(a) - \bar{N}(a))^2}{2\bar{N}(a)} \right] \quad (\text{E.13})$$

For the calculations to follow let us assume that the monostatic system is operating over a vertical path so that $\bar{\mu} = 1$ and $R \equiv z$. Further, it is assumed that for a first approximation the two way path of the laser beam is confined to a cylindrical volume whose cross sectional area equals the aperture area of the receiver (πB^2 , where B is the radius of the receiver aperture) and whose length equals the range, z . In addition assume that $z = 5$ km. and that $v^* = 3.0$ (power of Junge distribution) for which the constant,

c , in (2.1, Chapter 2) equals 3×10^{-15} . For such a size distribution calculations with the Mie equations show that $\tilde{\beta}_t^P$, given in (E.7) equals $1.8 \times 10^{-4} \text{ km}^{-1}$. Finally, it can be shown that the total mean number of particles contained within the cylindrical volume in a size interval Δa about a is given by

$$\bar{N}(a) \approx (ca^{-4} \Delta a) (\pi B^2 \int_0^{5\text{km}} N'(z) dz)$$

Using (E.2) and (E.6) the above relation simplifies to

$$\bar{N}(a) \approx (ca^{-4} \Delta a) (\pi B^2 \tau_T^P / \tilde{\beta}_t^P) \quad (\text{E.14})$$

Similarly, using (E.8) and noting that $\tau^P(0, R)$ at $R=z=5\text{km}$ equals τ_T^P a relation is developed for $N(a)$ in terms of $\bar{N}(a)$. This relation is based on the fact that $\Delta N_O / N_O$ equals $\Delta \bar{N}(a) / \bar{N}(a)$, so that

$$N(a) = \bar{N}(a) \pm \Delta \bar{N}(a) = \bar{N}(a) \pm (0.005 \bar{N}(a) / \tau_T^P) \quad (\text{E.15})$$

Finally, if the particulates have a water density (chosen for simplicity) and are in an environment with a temperature, $T = 300\text{K}$, then all the parameters have been specified to calculate T_N and Θ_N for various sized particles. Table E.1 shows the results of the calculations of T_N and Θ_N for $\tau_T^P = 0.1$ and 0.25 for particles of size a and within

range Δa , and for $B = 15$ cm (equal to the radius of the University of Arizona monostatic receiver aperture).

One can conclude from Table E.1 that reasonable times for the occurrence of fluctuation states in the particulate concentrations do not arise to cause optical depth variances which lead to a 1% fluctuation in the mean received flux, F_T ; an examination of Θ_N for the various particulate sizes and optical depths substantiates this conclusion. However, it must be remembered that the particulates are assumed to move by thermal motion.

An extension of the previous development for the effects of turbulent motion appears warranted. Referring to (E.10) and (E.11), it is noted that the probability per unit time for particle escape, P_O , depends on the mean velocity of the particles, \bar{v} . Using a mean turbulent velocity for all the particulates yields a good approximation to the turbulent process. Inspection of the equations for T_N and Θ_N (E.9 and E.13) shows that they are inversely proportional to \bar{v} . Therefore, a simple ratio of the mean thermal and turbulent velocities yields the corresponding fluctuation times for the turbulent motion in terms of the values of the thermal motion expressed in Table E.1; simply stated

$$\begin{pmatrix} T_N \\ \Theta_N \end{pmatrix}_{\text{turb}} = \left[\frac{\bar{v}_{\text{thermal}}}{\bar{v}_{\text{turbulent}}} \right] \begin{pmatrix} T_N \\ \Theta_N \end{pmatrix}_{\text{thrm}} \quad (\text{E.16})$$

Table E.1 - Fluctuation States for Particulates in Brownian Motion.

$$\tau_T^P = 0.1$$

$a; \Delta a (x10^{-6} \text{meters})$	$\bar{N}(a)$	$P_O (\text{sec}^{-1})$	$T_N (\text{sec})$	$\theta_N (\text{sec})$
0.01; 0.001	1.18×10^{13}	5.32	7.94×10^{-15}	10^{10^9}
0.1 ; 0.01	1.18×10^{10}	1.68×10^{-1}	2.50×10^{-10}	10^{10^6}
1.0 ; 0.1	1.18×10^7	5.32×10^{-3}	7.94×10^{-6}	10^{10^3}
8.0 ; 0.8	2.36×10^4	2.38×10^{-4}	8.90×10^{-2}	10^{10^2}
10.0 ; 1.0	1.18×10^4	1.68×10^{-4}	0.250	10^{64}

$$\tau_T^P = 0.25$$

"	2.95×10^{13}	"	3.18×10^{-19}	10^{10^8}
"	2.95×10^{10}	"	1.00×10^{-9}	10^{10^5}
"	2.95×10^7	"	3.18×10^{-5}	10^{10^3}
"	5.90×10^4	"	3.56×10^{-2}	2.0×10^7
"	2.95×10^4	"	0.1	1.1×10^4

Using reasonable values of $\bar{v}_{\text{turbulent}}$ (10-100 cm/sec) makes little changes in the results derived for the thermal motion. Only for the special case of $a = 10.0 \times 10^{-6}$ meters at $\tau_T^p = 0.25$ does $\Theta_N \sim$ few seconds, but at $a = 8.0 \times 10^{-6}$ meters Θ_N is again up to the thousands of seconds! Therefore, it is concluded that even for turbulent motion of the particulates fluctuations of 1% in F_T most likely do not occur.

Finally, the large values of Θ_N at each size interval shows that variations in $\tilde{\beta}_t^p$ caused by changes in the relative numbers of particulates in the Junge distribution are not too likely.

With regard to the molecules, Chandrasekhar shows that a 1% fluctuation in the air density for a spherical volume of radius 1 cm has a recurrence time, Θ_N , of $10^{10^{14}}$ seconds! Therefore, for the large volumes associated with the transmission paths of the laser-receiver system, fluctuations of 1% are virtually impossible.

LIST OF REFERENCES

- Asakura, T., Y. Kinoshita, M. Suzuki, 1969: Further correlation studies of gaussian-beam fluctuations caused by a random medium. Jour. Opt. Soc. Amer., 59, 913-920.
- Batchelor, G.K., 1959: The theory of homogeneous turbulence. University Cambridge Press, 197 pp.
- Battan, L.J., 1959: Radar meteorology. University of Chicago Press. 161 pp.
- Brown, W.P., 1971: Second moment of a wave propagating in a random medium. Jour. Opt. Soc. Amer. 1051-1059.
- Chandrasekhar, S., 1943: Stochastic problems in physics and astronomy. Rev. Mod. Phys., 15, 1-89.
- Clark, N.A., J.H. Lunacek, and G.B. Benedek, 1970: A study of brownian motion using light scattering. Amer. Jour. Phys., 6, 575-585.
- Collis, R.T.H., and M.G.H. Ligda, 1964: Laser radar echoes from the clear atmosphere. Nature, 203, 508.
- Curran, J.C., 1971: A numerical solution to the horizontally-inhomogeneous time-dependent transfer equation. Ph.D. dissertation, Department of Physics, University of Arizona, Tucson, 187 pp.
- deWolf, D.A., 1969: Are strong irradiance fluctuations log normal or Rayleigh distributed? Jour. Opt. Soc. Amer. 1455-1460.
- Eiden, R., 1966: The elliptical polarization of light scattered by a unit volume of atmospheric air. Appl. Opt., 5, 569-575.
- Elterman, L., 1964: Atmospheric attenuation model, 1964, in the ultraviolet, visible, and infrared regions for altitudes to 50 km. Environmental Res. Papers No. 46, Air Force Cambridge Res. Labs., Bedford, Mass.
- Fernald, F.G., 1972: Ruby lidar measurements of the scattering properties within the lower troposphere. Ph.D. dissertation, Department of Atmospheric Physics, University of Arizona, Tucson, 108 pp.

- Fischer, K., 1973: Mass absorption coefficients of natural aerosol particles in the $0.4\mu\text{m}$ - $2.4\mu\text{m}$ wavelength interval. Beitr. Phys. Atmos., 46, 89-99.
- Fuchs, N.A., 1964: The mechanics of aerosols. New York, Pergamon Press, 408 pp.
- Greytak, T., 1970: Light beating spectroscopy. Phys. of Quantum Electronics, M.I.T. Opt. Sci. Cent. Tech. Rep., 31, vol. 1, 195-226.
- Ho, T.L., 1969: Log-amplitude fluctuations of laser beam in a turbulent atmosphere. Jour. Opt. Soc. of Amer., 4, 385-390.
- _____, 1970: Coherence degradation of gaussian beams in a turbulent atmosphere. Jour. Opt. Soc. of Amer., 5, 667-674.
- Hinze, J.O., 1959: Turbulence. New York, McGraw-Hill Book Co., Inc. 586 pp.
- Holland, A.C., and J.S. Draper, 1967: Analytical and experimental investigation of light scattering from polydispersions of Mie particles. App. Opt., 6, 511-518.
- Holland, A.C., and G. Gagne, 1970: The scattering of polarized light by poly disperse systems of irregular particles. App. Opt., 9, p. 1113.
- Junge, C.E., 1963: Air chemistry and radioactivity. New York, Academic Press, 382 pp.
- Livingston, P.M., P.H. Deitz and E.C. Alcaraz, 1970: Light propagation through a turbulent atmosphere: measurements of the optical filter function. Jour. Opt. Soc. Amer. 925-935.
- MacKinnon, D.J., 1969: The effect of hygroscopic particles on the backscattering power from a laser beam. Jour. Atmos. Sci., 26, 500-510.
- Mandel, L., and E. Wolf, 1965: Coherence properties of optical fields. Rev. Mod. Phys., 2, 231-287.
- Marshall, J.S., and W. Hitschfeld, and P.R. Wallace, 1953: The interpretation of the fluctuating echo for randomly distributed scatterers. Part I. Can. J. Phys., 31, 962-1009.
- Mie, G., 1908: Beitrage zur Optik Truber Medien, Ann. Physik, vol. 25, p. 377.

- Papoulis, A., 1965: Probability, random variables, and stochastic processes. New York, McGraw-Hill, 583 pp.
- Poirier, J.L., and D. Korff, 1972: Beam spreading in a turbulent medium. Jour. Opt. Soc. Amer. 893-898.
- Quenzel, H., 1969: Influence of refractive index on the accuracy of size determination of aerosol particles with light-scattering aerosol counters. App. Opt. 8, 165-169.
- Rice, S.O., 1954: Selected papers on noise and stochastic processes. New York, Dover Publication, Inc. 377 pp.
- Smith, P.L., 1965: Interpretation of the fluctuations in optical radar echoes from the atmosphere. Proceedings on the Conference on Limitations of Optical Propagation Through the Atmosphere, Boulder, Colorado, 383-396.
- Smithsonian Meteorological Tables. Sixth rev. ed. Washington: The Smithsonian Institution, 1958.
- Tartarskii, V.I., 1961: Wave propagation in a turbulent medium. New York, McGraw-Hill.
- Uspensky, J.V., 1937: Introduction to mathematical probability. New York, McGraw-Hill, 411 pp.
- Wang, M.C., and G.E. Uhlenbeck. 1945: On the theory of brownian motion II. Rev. Mod. Phys., 17, 323-342.